The activity of the Rokko-Awaji fault zone and the Osakawan fault zone inferred from the subsurface geology in the urban area of Kobe

苦瓜，泰秀

(Degree)
博士（理学）

(Date of Degree)
2009-03-25

(Date of Publication)
2009-04-09

(Resource Type)
doctoral thesis

(Report Number)
甲4515

(URL)
https://hdl.handle.net/20.500.14094/D1004515

博　士　論　文

The activity of the Rokko-Awaji fault zone and the Osakawan fault zone inferred from the subsurface geology in the urban area of Kobe

神戸市街地の表層地質からみた六甲・淡路断層帯

と大阪湾断層帯の活動性の研究

平成 21 年 1 月

神戸大学大学院自然科学研究科

苦瓜　泰秀

Abstract

The Rokko-Awaji fault zone and the Osakawan fault zone are distributed at the northwestward area of the Osaka Bay. The Osakawan fault zone is approaching to the Rokko-Awaji fault zone at near the eastern urban area of Kobe. The relationship of these fault zones is influenced to earthquake risk management around the urban area. Some concealed faults have been discovered in the urban area from seismic reflection surveys. I used boring database and ground penetrating radar (GPR) to investigate the subsurface structures on these concealed faults. The linkage of two fault zones was discussed in this paper.

The topography is characterized with the Rokko Mountains, which is composed with the Late Cretaceous granite, and the Osaka Bay in the south of the mountains. It is considered to be produced by the east-west compressive stress and predominantly right-lateral strike-slip fault movement. The Osaka Bay is filled up with the sediments from the Late Pliocene to the Pleistocene, which are named as the Osaka Group. The marine clay layers, which are numbered from Ma-1 to Ma13, are included in the middle and upper subgroups.

The tectonics after the Middle Pleistocene was studied using deep boring data. The mountain side was uplifting at around the rate of 0.08 m/kyr. It is harmonized with the present topography. The subsurface geology was studied using the boring database ‘KOBE JIBANKUN’. In the urban area, the Holocene marine clay layer (Ma13) and the clay layer including the K-Ah ash had discontinuities along the southwestward

extension of the Ashiya fault.

Ground penetrating radar (GPR) method was applied to investigate some concealed faults. The survey lines were set along the Sumiyoshi River (L = 2,730 m) and the Ishiya River (L = 1,439 m). The used GPR system was GSSI SIR-2 pulse radar system with 100 MHz antennas. The GPR reflectors were compared with boring data and interpreted as the structures of sediments and anomalies of the concealed faults.

Three concealed faults are estimated between the Rokko-Awaji fault zone and the Osakawan fault zone. These faults distribute like step faults and locate near the central area of Kobe. Additional attentions have to be paid to determine a scenario earthquake in the future.

Contents

1. Objectives of the study

The South Hyogo Prefecture Earthquake in 1995 (Kobe earthquake) (M_{JMA} 7.3) occurred under the Akashi Straight between the Honsyu Island and the Awajishima Island in southwestern Japan. The fault broke with right-lateral strike-slip movement to southwestward and northeastward along the Rokko-Awaji fault zone. The southwestward fault appeared to the surface along the west coast of the Awajishima Island as the Nojima earthquake fault. On the other hand, the northeastward fault broke only in the deep underground and clear continuous ruptures were not found on the urban area of Kobe. However the strong earthquake motions as the intensity 7 were observed and the destructions of the urban area were widely occurred. The damaged area had the zonal distribution between the Rokko Mountains and the sea (e.g. Shimamoto, 1995).

Nigauri and Miyata (1998) studied deformed joints of house inlet casings in the urban area of Kobe. The result had two features.

1) The directions of moved casings were mainly northwest or southeast.
2) Surface casings had large movements.

These two results indicated that the reason of deformation was mainly strong S-waves, not because the liquefactions and land slides. From that reason the impulsive force was introduced as the parameter (*IF*-value) of the strong ground motion.

$$IF = d \times \sqrt{s} \quad (\mathrm{cm}^{3/2})$$

where, *IF*: Index of the impulsive force, *d*: Depth of the moved joint (cm) and *s*: Slip range between the joints (cm).

The distribution of the *IF*-value was not plain even in the area of seismic intensity 7. The large *IF*-value areas had the zonal or spotted distributions. The amplification of seismic waves was occurred on the soft ground condition (e.g. filled old river and pond) and along the faults from the comparison with detailed topographic map. The information of ground condition and the structural geology are necessary for detailed seismic zoning.

After the Kobe earthquake, many seismic reflection surveys took place in the urban area and the Osaka Bay. Several concealed faults have been found. For example, the Gosukebashi (Uzugamori) fault was thought to be extended to southwestward from the Rokko Mountains and connected to the Wadamisaki fault in the Kobe Port (Geo-Research Institute, 1998). The Wadamisaki fault was considered as one of the splay faults of the Osakawan fault (Huzita and Maeda, 1984).

The fault zone consists of many fault segments. There are at least nine fault segments inside ten kilometers from central Kobe. These fault segments are included in the middle of Rokko-Awaji fault zone (e.g. the Suma fault, the Suwayama fault and the Gosukebashi fault) and the northern part of Osakawan fault zone (the Wadamisaki fault, the Maya fault and the Rokko Island fault). These fault segments have around ten kilometer lengths. The *M* 6 class earthquake was estimated from the activity of single fault segment using Matsuda's empirical formula (Nigauri and Miyata, 2008).

When the energy of an earthquake is remained, the breakage of fault

segments propagates to the next fault segment. The 1596 Keicho-Fushimi earthquake (ca. *M* 7.5) is a former known destructive earthquake around Kobe area. The fault movement was propagated to the adjacent active fault zone, such as from the Arima-Takatsuki fault zone to the Rokko-Awaji fault zone (Lin *et al.* 1998).

Concerning about the earthquake disaster prevention, it is important to study the existence, activity and linkage of active faults. The study area was set between the eastern Rokko-Awaji fault zones and the northern Osakawan fault zone. The main objective of the study was to read the active fault linkage using geological information and GPR data.

2. Geological settings

The Hanshin area between Osaka City and Kobe City is located in the northern edge of the Osaka Bay basin. The geological structures are affected by the fault block movement after the Late Pliocene (e.g. Huzita and Kasama, 1982 and 1983). The fault movements are attracted by the east-west compressive stress. The Rokko Mountains are formed by the uplift of the Late Cretaceous granite which is also widespread under the Osaka Bay basin as the basement rock. (Figs. 2.1 and 2.2)

The Osaka Bay basin is filled up with after Pliocene sediments (e.g. Katoh *et al.*, 2008). The sediments are named as the Osaka Group and divided into the three subgroups. The middle and upper subgroups are characterized the rhythmical sedimentation of the marine clay layers and coarse grained layers. The marine clay layers are called the numbers (Ma-1 to Ma13) from the bottom. The ages of the layers have been detected using several volcanic ash beds. The Ma-1 layer was older than 1 Ma (Late Pleistocene) and the Ma13 layer was the Holocene clay. Heights of the marine clay layers have been used to read the tectonic movement.

The Rokko-Awaji fault zone is extended southwest to northeast almost parallel to the Rokko Mountains and the Awaji-shima Island. But in the eastern Rokko Mountains area, several faults from northeast to southwest distribute parallel and cross the Rokko Mountains (e.g. the Gosukebashi fault, the Yahatadani fault, the Ashiya fault, the Koyo fault and the Nishinomiya flexure zone).

The Gosukebashi fault is one of the long segments among them. The length is about 14 km and it reaches to the Arima-Takatsuki fault zone at the northeastern tip. The right-lateral strike-slip movement is read geologically. The Paleozoic shale and the Mesozoic granite porphyry dike are dislocated right-laterally 2 km across the fault. The Yahatadani fault runs through southern edge of the granite porphyry dike at the Yahatadani valley (Miyata and Nigauri, 2008). The Ashiya fault consists of the southeastern borderline of the Rokko granite and the Osaka Group. The terrace deposits of the Osaka Group are deformed on the Koyo fault. The Nishinomiya flexure zone is a concealed fault under the urban area. The northeastward tip continues to the Itami fault, the Nobatake fault and the Arima-Takatsuki fault zone (HERP, 2006).

The Osakawan fault zone has become gradually cleared using the seismic reflection surveys (e.g. Yokokura *et al.*, 1998). The fault zone is almost parallel to the Rokko-Awaji fault zone and separates from 10 km to east. The main fault splays to the Wadamisaki fault, the Maya fault and the Rokko Island fault at the offshore of Kobe. These faults extend to north-northeastward and approach to the eastern urban area of Kobe (e.g. Huzita and Maeda, 1984) (Fig. 2.3).

After the 1995 Kobe earthquake, several seismic reflection surveys were carried out at the urban area and the port of Kobe (compiled in Geo-Research Institute, 1998). From the analysis some faults in the Rokko Mountains have been extended to under the urban area as concealed faults and flexure zones. But the relationship of the Rokko-Awaji fault zone and the Osakawan fault zone has not yet been

entirely solved, because of thick covered sediments.

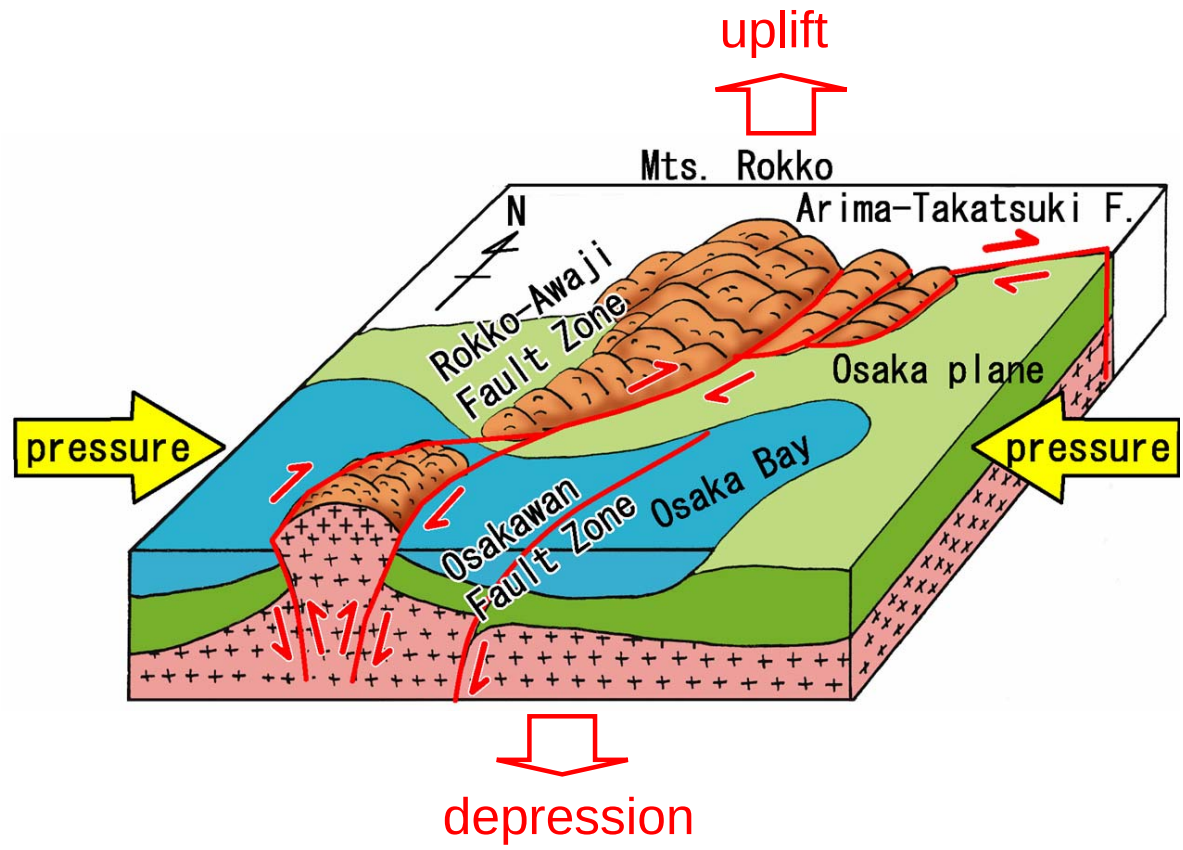

Fig. 2.1 The tectonic model of the Rokko Mountains uplift.

The right-lateral and reverse fault movements are playing the important roles to create the topography.

Geological map of Hanshin area (Geological survey of Japan, 1982, 1983)

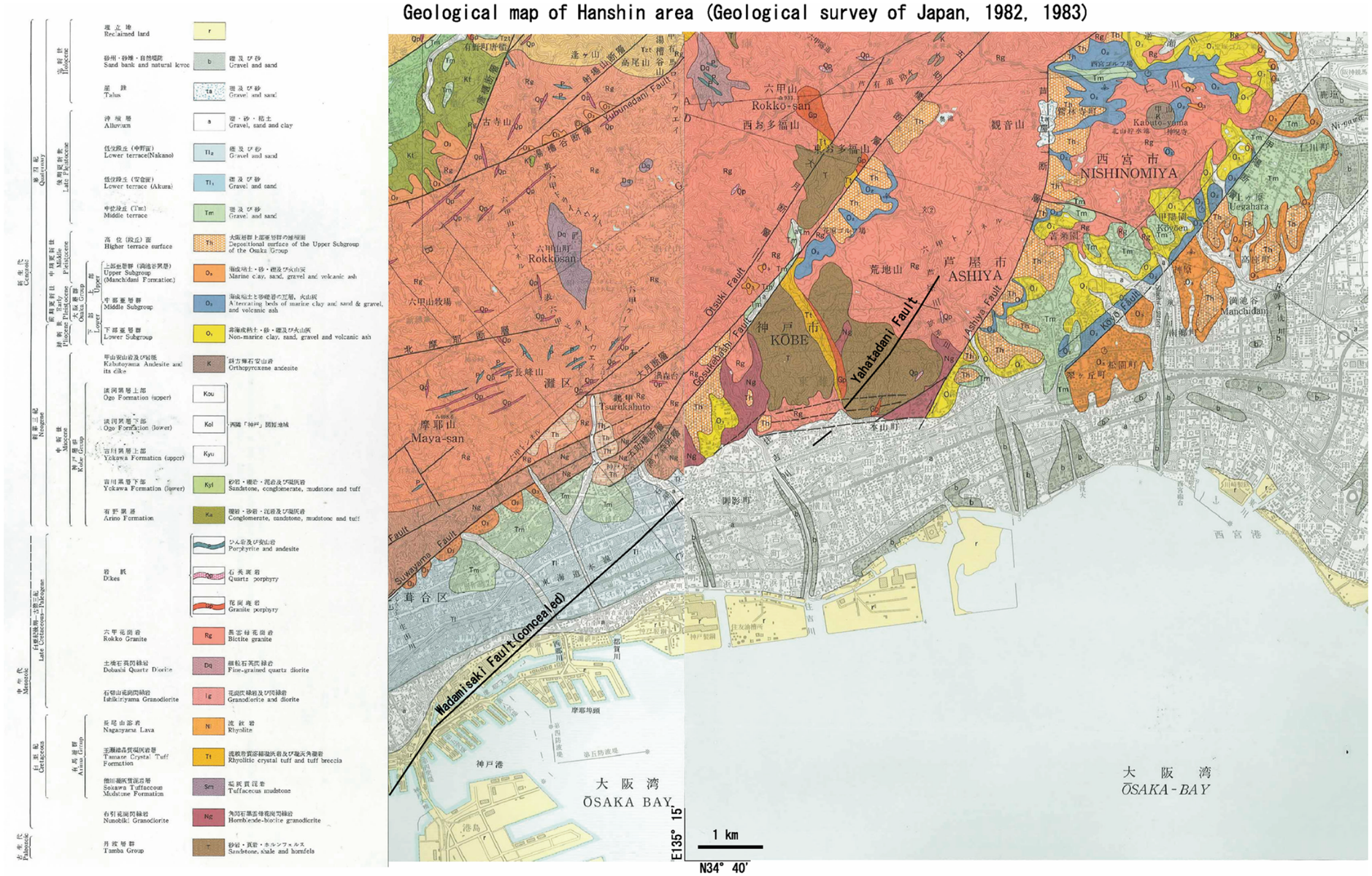

Fig. 2.2 The Geological map of Hanshin area modified Geological survey of Japan, 1982 and 1983. The Yahatadani fault was reported in Miyata and Nigauri (2008). The Wadamisaki fault was detected from seismic reflection surveys and boring data.

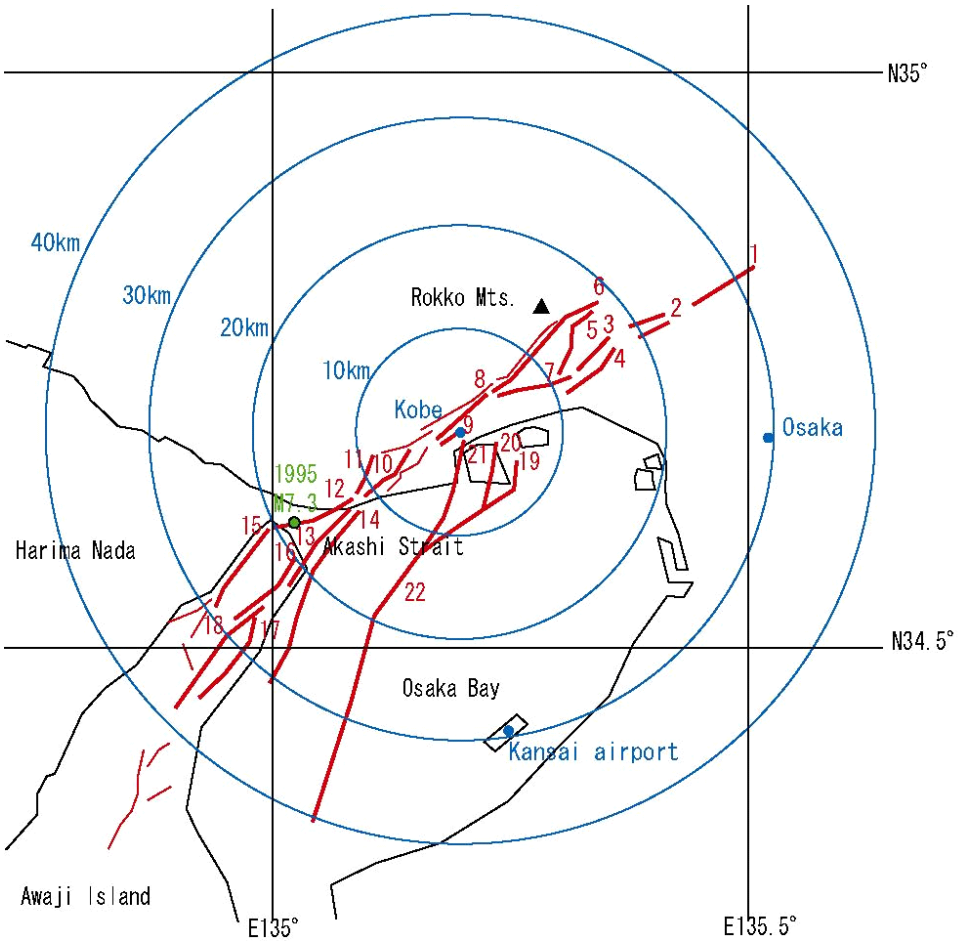

Fig. 2.3 Active fault distributions around Kobe City. Definition of the faults is followed The Headquarters for Earthquake Research Promotion (2005 and 2006). The fault names are as follows, 1. Nobatake fault, 2. Koya-ike subsidence zone and Itami fault, 3. Koyo fault, 4. Nishinomiya flexure zone, 5. Ashiya fault, 6. Gosukebashi fault, 7. Okamoto fault, 8. Suwayama fault, 9. Motomachi flexure zone, 10. Suma fault, 11. Yokoo-yama fault, 12. Taka-iso fault, 13. Kariya fault, 14. Kariya-oki fault, 15. Nojima fault, 16. Kusimoto fault, 17. Higashi-ura fault, 18. Nodao fault, 19. Rokko Island fault, 20. Maya fault, 21. Wadamisaki fault, 22. Osakawan fault.

3. Tectonics read from deep borings in the eastern Kobe area

The basement rock distributed around the south of the Rokko Mountains is sharply subsided toward the urban area. It is thought to be divided into several fault brocks. But information of the fault is very limited because of thick covered sediments. Some seismic reflection surveys were operated in the urban area and the Osaka Bay to research the existence of concealed faults. Several faults were discovered as the discontinuities of basement rock surfaces and flexures of covered sediments. More detailed surveys have to be operated to confirm the activity of such faults. Some deep boring surveys were also operated in order to investigate the geological structure and sedimentation.

To investigate the fault movement around the study area, I selected three borings (Fig. 3.1). The first boring was the GS-K1, which was in the Uozaki-hama, the seaside area of Higashinada Ward. The depth was 1,700 m (reached to the basement rock). The second boring was the GS-K3, which was in the Ishiya-gawa Park, Nada Ward. The depth was 680 m and the bottom reached under the Ma-1 layer, the lowest marine clay layer of the Osaka Group. The third boring was the HG-C, which was in the Maya wharf, Nada Ward. The depth was 583 m and the bottom was the Ma1 layer. The detail specs of the borings are shown in the Table 3.1.

Fig. 3.1 shows the three boring points. Dark blue lines indicate seismic reflection survey lines. Some concealed faults have been detected with the flexures of sediments. The flexure zones are expressed

by the green colored zones. But a concealed fault was not imaged inside the triangle of the three boring points. Then the comparison of the sediments using the height of volcanic ash beds and the marine clay layers were studied to check the fault movements between the each boring point. The Osaka Group has been widely studied and the general consensus of the stratification has been established (e.g. Ichihara, 1993). The age of layer was determined by using volcanic ash beds. The used ashes in this study were as follows, AT (29 ka between Ma13 and Ma12), Wada (340 ka between Ma10 and Ma9), Kasuri (420 ka included Ma8), Sayama (840 ka including Ma3), Azuki (870 ka near the bottom of Ma3), Pink (1050 ka above the Ma1) and Lower Yellow (1060 ka, included Ma-1). The boundary of Brunhes epoch and Matsuyama epoch (780 ka) was recorded in the Ma4 layer (Katoh *et al.*, 2008).

The relative rates between the each boring point were obtained from the differences of the elevation of the volcanic ash beds. For example, the elevations of the Pink ash bed were -592m at the GS-K1, -493m at the GS-K3 and -556m at the HG-C respectively. The Pink bed was about 15m above the marine clay Ma1 layer. It means that the Pink bed had been on sub horizontal plane when the ash had been fall. The differences of the levels indicated the relative movement between the two boring points. They are shown in Figs. 3.2, 3.3 and 3.4. The rate of the movement (elevation gap / age of the layer) was obtained from the comparison with the gap of several volcanic ash beds. The Rokko Mountain side was rising constantly after Middle Pleistocene. The GS-K3 side was moving upward at the rate of 0.07 m/kyr against the

GS-K1 side (Fig. 3.2). Between the HG-C and the GS-K3, the GS-K3 side was moving upward at the rate of 0.08 m/kyr (Fig. 3.3). The elevation gaps became larger (more than 100 m) at the deeper layers between these points. On the other hand, comparison with seaside data, between the GS-K1 and the HG-C, the movement was not stable (Fig. 3.4). But relative elevation gap was entirely small, less than 21 m.

Table 3.1 Specifications of deep borings used in the study.

Site Name	HG-C	GS-K3	GS-K1
Latitude	N 34°41’48”	34°43’3”	34°42’9”
Longitude	E 135°13’51”	135°14’58”	135°16’35”
Depth (m)	583	680	1700
Ground level (m)	2.1	34.67	2.68
Ground level before the land fill（m）	-8.7	31.67	-9.9
The bottom level (m)	-580.9	-645.33	-1697.32

Notice: Ground level before the land fill was estimated from the near another boring data (Kobe City, 1999) before the land fills.

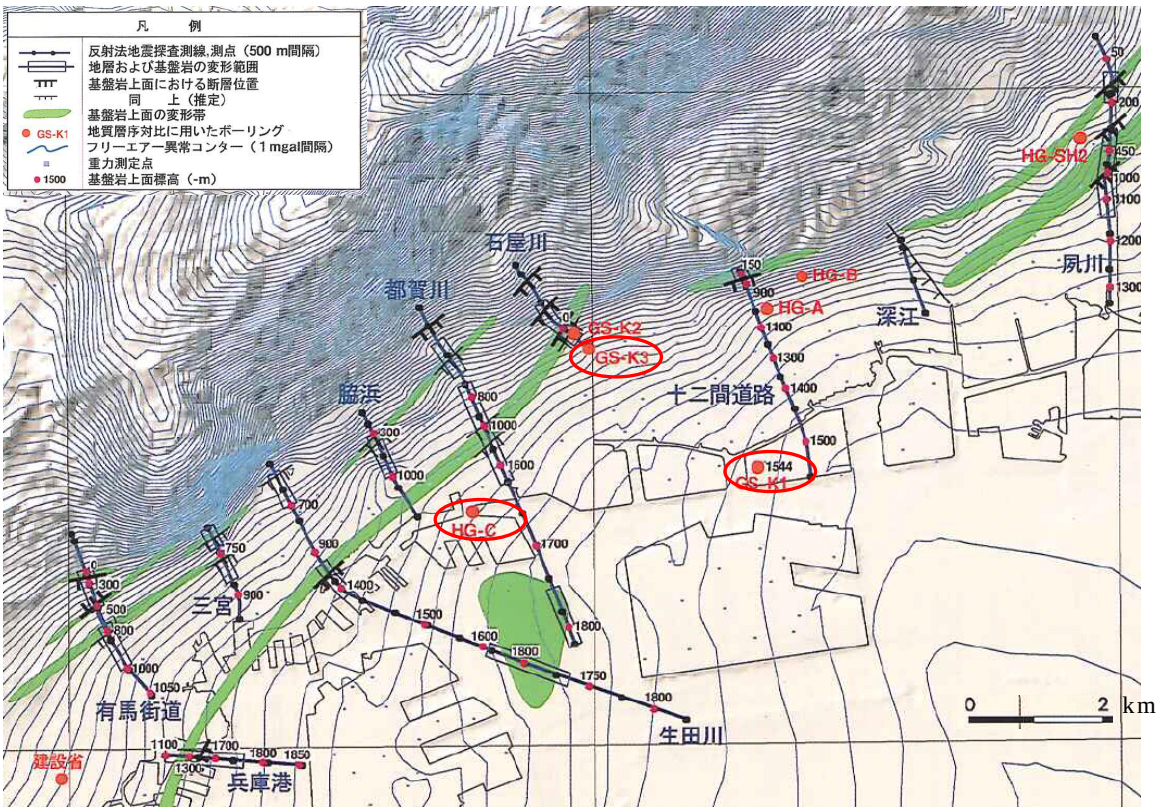

Fig. 3.1 Index map. The map was arranged of the new Kansai ground (1998). Red circles: boring point. Dark Blue line: the seismic reflection survey line. Green colored area: deformation zone of the basement rock.

Boring (GS-K3)				Boring (GS-K1)				Age (ka)	Elevation gap K1-K3
Height	Depth	Marine Clay	tephra	Height	Depth	Marine Clay	tephra		
34.67	0	Ground Surface		2.7		Ground Surface			
32	3	bottom of the fill	before filling	-9.9		Surface of Ma13	before landfill	0	-42
				-23	26.15		Aira-Tanzawa	29	
				-65	68	Ma12		100	
				-87	90	Ma11(3)			
				-99	102	Ma11(2)			
				-114	117	Ma11(1)			
				-155	158	Ma10			
				-172	174.75		Naruohama IV		
-129	164	Ma9 ?		-199	202	Ma9			-70
				-243	245.32	Ma8	Kasuri	420	
-212	247	Ma7		-282	285	Ma7			-70
-229	264	Ma6		-306	309	Ma6			-77
-262	296.41	Ma5	Hacho-ike	-348	350.90	Ma5	Hacho-ike		-86
-295	330	Ma4	(B/M Boundary)	-392	395	Ma4		780	-97
				-419	422.10	Ma3	Sayama	840	
-339	373.37	Ma3	Azuki	-441	443.85	Ma3	Azuki	870	-102
-355	390	Fague/Metasequoia Boundary		-467	470	Fague/Metasequoia Boundary			-112
-387	422	Ma2		-491	494	Ma2			-104
-426	460.20		Komyo-ike III	-534	536.53		Komyo-ike III		-108
-448	482.95		Pink	-563	565.55		Pink	1050	-115
-460	495	Ma1		-579	582	Ma1			-119
-524	558.95	Ma0	Lower Yellow	-645	648.00	Ma0	Lower Yellow	1060	-121
-559	594	Ma-1		-685	688	Ma-1			-126

notice: The heights of the marine clay are middle of the layer.

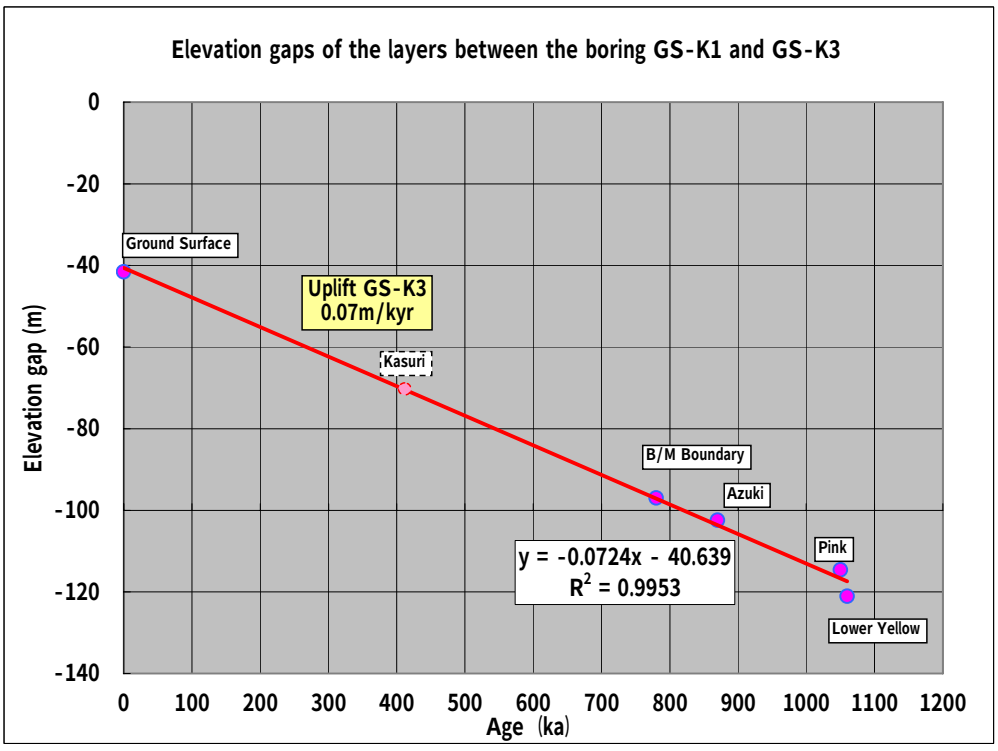

Fig. 3.2 The comparison of the boring data (GS-K1 and GS-K3) and the elevation gaps of the layers.

Boring (GS-K3)				Boring (HG-C)				Age (ka)	Elevation gap C-K3
Height	Depth	Marine Clay	tephra	Height	Depth	Marine Clay	tephra		
34.67	0			2.1	0				
32	3	bottom of the fill	before filling	-8.7		Surface of Ma13	before landfill	0	-43
				-10	12.5	Ma13			
				-71	73.5	Ma12			
				-175	177	Ma10			
				-207	209		Wada	340	
-129	164	Ma9 ?		-220	222	Ma9			-91
				-264	266	Ma8	Kasuri	420	
-212	247	Ma7		-298	300	Ma7			-86
-229	264	Ma6		-323	325	Ma6			-94
-262	296.41	Ma5	Hacho-ike	-361	363	Ma5			-99
-295	330	Ma4	(B/M Boundary)	-403	405.16	Ma4	B/M Boundary	780	-108
-339	373.37	Ma3	Azuki	-443	445.46	Ma3	Azuki	870	-105
-355	390	Fague/Metasequoia Boundary							
-387	422	Ma2		-483	485.5	Ma2			-96
-426	460.20		Komyo-ike III						
-448	482.95		Pink	-544	545.61		Pink	1050	-95
-460	495	Ma1		-561	563.5	Ma1			-101
-524	558.95	Ma0	Lower Yellow					1060	
-559	594	Ma-1							

notice: The heights of the marine clay are middle of the layer.

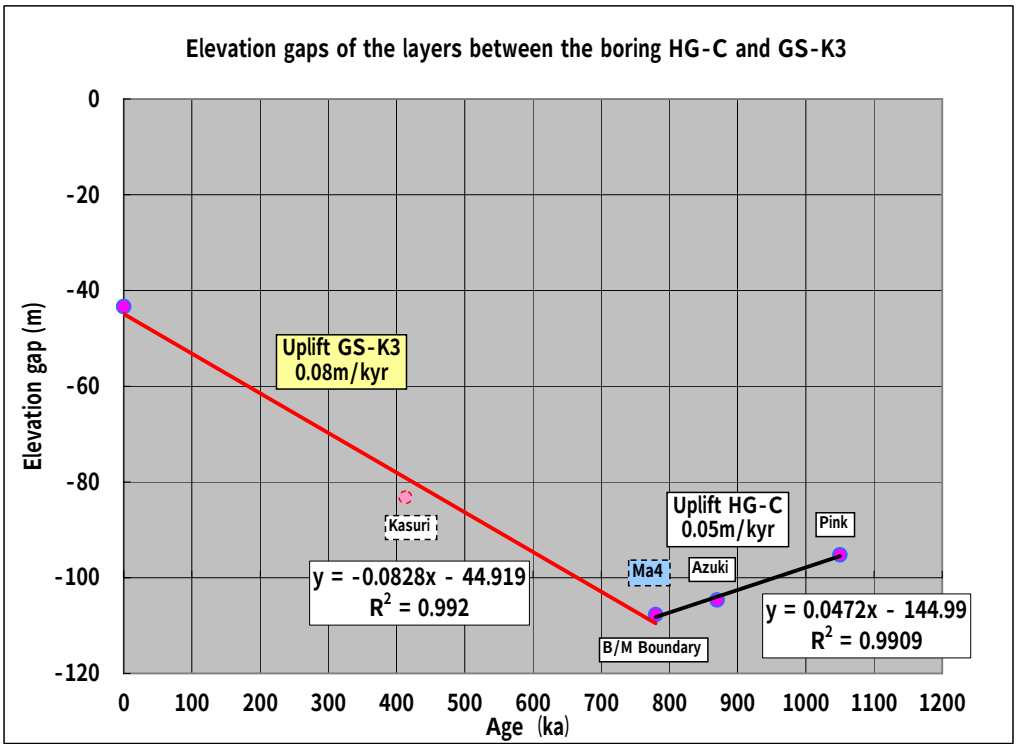

Fig. 3.3 The comparison of the boring data (HG-C and GS-K3) and the elevation gaps of the layers.

Boring (HG-C)				Boring (GS-K1)				Age (ka)	Elevation gap K1-C
Height	Depth	Marine Clay	tephra	Height	Depth	Marine Clay	tephra		
2.1	0	Ground Surface		2.68	0	Ground Surface			
-8.7		Surface of Ma13	before landfill	-9.9		Surface of Ma13	before landfill	0	-1
-10	12.5	Ma13							
				-23	26.15		Aira-Tanzawa	29	
-71	73.5	Ma12	(Aso-4 to Aso-3)	-65	68	Ma12	(Aso-4 to Aso-3)	100	6
				-87	90	Ma11(3)			
				-99	102	Ma11(2)			
				-114	117	Ma11(1)			
-175	177	Ma10		-155	158	Ma10			20
				-172	174.75		Naruo-hama IV		
-207	209		Wada					340	
-220	222	Ma9		-199	202	Ma9			21
-264	266	Ma8	Kasuri	-243	245.32	Ma8	Kasuri	420	21
-298	300	Ma7		-282	285	Ma7			16
-323	325	Ma6		-306	309	Ma6			17
-361	363	Ma5		-348	350.90	Ma5	Hacho-ike		13
-403	405.16	Ma4	B/M Boundary	-392	395	Ma4		780	11
				-419	422.10	Ma3	Sayama	840	
-443	445.46	Ma3	Azuki	-441	443.85	Ma3	Azuki	870	2
-483	485.5	Ma2		-491	494	Ma2			-8
				-534	536.53		Komyo-ike III		
-544	545.61		Pink	-563	565.55		Pink	1050	-19
-561	563.5	Ma1		-579	582	Ma1			-18
				-645	648.00	Ma0	Lower Yellow	1060	
				-685	688	Ma-1			

notice: The heights of the marine clay are middle of the layer.

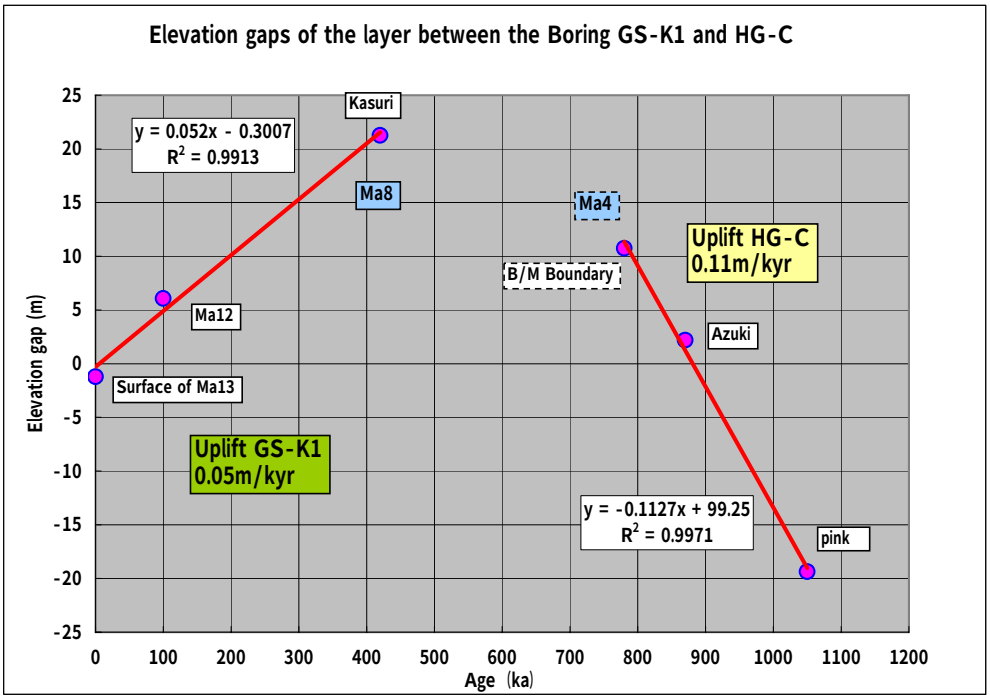

Fig. 3.4 The comparison of the boring data (GS-K1 and HG-C) and the elevation gaps of the layers.

4. Concealed fault research using boring database in the eastern Kobe area

The urban area of Kobe is a highly concentrated area with buildings and infrastructures. There are many boring data for the constructions. About 9,000 boring data were collected and input to the GIS system named KOBE JIBANKUN (Kobe City, 1999). The subsurface stratification and N-value were main information.

The urban area is mainly on the complex Holocene fans which are composed of the debris flow deposits from the Rokko Mountains. The soil includes mainly cobbles, gravels, sands and sometimes the inclusion of thin clay layers. The clay layers are continuous by comparison. They have been very useful in the study of the sedimentary process. Some tephras were recorded in various boring data. The K-Ah ash is one of the widespread tephras around southwestern Japan in 7,330 years ago. On the other hand, marine clay the Ma13 (after 10 ka) and the Ma12 (70~130 ka) are distributed near the seaside area. They have been used as good indicators to determine the sea levels in the past around the Osaka Bay because they gradually subsided under the sea (e.g. Huzita and Kasama, 1982 and 1983).

In this study, four geological east - west layer sections were analyzed between the Ashiya fault and the Maya fault in the eastern Kobe area (Fig. 4.1). The Maya fault was detected in several east-west geological sections between the Port Island and the Rokko Island (Huzita and Maeda, 1984). The Ashiya fault was known in the eastern

Rokko Mountains. The a-b section crossed the already known the Maya fault. The c-d section was along the coast line of landfill area. The e-f line was along the past natural coastline. And the g-h line was along the Route 2.

1) a-b section (Fig. 4.2)

The northern tip of the Maya fault was detected as an elevation gap of the Ma12 marine clay layer between the Port Island and the Rokko Island. The elevation of the upper side of the Ma12 layer was different more than ten meters, the western side was up. The bottom of the Ma13 layer was also ten meters higher at the western side.

2) c-d section (Fig. 4.3)

The Ma13 layer was traced along the section. But the thickness was different at around the middle of the section. The thickness was larger (ca. 10~15m) through the eastern side. Through the western side, it became less than five meters.

3) e-f section (Fig. 4.4)

The continuous Ma13 layer distributed only at the eastern side of the profile. The bottom level of the Ma13 layer was TP-20m at point f, and it sharply rose around the center of the profile. The upper side of the Ma13 layer was undulated several meters. It is considered the influences of the constructions of reclaimed lands. The original Ma13 layer is thought to be distributed the zone of TP-5 to TP-20m. The mouth of the Sumiyoshi River crosses the profile. The sandy soils were carved the Ma13 clay layer.

4) g-h section (Fig. 4.5)

The Holocene marine clay layer (Ma13) was not distributed along the section because the section was apart from the coast line. The facies were changed frequency. The relative clay rich layers zone including the K-Ah tephra (Machida and Arai, 1978) were selected to read the movement. The thickness of the layer was about 10 m at the eastern side of the section, but gradually it became thin towards the west. The raised area was the Sumiyoshi River. The clay layer was disappeared near the river.

The detected level changes of Holocene clay layers were arranged in northeast to southwest direction. The changes indicated commonly that the movements of western sides are up and eastern sides are down. It was harmonized with the tectonics read from the deep boring analysis written in the previous section.

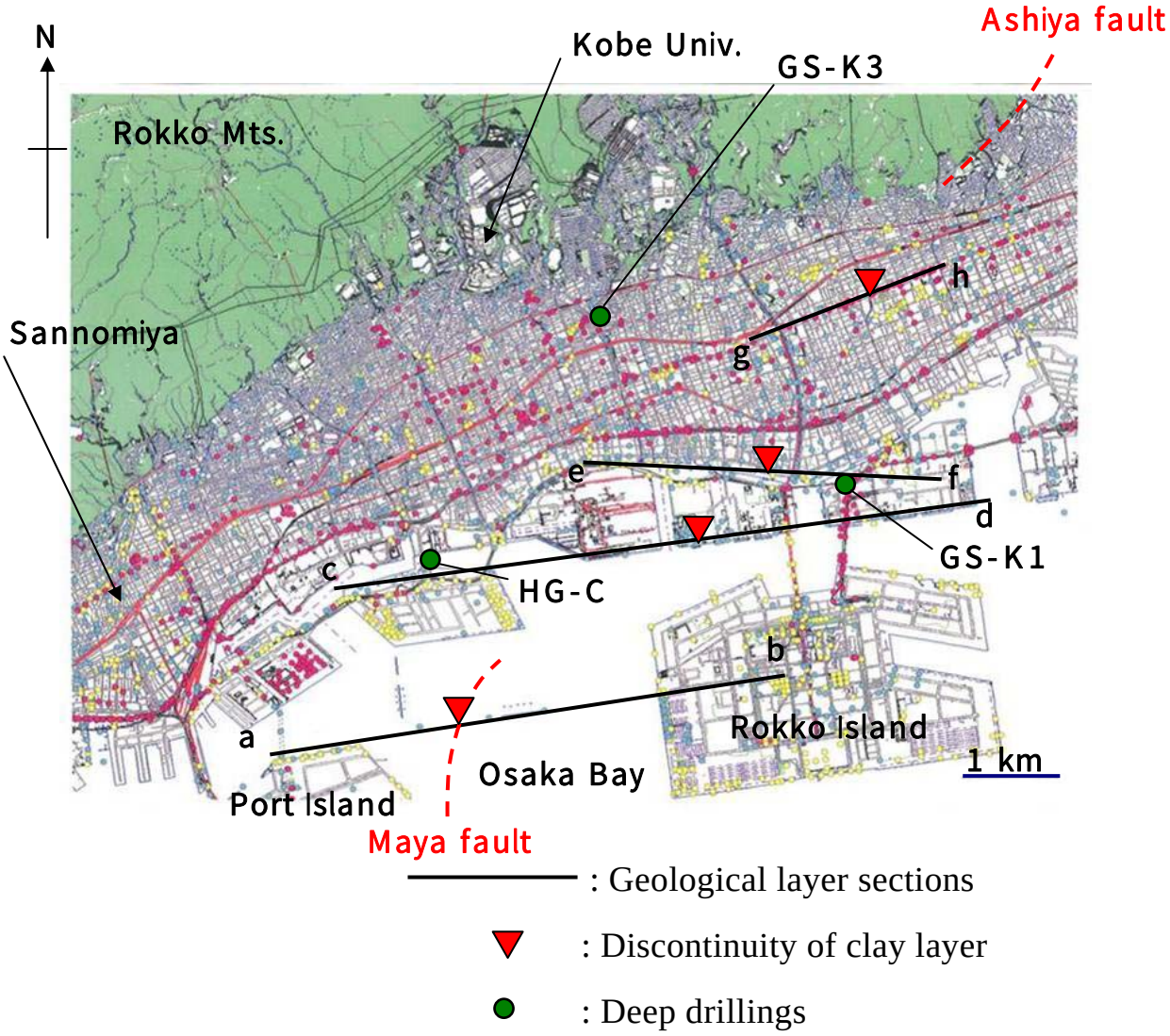

Fig. 4.1 The map of the geological layer sections. The base map was from the boring database 'KOBE JIBANKUN'. The blue, yellow and red small circles indicate boring sites in the database.

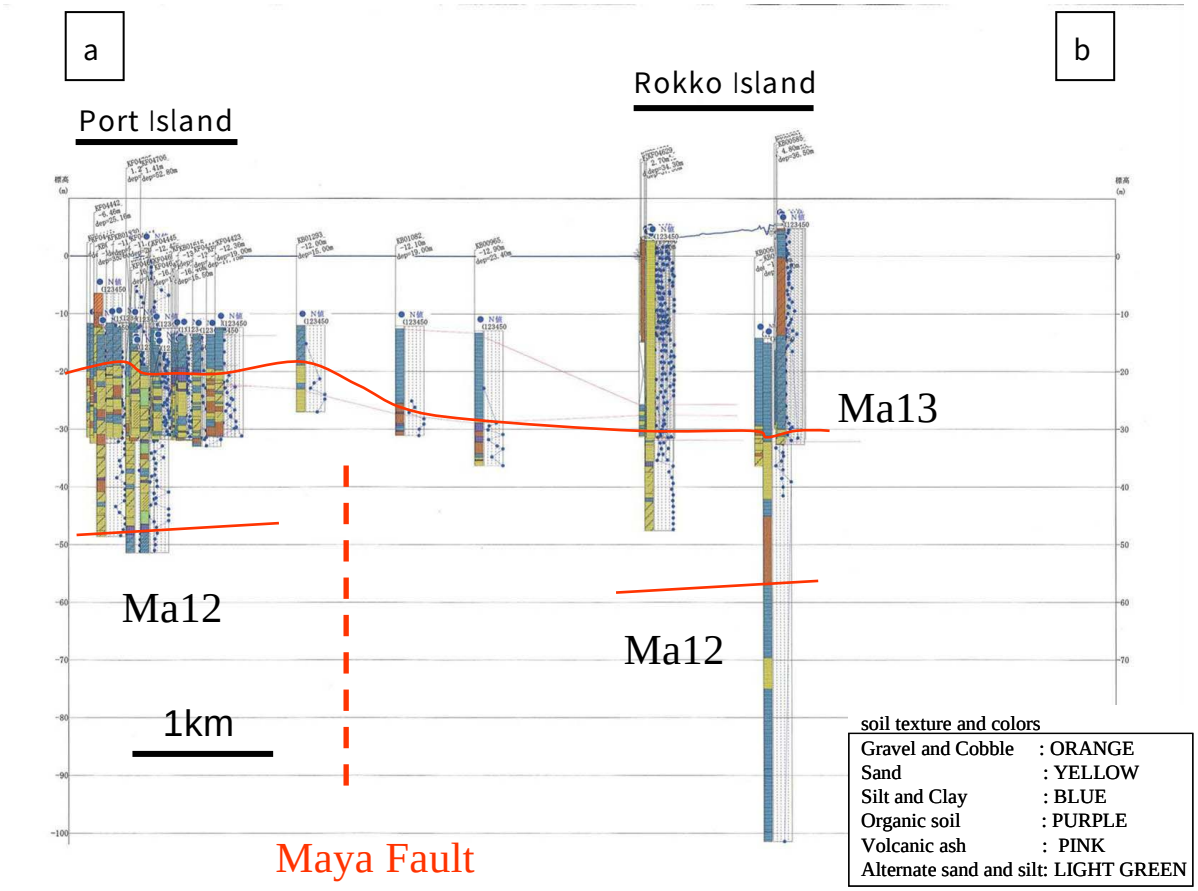

Fig. 4.2 The geological section between the Port Island and the Rokko Island from the boring database 'KOBE JIBANKUN'. The position is shown in Fig. 4.1.

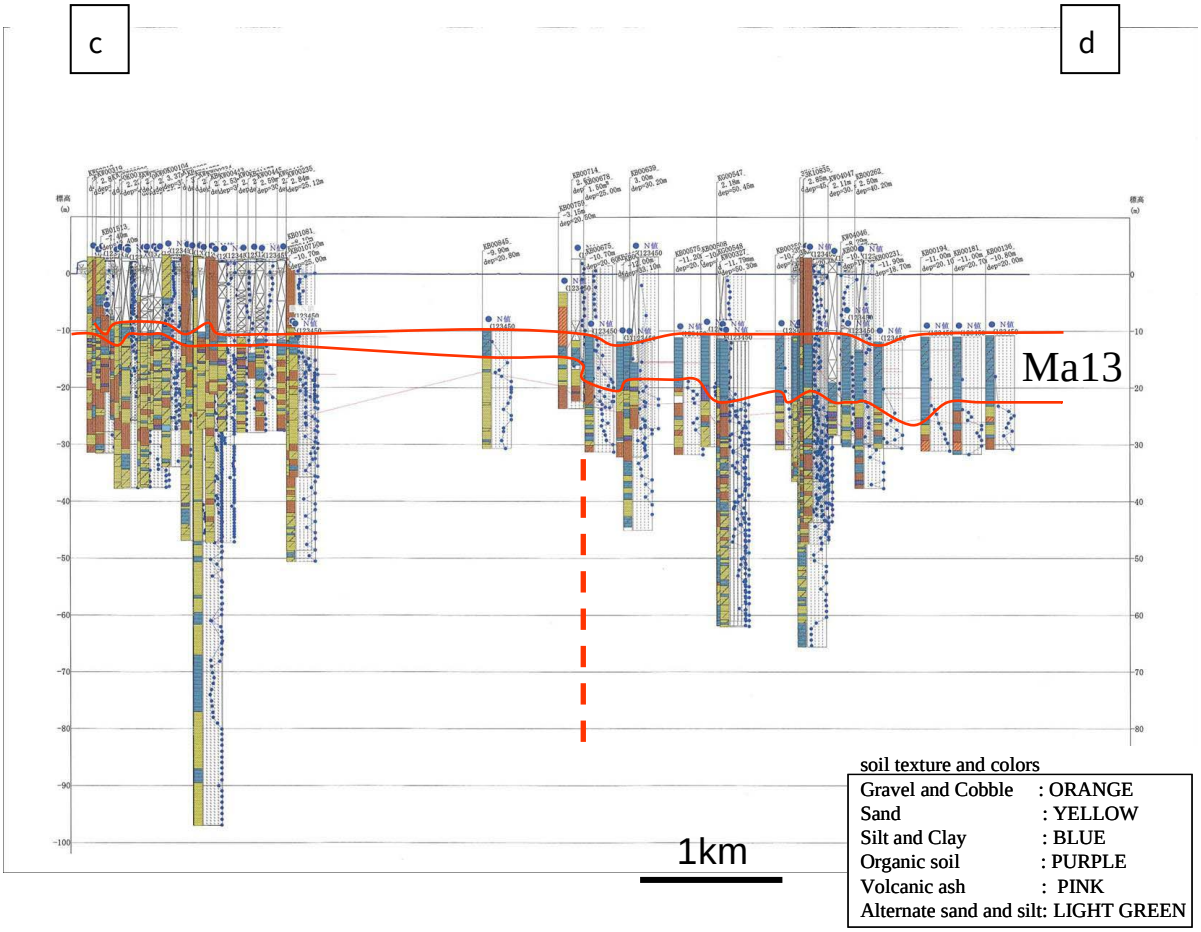

Fig. 4.3 The geological section along the coast line of landfill area from the boring database 'KOBE JIBANKUN'. The position is shown in Fig. 4.1.

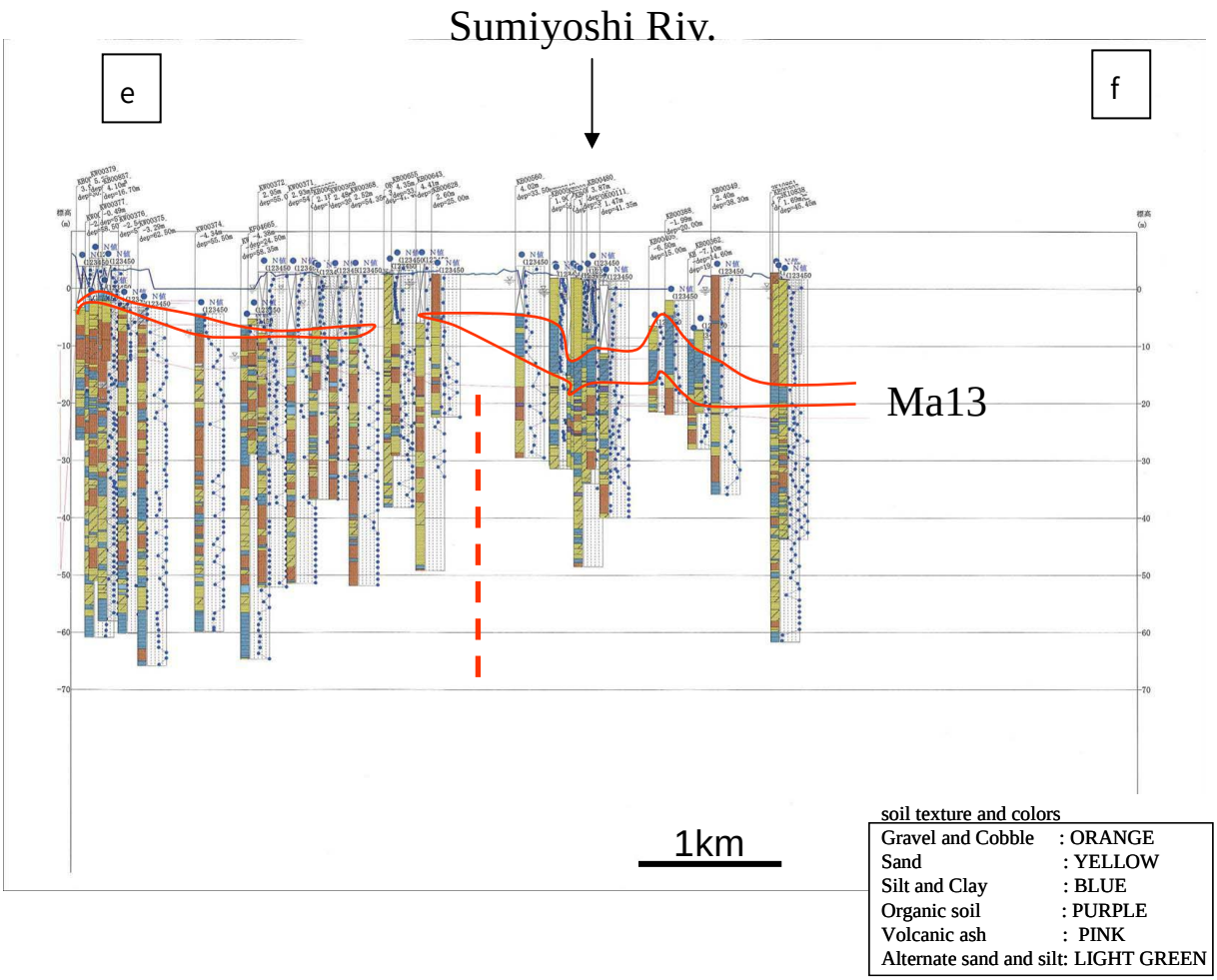

Fig. 4.4 The geological section along the coast line from the boring database 'KOBE JIBANKUN'. The position is shown in Fig. 4.1.

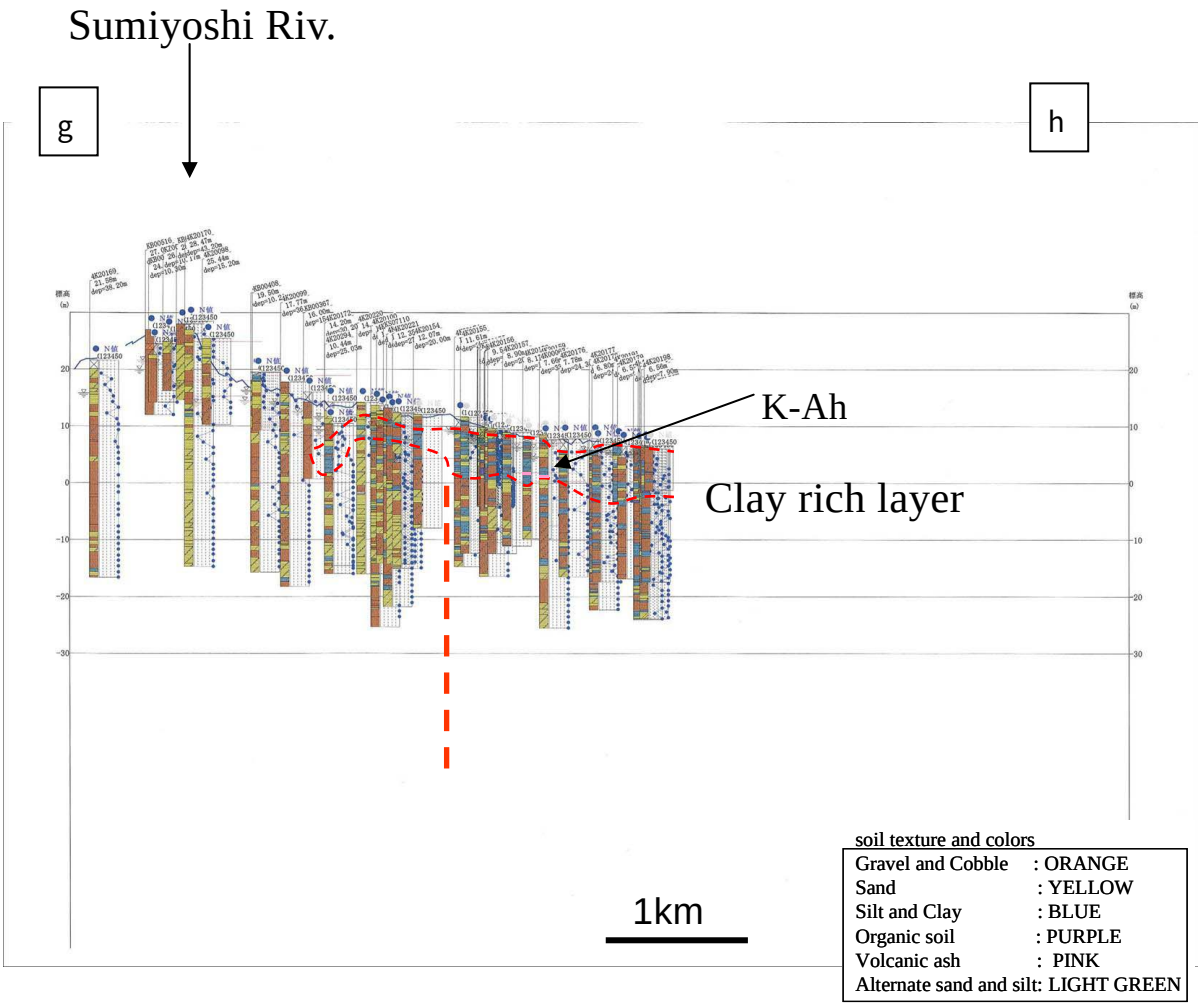

Fig. 4.5 The geological section along the Route 2 from the boring database 'KOBE JIBANKUN'. The position is shown in Fig. 4.1.

5. Ground penetrating radar image of concealed faults in the eastern urban area of Kobe

5.1 Ground penetrating radar method

Ground penetrating radar (GPR) is one of the geophysical methods to investigate the underground structures. GPR shots downward electromagnetic (EM) waves and receives the reflection waves from underground reflectors. The reflection occurs at the boundary of EM wave velocities (Fig. 5.1). The wave velocity represents as follows:

$$v = \frac{C}{\sqrt{\varepsilon_r}} \quad (1)$$

where v, C and ε_r are EM velocity, speed of light (30 cm/ns) and relative dielectric permittivity, respectively. The relative dielectric permittivity has a property which is changed depends on the soil and water content. Table 5.1 shows the example. A massive and dry material such as rock indicate a fast EM velocity, on the other hand a water content soil such as clay and silt indicate a slow EM velocity.

At the field the unit of two antennas (transmitter and receiver) is towed slowly and collected the reflection data. The method is called a profile measurement. The record format is distance (horizontal axis) and time (vertical axis). The frequency of antennas have to be chosen properly depends on the purpose of the study. The low frequency waves reach to deep underground, but have low resolution and the high frequency waves have opposite property.

To know the EM wave velocity, a wide angle measurement is carried out. The wide angle measurement uses two separate antennas. One antenna is used as a transmitter and the other is used as a receiver, both antennas are moved slowly to opposite sides each other with the same speed. The EM wave velocity is calculated as follows,

$$t = \frac{\sqrt{4d^2 + X^2}}{V} \quad (2\text{-}1)$$

$$t^2 = \frac{4d^2}{V^2} + \frac{X^2}{V^2} \quad (2\text{-}2)$$

where t, d and X are two-way travel time, depth to the reflector and separation of antennas respectively. If the data are plotted on the X^2-t^2 axes. The EM wave velocity is determined by using the gradient a.

$$a = \frac{1}{V^2} \quad \text{then} \quad V = \frac{1}{\sqrt{a}} \quad (3)$$

The depth of reflector is presented as b from the interception of t^2-axis.

$$b = \frac{4d^2}{V^2} \quad \text{then} \quad d = \frac{V\sqrt{b}}{2} \quad (4)$$

5.2 GPR Survey

The ground penetrating radar (GPR) system was the GSSI SIR-2 pulse radar and the 100 MHz antenna. The time range of records was set 150 ns or 250 ns. The EM velocity was determined 10 cm/ns from the result of several wide angle measurements in the urban area of Kobe. The velocity was assumed even through the profile. The depths of the

profile corresponded to 7.5 m and 12.5 m with the ranges were 150 ns and 250 ns respectively. The horizontal position was collected with one meter interval markers in the data. The original data was processed by high cut (Boxcar filter 400 MHz) and low cut (Boxcar filter 25 ~ 40 MHz) filtering using the RADAN 6 software system for contrast layer continuities.

The survey lines were set along the rivers. The first line was along the Sumiyoshi River. The length was 2,730m. The second line was along the Ishiya River. The length was 1,439m. The survey line positions were selected where the seismic reflection survey data was not exist (Fig. 5.2).

5.3 The Sumiyoshi River GPR survey line

1) Northern part (Fig. 5.3)

The survey line was located between the Ishiya River seismic reflection survey line and the Juniken Road seismic reflection survey line. The line was set on the promenade along the left side of the river.

The northern part of the Yamate arterial road had steep gradient over five degrees. The soil contained mainly sands, gravels and cobbles. The N-values were almost more than 50, instead of sand and clay thin beds. The GPR imaged continuous and parallel reflection. They were interpreted as the facies of fan sediments.

Between the Yamate arterial road and the Route 2, the gradient became a little gentle to four degrees. The soil contained mainly sand

and gravel. In addition thin sand and clay beds were seen in the interval of several meters. Three continuous sand beds were seen around the depth of 10, 20 and 25 meters. The AT tephra (29,000 yBP) was detected under the 10 meter depth bed at the boring KS07114 (Kobe City, 1999). These beds were traced to at least the north of the Yamate arterial road. The GPR reflection surfaces had curved upward wavy shapes. They were considered as the end of the fan deposits.

2) Southern part (Fig. 5.4)

From the Route 2 to the middle of the profile, the gradient became two to three degrees. The soil contained mainly sands and gravels. The N-values were around 30~40. The reflector surfaces were clear and continuous. They were identified as gravel fan deposits.

The northern part of the Hanshin Railway, the gradient became one to two degrees. The soil contained mainly sand. The N-values were around 30~40. The GPR reflection became a little weak because of the small amount of gravels.

Between the Hanshin Railway and the Route 43, the gradient was one to two degrees. The soil contained sand and gravel. N-values became small to the south. The GPR reflector surface had complex shape.

At the southern part of the Route 43, the loose sandy sediments were distributed at the surface. The N-values were around 10~20. The GPR reflections from sand bar deposits were inclined to seaward. Near the coast line area, the alluvium marine clay Ma13 layer was distributed at the depth under seven meters. But the radar waves were reduced by the sea water.

5.4 The Ishiya River GPR survey line

1) Northern part (Fig. 5.5)

The survey line was located at the southern extension of the Ishiyagawa seismic reflection line. The soil contained mainly sands and gravels. Thin clay layers sometimes existed, but their continuities were not good. The N-values were not constant (varied around 10 ~ 50). The Mikage flexure zone which has been found by the seismic reflection survey along the Ishiya River was crossing the middle of the profile. The sand layer at the elevation of around 25 m on the hanging wall was connected to the sand layer at the elevation of around 5 m on the footwall. The layer boundaries corresponded to the difference of the strength of GPR reflection. The underground flow of the Ishya River sprang around the south of boring 3K00017. The GPR image became a little dark color. The discontinuities of the GPR reflection were seen at the zone.

2) Southern part (Fig. 5.6)

The ten meters thick fan sediments were distribute at the surface of the terrace sediments. Some horizontal thin clay beds were distributed under the fan sediments. They were traced at the southern side of the Hanshin Railway. The N-values were almost fifty, but ten to thirty in thin beds. The GPR images were inclined to the south depend on the structure of fan sediments. The sand bar sediments were distributed between the Route 43 and the coast line. The N-values were ten to twenty.

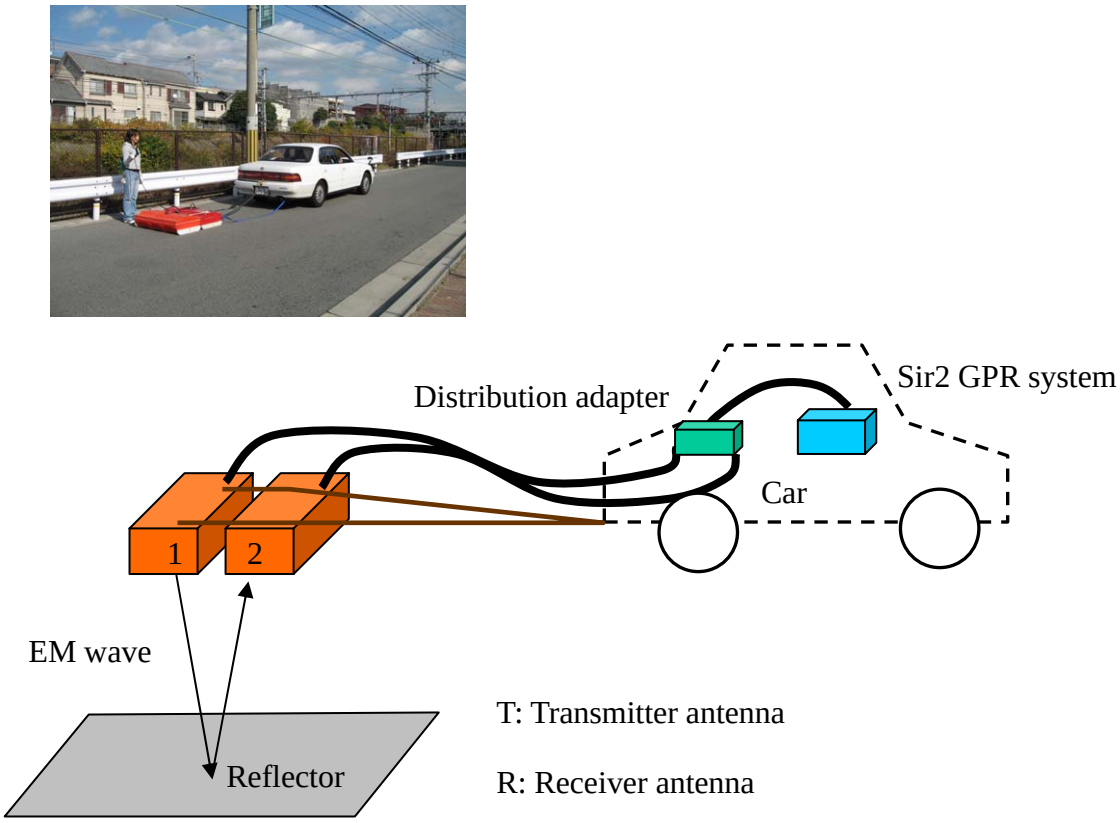

Fig. 5.1 The model of GPR method

Table 5.1 Relative dielectric permittivity and velocity of electromagnetic wave of rock and soil, after Uchida (1984).

Material	Relative dielectric permittivity	Velocity (cm/ns)
Granite	4	15
Andesite	2	21
Gabbro	3	17
Basalt	4	15
Tuff	6	12
Limestone	7	11
Marble	6	12
Soil (20% of water content)	10	9.5
Soil (0% of water content)	4	15
Water	81	3.3

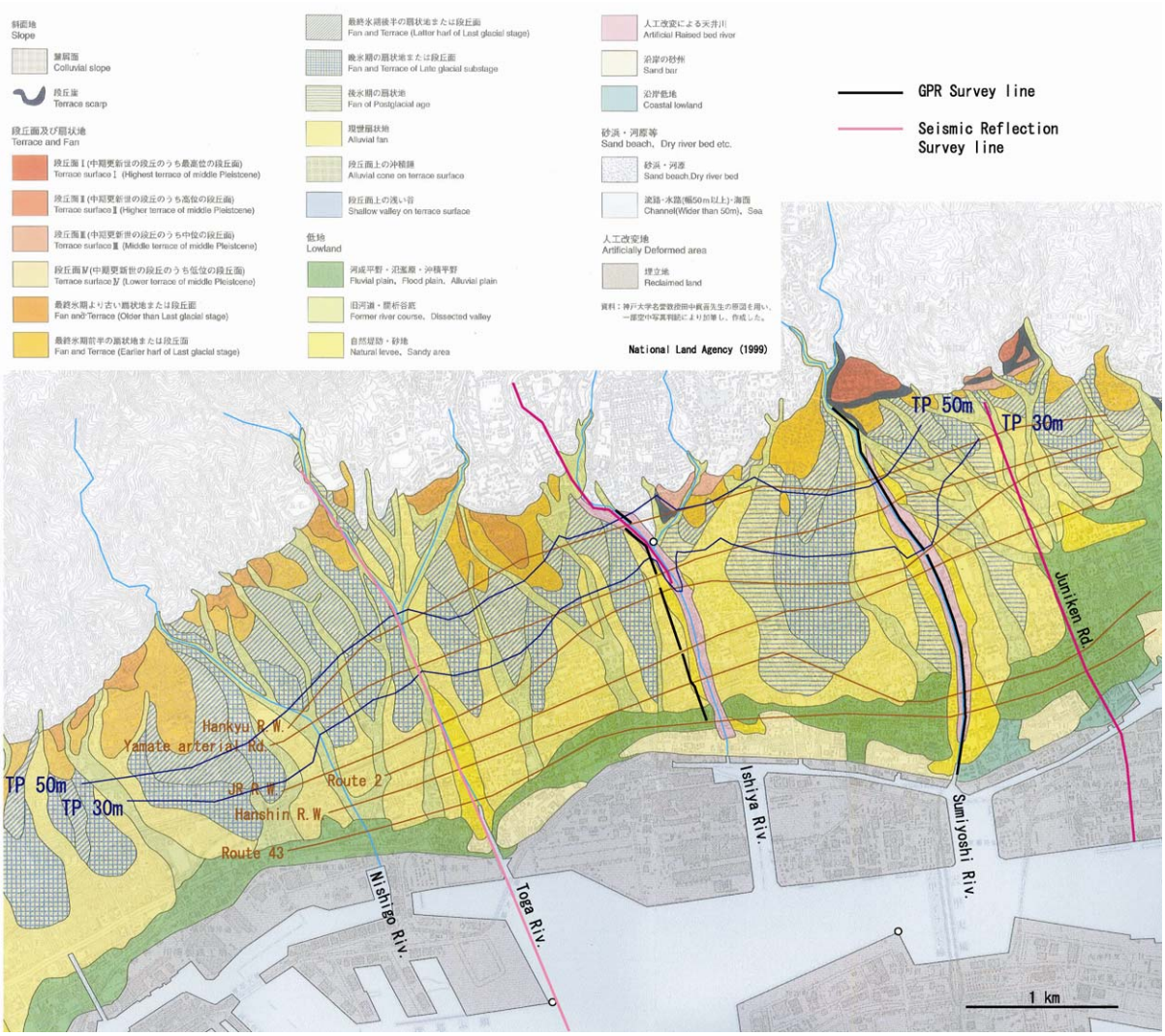

Fig. 5.2 GPR survey lines and seismic reflection lines on the detailed topographic map (National Land Agency, 1999).

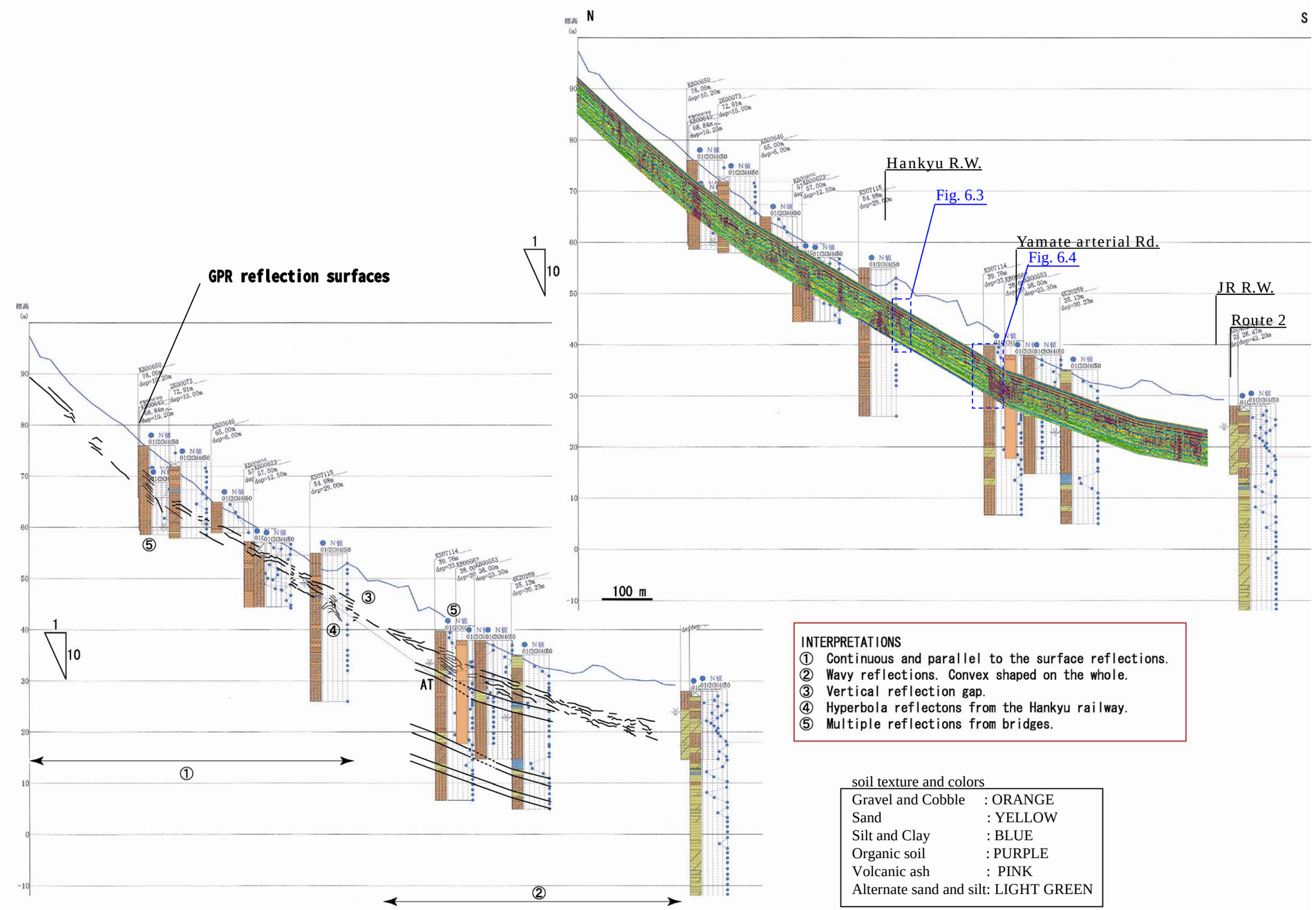

Fig.5.3 GPR survey profile. Northern part of the Sumiyoshi River section. The boring data were from the database ‘KOBE JIBANKUN’ (Kobe City, 1999).

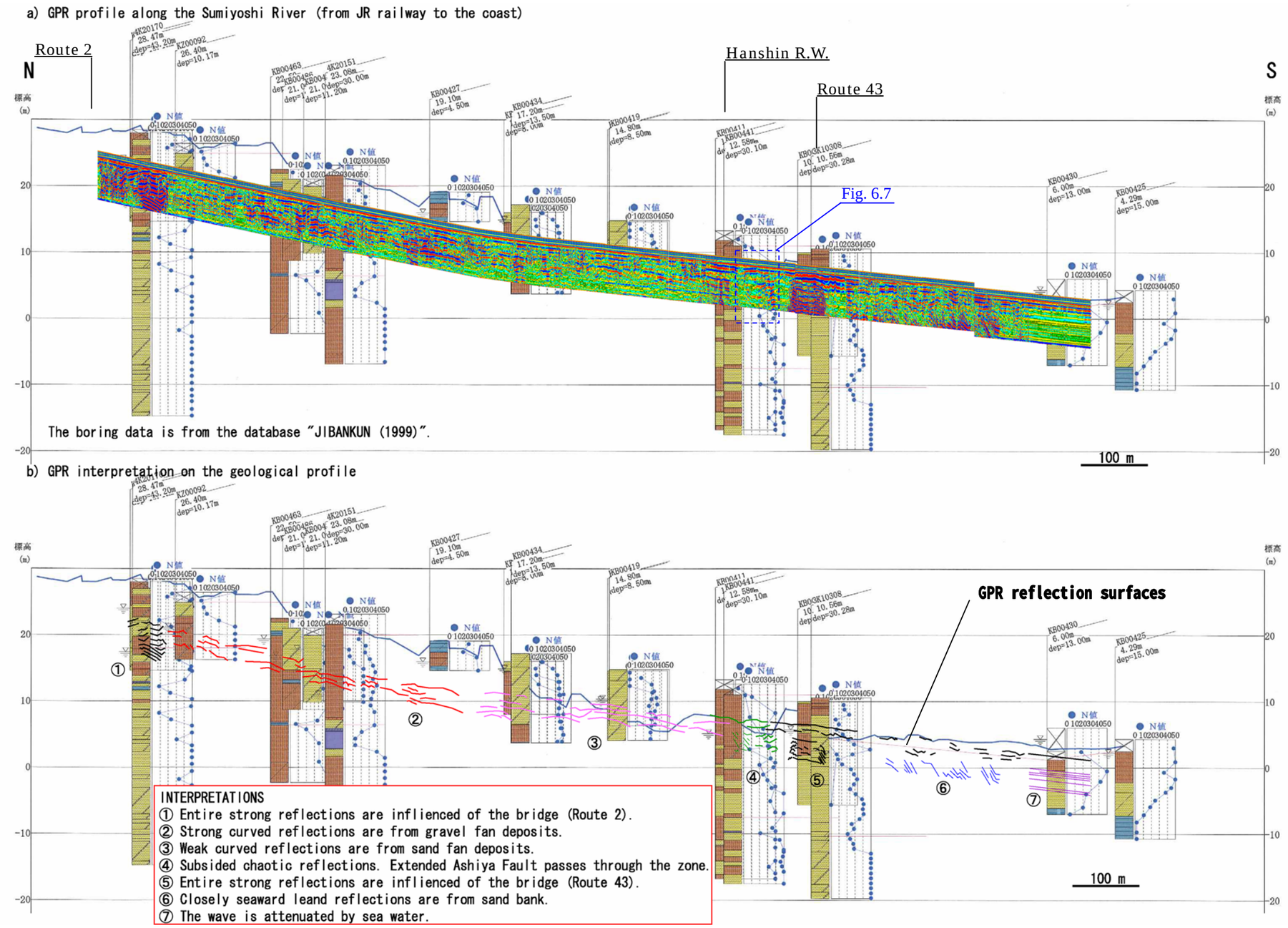

Fig.5.4 GPR survey profile. Southern part of the Sumiyoshi River section. The boring data were from the database ‘KOBE JIBANKUN’ (Kobe City, 1999).

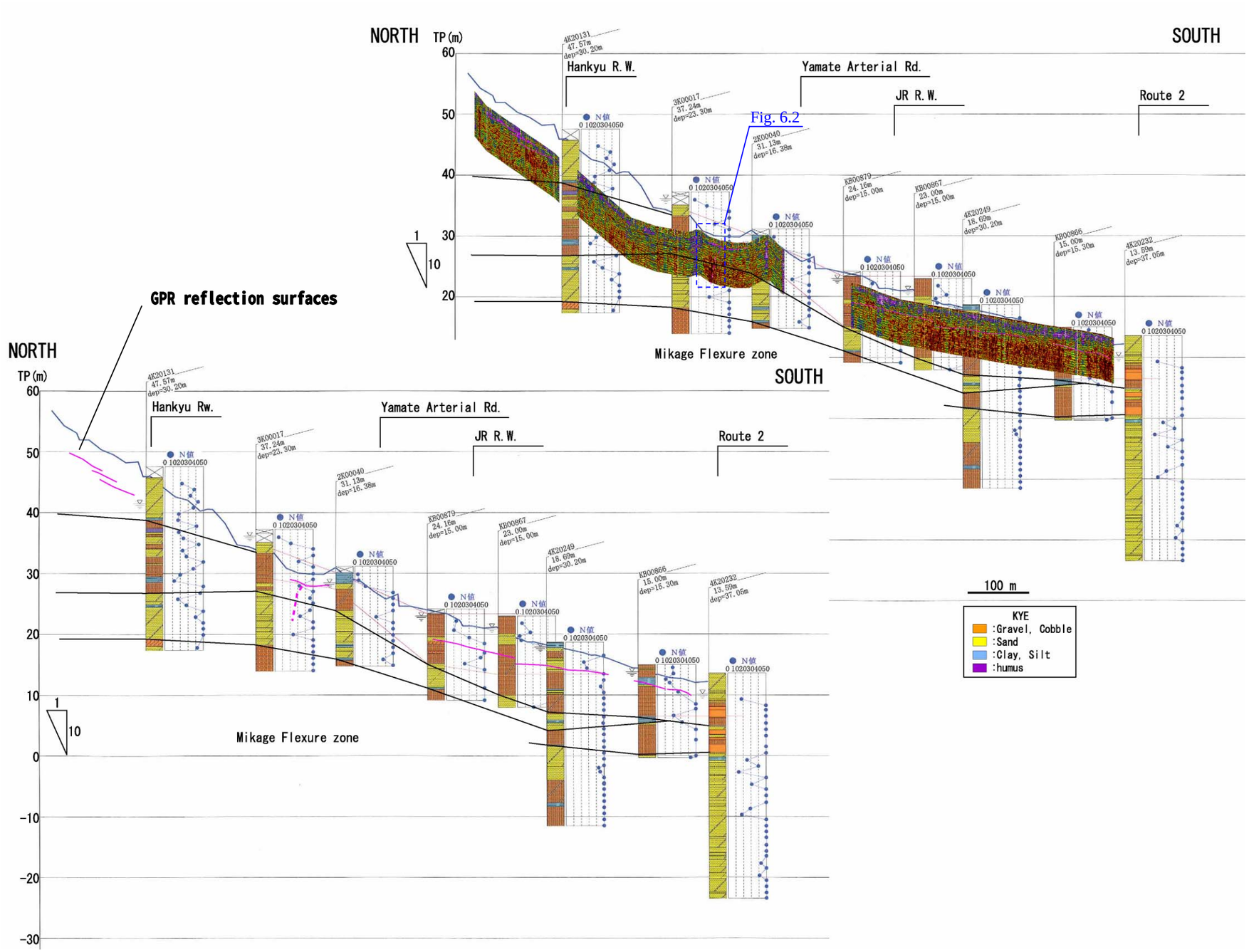

Fig.5.5 GPR survey profile. Northern part of the Ishiya River section. The boring data were from the database ‘KOBE JIBANKUN’ (Kobe City, 1999).

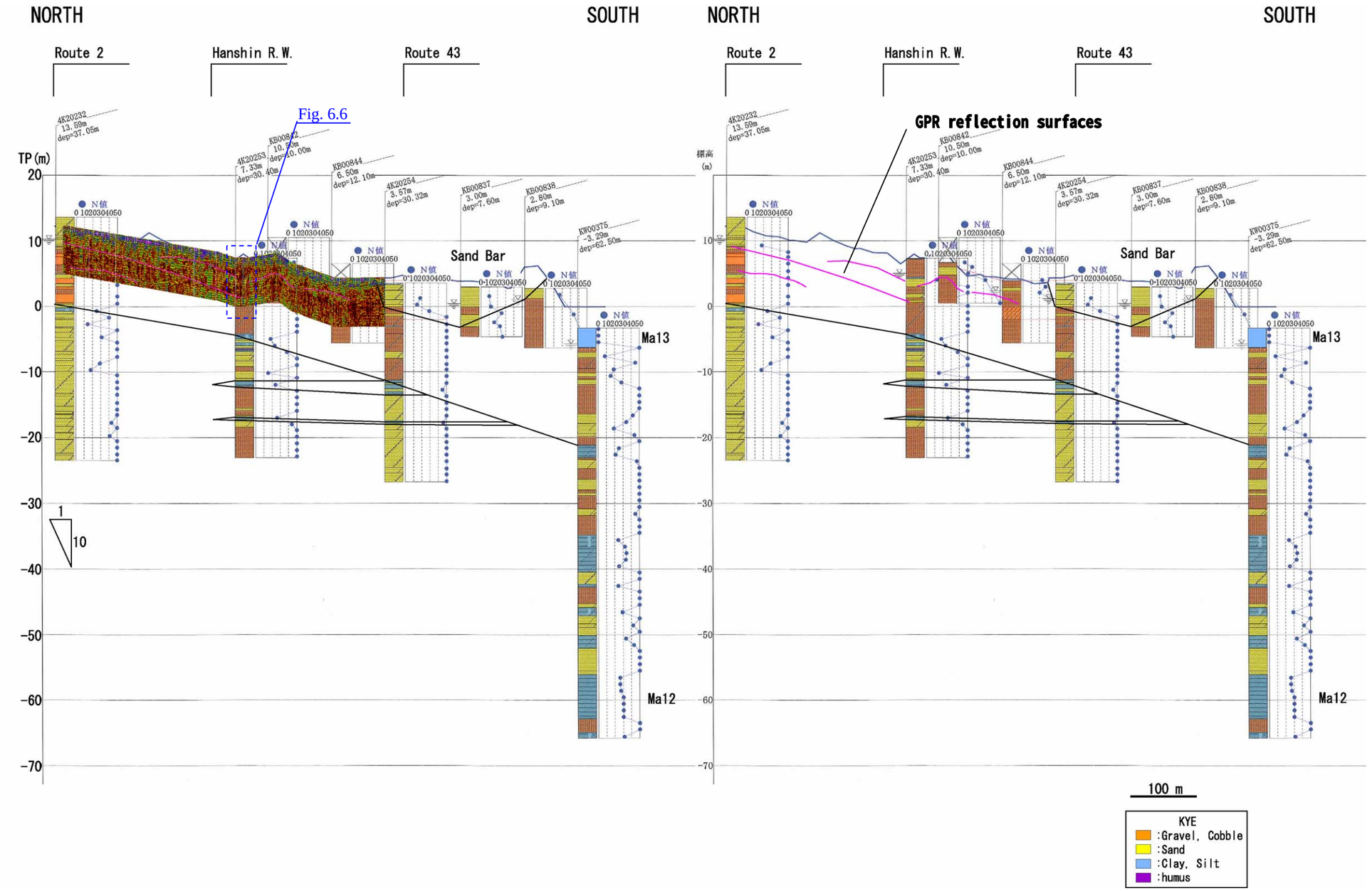

Fig.5.6 GPR survey profile. Southern part of the Ishiya River section. The boring data were from the database ‘KOBE JIBANKUN’ (Kobe City, 1999).

6. Discussion

6.1 Concealed faults in the urban area of eastern Kobe

Some concealed faults have been analyzed on the seismic reflection survey profiles. Along the Toga River, two faults, TF1 and TF2 have been found under the urban area (Line TR in Fig. 6.1). The TF2 fault was considered the Wadamisaki fault which is one of the splay faults of the Osakawan fault zone. But the TF1 fault was not determined the relations with other faults. Along the Ishiya River section, the IF1 fault has been clearly imaged with the Mikage flexure zone. The Mikage flexure zone was also imaged in the subsurface geological section along the Ishiya River (Fig. 5.5).

The IF1 fault has been connected to the TF2 fault (the Wadamisaki fault). The existence of another fault at the south of the IF1 fault has not detected because the Ishiya River seismic reflection survey line has not been extending to the coast line (Fig. 6.1 Line IR). In this study, the GPR survey provided the subsurface structure information (Fig. 5.6).

Miyata *et al.* (2006) reported a new found active fault which extends from northeast to southwest between the Gosukebashi fault and the Ashiya fault in the Rokko Mountains. The fault was named as the Yahatadani fault. It has been traced to the southwestern direction in the urban area using GPR surveys. The further extension crosses the GPR line of the northern Sumiyoshi River (Fig. 5.3) and the southern Ishiya

River (Fig. 5.5), and reaches to the TF1 fault.

From the distributions of the subsurface clay layer discontinuity (Fig. 4.1) the Ashiya fault is considered to extend southwestward to the urban area. The estimated line crosses the southern Sumiyoshi River GPR section (Fig. 5.4). But along the Juniken Road seismic reflection survey section (Line Ju in Fig. 6.1), any concealed faults have not be found in the urban area. The faults have been detected only at the north of the section (The F1 and the F2 in Fig. 6.8c). They are near the southern edge of the Rokko Mountains.

6.2 GPR images of a concealed fault

Fig. 6.2 shows a detailed GPR analysis along the Ishiya River on the Mikage flexure zone. The position is shown in Fig. 5.5. The curvature of the flexure became large around there. The characteristic anomaly appeared in the dark zone at the middle lower section. The lines are read as upward branched shape. The discontinuities of beds are identified to around the depth of 2.5 m.

The extension of the Yahatadani fault was estimated on two anomalies in the GPR profile along the Sumiyoshi River (Figs. 6.3 and 6.4). The position is shown in Fig. 5.3. The layer of strong reflection had a gap of elevation at the distance of eighteen meters in Fig. 6.3. That type of image is similar to a vertical displaced fault.

Several inclined reflections to north were seen in Fig. 6.4. They have

an opposite direction of the slope. The connection of layers were deformed or cut near the inclined reflections. The structures are considered to the interaction of the reverse fault movements and the soft sediments.

The two GPR imaged deformations are thought to have a same root. The interpretation of the flower structure is shown in Fig. 6.5. The fault was analyzed as single line on the seismic reflection profile at the depth of over three hundred meters (Fig. 6.5). The discontinuities of reflectors were sharply identified. But the shallower zone, the reflection patterns represented flexures. The estimated deformed zone on the fault has the width of about two hundred meters. It is impossible to read such the detail deformation only from a seismic reflection survey profile. GPR images provide useful information to assess an active fault especially in an urban area where a trench excavation research is difficult.

The southern part of the Ishiya River is between the TF1 fault and the extension of the Yahatadani fault. The estimated fault passes around the middle of the image in Fig. 5.6. At the southern part of the profile, two continuous clay layers were detected from the boring data at least the southern part of the Hanshin Railway. On the other hand, the GPR reflections were relatively continuous at the northern part of the profile. Several vertical dark lines were shown in the GPR image in Fig. 6.6. The type of anomaly is similar to the image of the Mikage flexure zone in Fig. 6.2.

The extension of the Ashiya fault passes between fan sediment area

and sand bar sediment area in the southern Sumiyoshi River section (Fig. 5.4). The confused reflections were shown in the distance 10 to 20 m at the time of 50 to 150 ns (Fig. 6.7). They are analyzed as filling deposits in cracks. That type of reflections was also seen around the distance 30 m at the time of 100 ns. At the ground surface the inclination of the river was changed around the distance of 28 m and the steps were putted on the river bed. The both sides of river revetments were repaired approximately after the 1995 Kobe Earthquake (Plate 6.1). There is a possibility that these features are related the strong movement during the Kobe earthquake, trapped through the concealed fault.

6.3 The problem of the extension of the Ashiya fault and the Juniken Road seismic reflection profile

In the previous studies, the Ashiya fault was thought to be continued to the Okamoto fault (e.g. Okada and Togo, 2000) along the southern border of the Rokko Mountains, because a concealed fault was not analyzed under the urban area from the seismic reflection survey (Yokota *et al.*, 1997, Fig. 6.8c) along the Juniken Road (line i-j in Fig. 6.8a). In the profile, continuous reflectors between the depths 0 to 700 meters were identified as marine clay layers of the Osaka Group. The Ma0 and Ma1 layers were analyzed from the coast line to the location around 2,200 m. And the Ma3 to Ma10 layers were analyzed almost entirely the profile near the faults F1 and F2.

Fig. 6.8b shows the layer section estimated between two deep boring GS-K1 (Geo-Research Institute, 1998) and HG-A (Takemura *et al.*, 1997). In the boring GS-K1 all the marine clay layers of the Osaka Group were detected. The upper parts from the Ma9 to Ma12 layers are shown in Fig. 6.8b. On the other hand, the HG-A detected only one marine clay layer. The Ma number was uncertain, but concerning about the seismic reflection survey profile, the layer was considered as Ma9 (Takemura *et al.*, 1997). The thicknesses of the Ma9 layer were 25.4 m at the GS-K1 point and 4.38 m at the HG-A point. They were thought to be gradually thin to the north. And upper marine clay layer (Ma10, Ma11 and Ma12) were not distributed at the HG-A point.

A seismic reflection survey method is good at to image the shapes of layers. But it is difficult to read gradual thickness changes of layer because of its resolution. The reflection surface from the Ma10 layer was thought to be continued through the profile near the fault F2 (Fig. 6.8c). But actually the Ma10 layer was changed to the terrace sediments depend on the boring data (Fig. 6.8b). It indicates that a continuous reflection surface is not always represented a same layer geologically. Both geological and geophysical information are needed to determine a concealed fault. This problem proposes the difficulty of detecting fault using seismic reflection surface shapes.

I insist the possibility of the existence of a concealed fault across the Juniken Road seismic reflection line around the distance 2,200 m from geological data and the anomalies on GPR images. In addition the base

rock line was kinked under the point (Fig. 6.8c). The strike of fault was estimated northeast to southwest same as the other faults in the eastern Rokko Mountains (Fig. 6.8a). It was estimated a right-lateral strike-slip fault under the east-west-directional regional crustal stress. If a fault plane has a nearly vertical fault plane and a dominant strike-slip component rather than dip-slip component, the fault is generally difficult to appear on the seismic reflection profile.

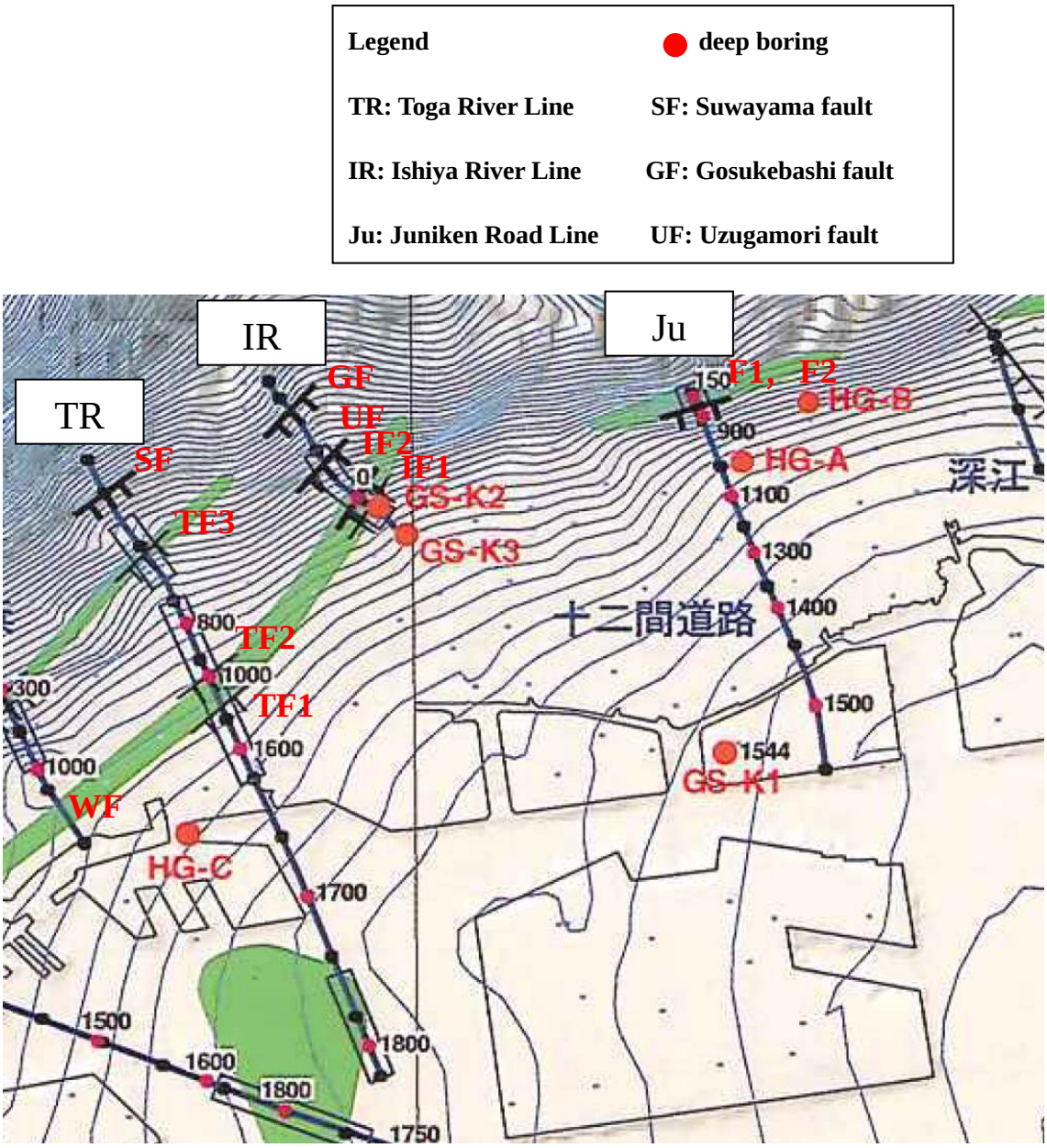

Fig. 6.1 Distribution of faults detected by seismic reflection surveys. The base map was after Geo-Research Institute (1998).

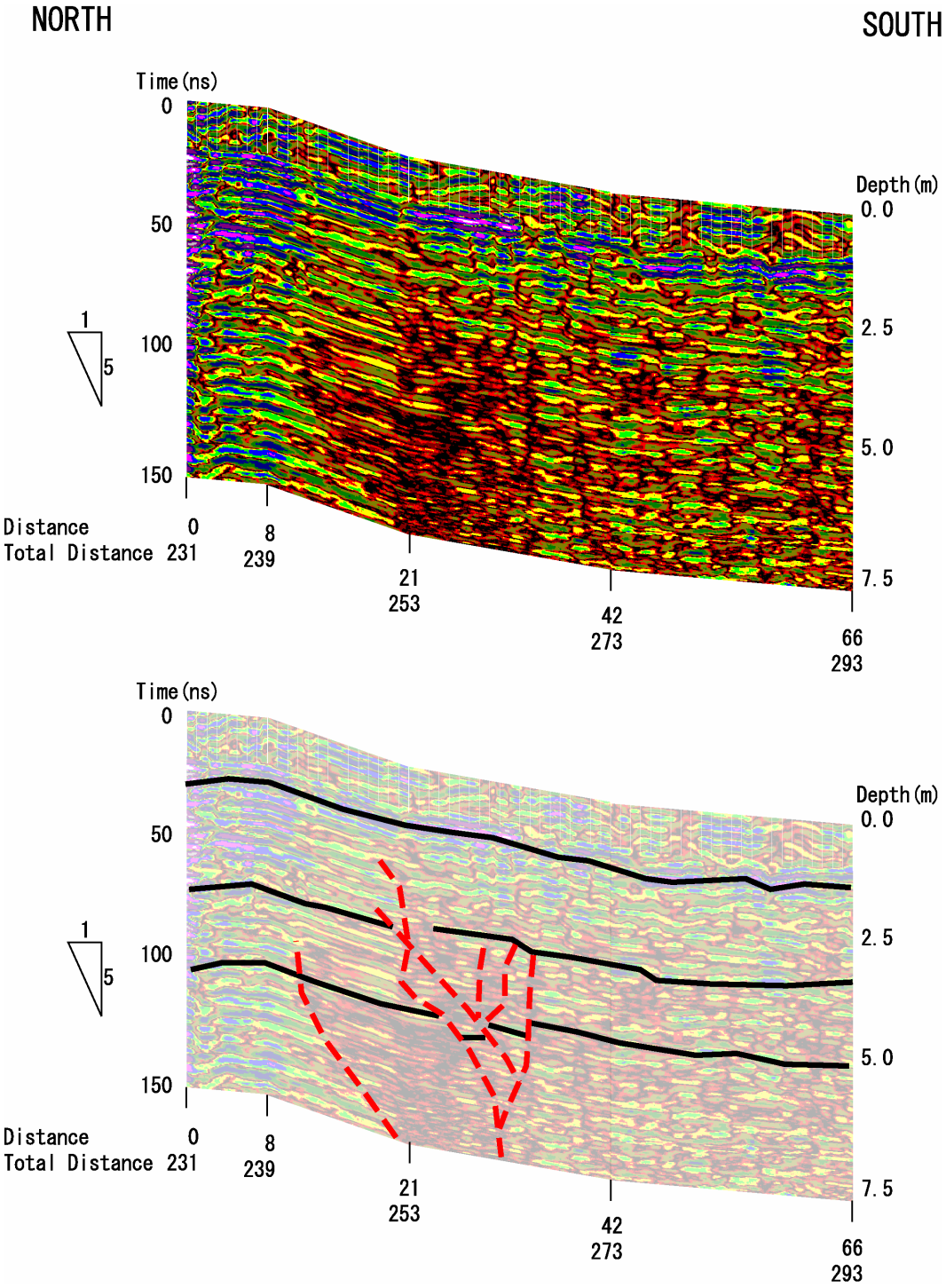

Fig. 6.2 The GPR image on the Mikage flexure zone. The position is shown in Fig. 5.5.

NORTH SOUTH

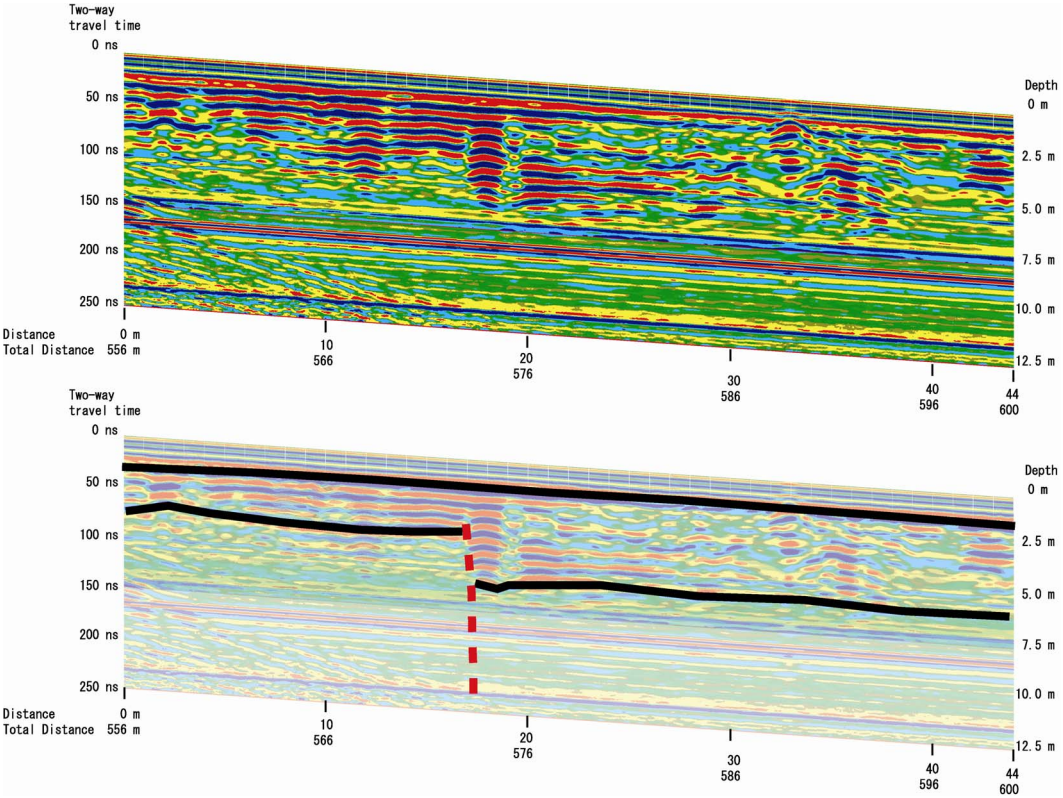

Fig. 6.3 The GPR image from the northern part of the Sumiyoshi River. The position is shown in Fig. 5.3. The red dotted line is the interpretation of the extension of the Yahatadani fault. Strong straight lined reflections around 150 ns, 170ns and 230ns are irremovable mechanical noises.

NORTH SOUTH

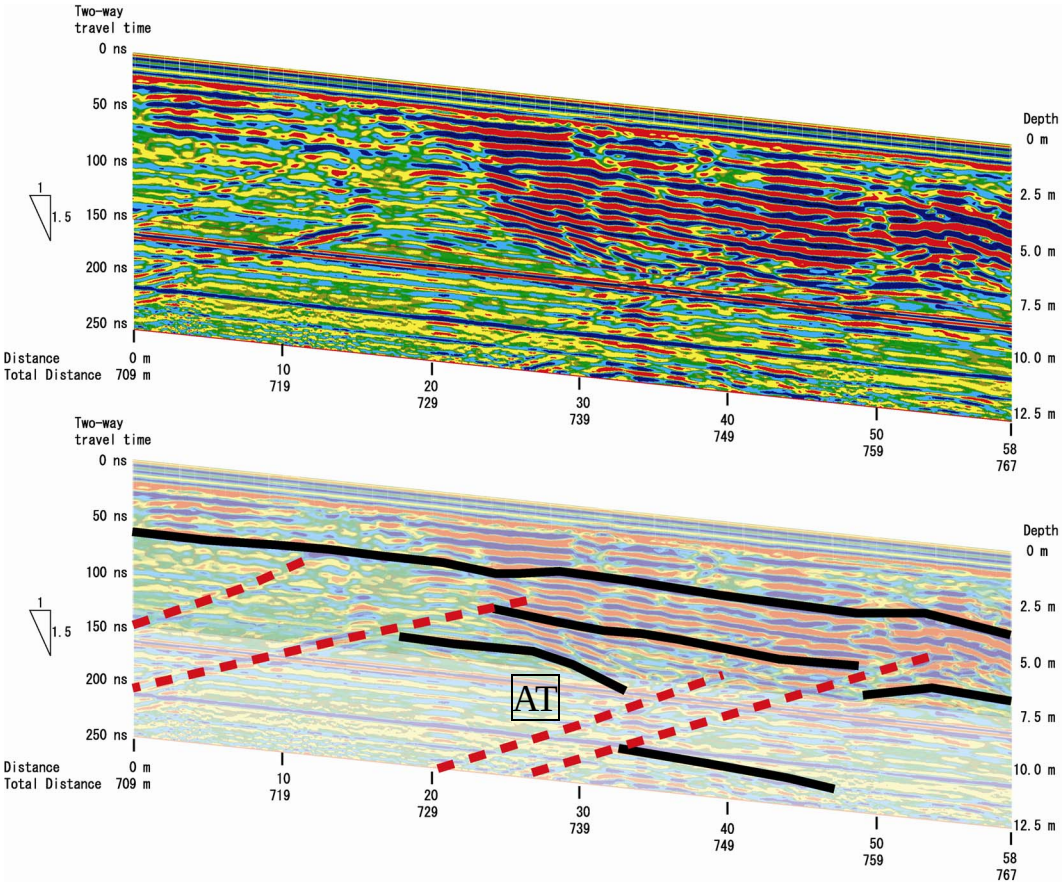

Fig. 6.4 The GPR image from the northern part of the Sumiyoshi River. The position is shown in Fig. 5.3. The red dotted lines are the interpretation of the extension of the Yahatadani fault. AT indicates the Aira-Tanzawa tephra from boring data in Fig. 5.3. Strong straight lined reflections around 170ns and 220ns are irremovable mechanical noises.

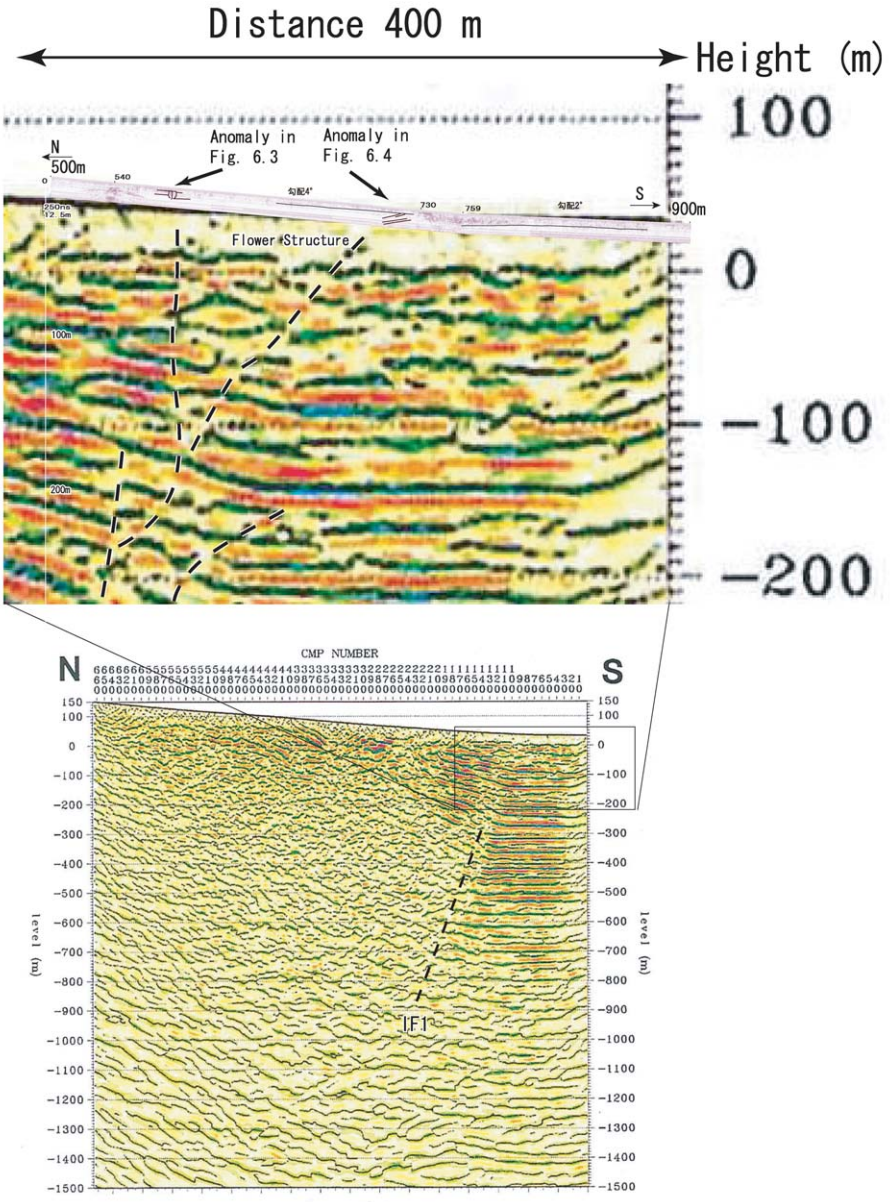

Fig. 6.5 The GPR image on the seismic reflection profile. The GPR image covers the anomaly zone in Figs. 6.3 and 6.4. The seismic reflection profile is line IR in Fig. 6.1.

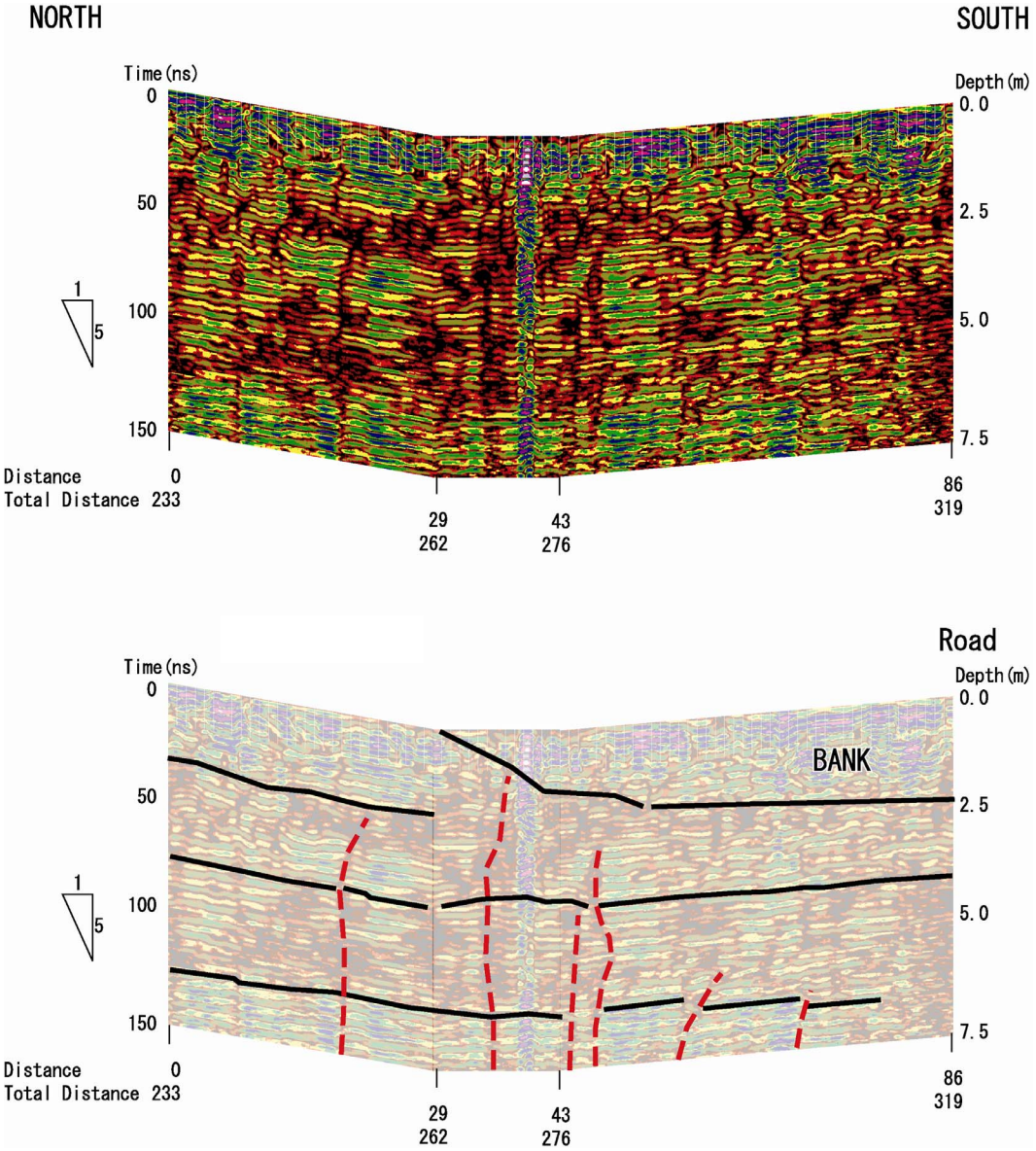

Fig. 6.6 The GPR image from the southern part of the Ishiya River. The position is shown in Fig. 5.6. The red dotted lines are the interpretation of faults between the TF1 fault and the Yahatadani fault.

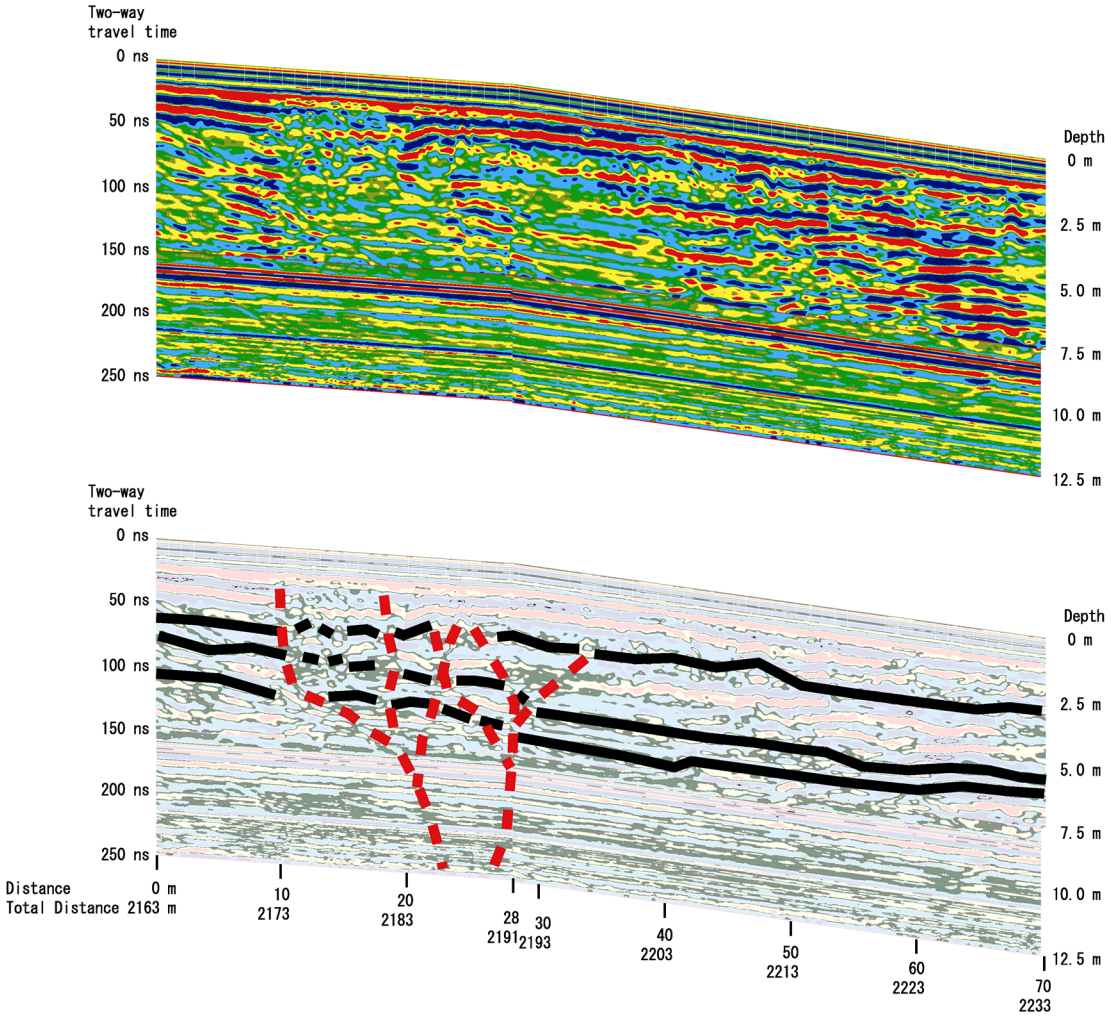

Fig. 6.7 The GPR image on the extension of the Ashiya fault. The position is shown in Fig. 5.4. Strong straight lined reflections around 170ns and 220ns are irremovable mechanical noises.

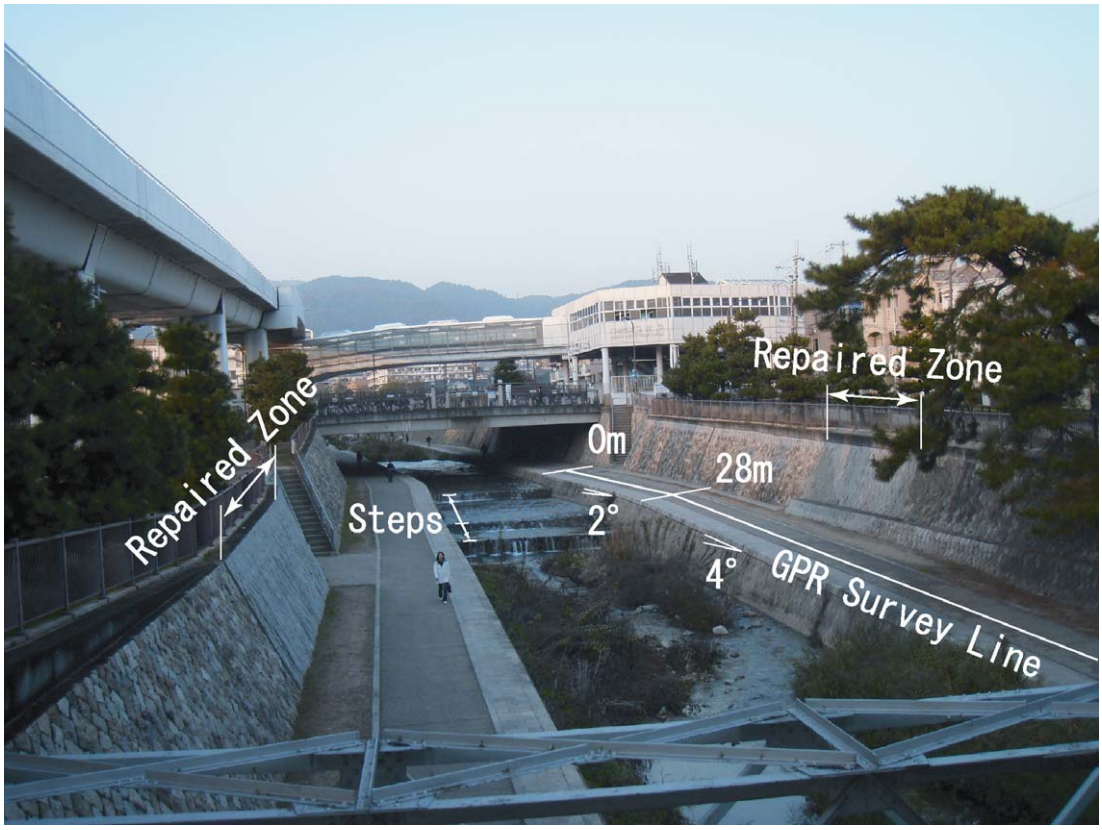

Plate 6.1 The situation around the survey area in Fig. 6.7.

Fig. 6.8 The Reinterpretation of the seismic reflection line along the Juniken Road. a) The map of fault position. The Okamoto fault was written in Okada and Togo, 2000. The Yahatadani fault was supposed to be continued to the F2 fault on the line i-j (Miyata *et al.*, 2006). b) The geological layer section from deep borings. The Ma9 layer in HG-A was estimated by Takemura *et al.*, 1997. c) The seismic reflection line along the Juniken Road. The interpretations of Ma0, Ma1, Ma3, Ma5, Ma7 and Ma10 were from Yokota, *et al.* (1997). The line of Ma9 was added by author.

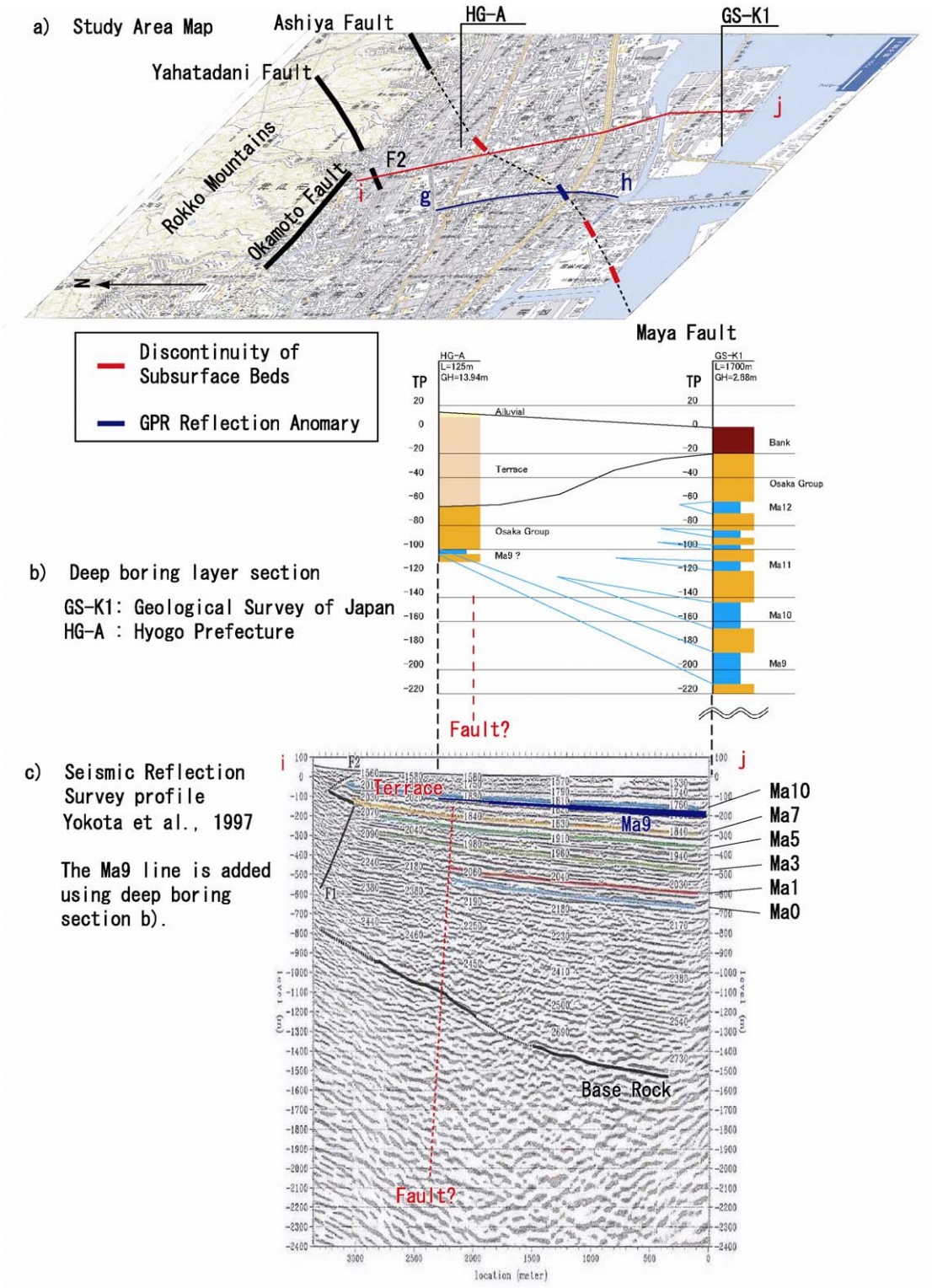
a) Study Area Map
Ashiya Fault
HG-A
GS-K1
Yahatadani Fault
Rokko Mountains
Okamoto Fault
F2
i
g
h
j
N
Maya Fault
Discontinuity of Subsurface Beds
GPR Reflection Anomary
b) Deep boring layer section
GS-K1: Geological Survey of Japan
HG-A : Hyogo Prefecture
HG-A
L=125m
GH=13.94m
GS-K1
L=1700m
GH=2.88m
TP
Alluvial
Terrace
Osaka Group
Ma9 ?
Bank
Osaka Group
Ma12
Ma11
Ma10
Ma9
Fault?
c) Seismic Reflection Survey profile
Yokota et al., 1997
The Ma9 line is added using deep boring section b).
F1
F2
Terrace
Ma9
Ma10
Ma7
Ma5
Ma3
Ma1
Ma0
Base Rock
Fault?
location (meter)

7. Conclusions

The relationship between the Rokko-Awaji fault zone and the Osakawan fault zone in the eastern urban area of Kobe was discussed in this paper, based on the following geological records and GPR survey results;

(1) The Rokko Mountain side was rising after middle Pleistocene. The rate was constant around 0.08 m/kyr. It is not large because the fault movements are estimated mainly right-lateral strike-slip but their fault movements have been accumulating. The movements are harmonized with a present topography.

(2) The existence of an active concealed fault between the Ashiya fault and the Maya fault was estimated from Holocene clay layer's discontinuities in the layer sections created from boring database. The detected faults were arranged in northeast to southwest direction. The main movement is expected to be right-lateral strike-slip because of the stress field in southwestern Japan.

(3) GPR images on the concealed faults appeared with the next features. 1. Branch to upward shape, 2. Reflectors level gap, 3. Dark colored vertical cracks and 4. Gentle inclined reflections against the slope. These features are thought to be the effects of the past fault movements.

Judging from these data, the Rokko-Awaji fault zone and the Osakawan fault zone are supposed to be closely related. At least three

concealed faults are estimated in the urban area between the two fault zones. These faults are arranged in Fig. 7.1. They distribute like step faults which are located near the center of Kobe (inside 10 km circle). These faults have to be considered for prevention of urban earthquake disasters in Kobe.

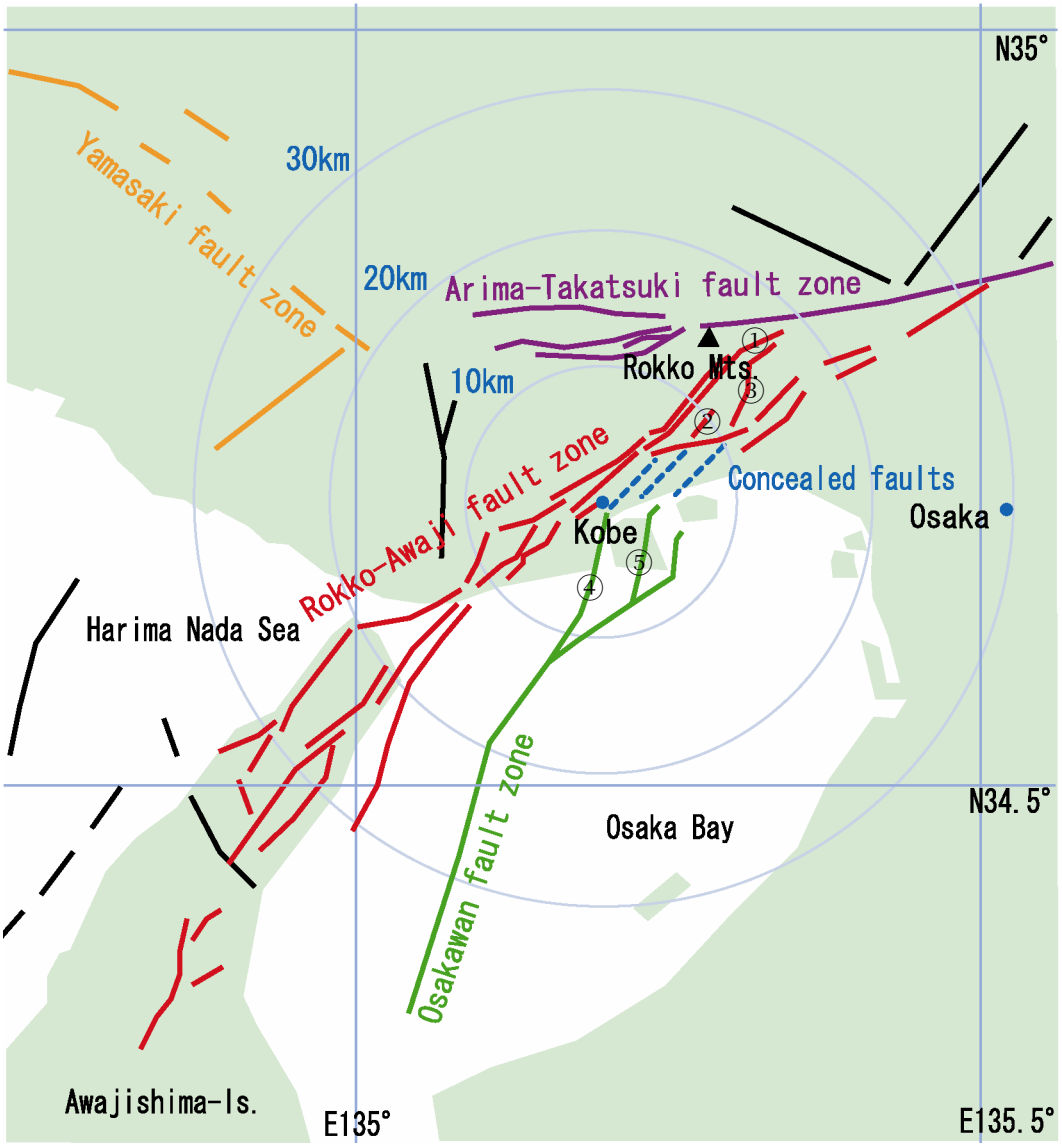

Fig. 7.1 Distribution of active faults around Kobe area. Blue dotted lines indicate concealed faults which were surveyed in this study. The fault names are as follows. ① : Gosukebashi fault, ② : Yahatadani fault, ③ : Ashiya fault, ④ : Wadamisaki fault, ⑤ : Maya fault.

Acknowledgements

This study was partly supported by a Grant-in-Aid for Scientific Research from Japanese Ministry of Education and Science, Japan (Project no. 16340154) and the fund form the Research Center for Urban Safety Security, Kobe University.

I wish thank Prof. T. Miyata for proper advices and helpful supports for all part of this study. Ms A. Hirai and Mr. S. Ueoka assisted very kindly in my field works of GPR survey. All members of tectonics seminar gave useful suggestions through discussions.

I wish thank the Eight Consultants co. ltd. for the permission of the study. My daily routine had been always supported with my workmates especially in Kansai branch.

References

Geo-Research Institute, 1998: The new Kansai basement –between Kobe and Hanshin area-, 270p (in Japanese)

Huzita, K., Kasama, T., 1982, Geology of the Osaka-Seihokubu district. Quadrangle Series Scale 1:50,000, Geol. Surv. Japan, 112p. (in Japanese with English abstr.)

Huzita, K., Kasama, T., 1983, Geology of the Kobe district. Quadrangle Series Scale 1:50,000, Geol. Surv. Japan, 115p. (in Japanese with English abstr.)

Huzita, K., Maeda, Y., 1984, Geology of the Suma district. Quadrangle Series Scale 1:50,000, Geol. Surv. Japan, 101p. (in Japanese with English abstr.)

Ichihara, M., 1993, The Osaka Group, 340p. (in Japanese)

Iwabuchi, Y., Nishikata, H., Noda, N., Yukimatsu, T., Taga, M., Miyano, M., Sakai, K. and Fukazawa, M., 2000: Basement and Active Structures Revealed by the Seismic Reflection Survey in Osaka Bay. *Report of Hydrographic Researches*, **36**, 1-23. (in Japanese with English abstr.)

Katoh, S., Okada, A. and Sangawa, A., 2008: Active faults in the Rokko Mountains, Awaji Island and Osaka Bay area, and Quaternary development of the Osaka and Harimanada sedimentary basins, western Japan. *The Quaternary Research*, **47**, (4), 233-246. (in Japanese with English abstr.)

Kobe City, 1999. Geological database ‘KOBE JIBANKUN’ URL:

http://www.kobe-toshi-seibi.or.jp/matisen/jibankun/index.htm

Lin, A., Maruyama, T. and Miyata, T. (1998): Paleoseismic events and the 1596 Keicho-Fusimi large earthquake produced by the slip on the Gosukebashi fault at the eastern Rokko Mountains, Japan. *The Island Arc*, **7**, 621-636.

Machida, H. and Arai, F., 1978. Akahoya Ashi – A Holocene Widespread Tephra Erupted from the Kikai Caldera, South Kyusyu, Japan. *Quaternary Research*, **17**, 3, 143-163. (in Japanese)

Miyata, T., Nigauri, Y., 2008, Assessment of an urban active fault using GPR, Eastern Kobe Japan. AOGS2008, SE84-D5-PM2-102-012, CD-Rom.

Miyata, T., Tanaka, K., and Ishibashi, K., 2006., Preliminary report of the GPR survey for a newly-found hidden fault beneath the Juniken road, Higashinada-ku, Kobe –Connection of the active faults in between the Rokko Mountains and the Osaka Bay-., Report of Research Center for Urban Safety and Security Kobe University March 2006. 255-262. (in Japanese)

Nigauri, Y. and Miyata, T., 1998: Distribution of impulsive force from deformed house inlets in Kobe during the 1995 Southern Hyogo Prefecture Earthquake, *Jour. Geol. Sci. Japan*, **104**, 199-209. (in Japanese with English abstr.)

Nigauri Y. and Miyata T., 2008. Importance of the Active fault Researches for effective earthquake risk management. Proc. of Society for Social Management Systems –Infrastructure and Environment 6-8 March 2008 Kochi, Japan, SMS08-132,

CD-Rom and Internet.

Okada, A., and Togo, M., 2000. Active Faults in Kinki District. University of Tokyo Press, Tokyo. (in Japanese)

Shimamoto, T., 1995: The mystery of seismic disaster zone., *Kagaku*, **65**, 195-198. (in Japanese)

Takemura, K., Katoh, S., Inoue, Y., Ishizawa, K., Ohshika, A., Herai, M., Nojiri, S., Danhara, T., Hayashida, A., and Sano, M., 1997. Stratigraphy of subsurface sediments in the south of Rokko Mountains –Drilling samples from Maya Wharf and Higashinada, Kobe City, Japan-. The Museum of Nature and Human Activities, Hyogo Prefecture, ed., The great Hanshin-Awaji earthquake and the Rokko tectonics, The report of active structures in the seismic zone of the Hyogo-ken Nanbu earthquake, 10-56. (in Japanese)

The Headquarters for Earthquake Research Promotion, 2005: The long term assessments of the Osaka-wan fault zone, 17p. (in Japanese)

The Headquarters for Earthquake Research Promotion, 2006: The long term assessments of the Rokko-Awajishima fault zone, 59p. (in Japanese)

Uchida, T., 1984: Present electromagnetic method for a fault investigation, *Butsuri-Tanko*, **37**, 69-85.

Yokokura, T., Kato, N., Yamaguchi, K., Miyazaki, T., Ikawa, T., Ohta, Y., Kawanaka, T., and Abe, S. 1998: Seismic profiling of deep geological structure in the Osaka Bay area. *Bull. Geol. Surv. Japan*, **vol. 49（11）**, p. 571-590. (in Japanese with English abstr.)

Yokokura, T., 2000: The Osakawan fault. -An active fault under the sea-. *Kagaku*, **70**, 16-18. (in Japanese)

Appendix

GPR Survey index map

Sumiyoshi River GPR Sections

調査名　　住吉川左岸地中レーダ探査

調査日　　2006/11/25　　天候:晴れ　　調査者:宮田、苦瓜　　測線No.1～7

距離	累加距離	変化点	方向	勾配（度）	地中構造物	河川構造物	橋梁	ファイル名	レンジ	ゲイン								備考
0	0				測定開始、コンクリート石畳始め	堰堤下流23m地点		9	150	-1	7	25	42	53	58			
35	35					清流の道公園に至る階段		10	250	-5	10	30	45	47	48	57	68	
68	68				堰堤始め	落差工始め												
70	70	方向勾配	S46E	2	堰堤終り													
74	74	勾配		14	暗渠始め													
77	77	勾配		10	暗渠終り													
87	87	勾配		8														
89	89	勾配		0														
100	100	方向	S40E		測定終了													
6	106	勾配		5		落差工終り		11	250									
13	113	方向勾配	S38E	4				12	150									
26	126	方向	S32E															
70	170	方向勾配	S26E	2		落差工始め												
84	184					落差工終り												
91	191				暗渠始め													
93	193				暗渠終り													
100	200	方向	S8E		測定終了													
4	204						新落合橋始め	13	150									
14	214	勾配		5				14	250									
20	220						新落合橋終り											
23	223	方向	N4E															
42	242				コンクリート石畳終り、アスファルト始め													
45	245				堰堤始め	落差工始め												
47	247				堰堤終り													
53	253	勾配		2														
60	260					落差工終り												
98	298				堰堤始め	落差工始め												
100	300	方向勾配	NS	5	堰堤終り、測定終了													
22	322					落差工終り		15	250									
57	357				堰堤始め	落差工始め		16	150									
58	358	方向	S10E															
59	359				堰堤終り													
88	388					落差工終り												
100	400	方向	S14E		測定終了													
16	416				堰堤始め	落差工始め		17	150									
18	418				堰堤終り			18	250									
53	453					落差工終り												
64	464						観音橋始め											
65	465	方向	S20E															
73	473						観音橋終り											
77	477				距離板　2.0km													
79.5	479.5				堰堤始め	落差工始め												
81.5	481.5				堰堤終り													
100	500				測定終了	落差工終り												
34	534						阪急始め	19	250									
35	535					落差工始め		20	150									
44	544						阪急終り											
55	555					落差工終り												
66	566					護岸階段始め												
73	573					護岸ブロック補修始め												
85	585					護岸階段終り												
89	589				暗渠始め													
90	590				暗渠終り													
95	595				堰堤始め	護岸ブロック補修終り、落差工始め												
97	597				堰堤終り													
100	600				測定終了													
15	615					落差工終り		21	150									
60	660				堰堤始め	落差工始め		22	150									0-10m
62	662				堰堤終り			23	250									
80	680					落差工終り		24	250									0-20m
100	700		S28E	4	測定終了													

調査名　　住吉川左岸地中レーダ探査
調査日　　2006/12/2　　天候:晴れ昼すぎ一時雨　　調査者:宮田、苦瓜　　測線No.8～15

距離	累加距離	変化点	方向	勾配(度)	地中構造物	河川構造物	橋梁	ファイル名	レンジ	ゲイン								備考
0	700							25	250	-5	10	30	45	47	48	57	68	
11	711						水管橋	26	150	-1	7	25	42	53	58			
25	725				堰堤始め													
27	727				堰堤終り													
29	729						水管橋											
30	730						水道橋始め(山手幹線)											
59	759						水道橋終り											
62	762	勾配		4			水管橋始め											
65	765						水管橋終り											
70	770					階段始め												
90	790					階段終り												
100	800				堰堤	落差工始め												
28	828					落差工終り		27	150									
30	830					道路に上る階段(前回調査基点)		28	250									
75	875	方向	S28E		堰堤始め	落差工始め		29	250	-5	10	30	45	52	52	63	75	再測定
76.5	876.5				堰堤終り													
84	884					落差工終り												
100	900																	
21	921					階段始め		30	250									
51	951					階段終り		31	150									
61	961				堰堤始め	落差工始め												
62	962	勾配		2	堰堤終り													
75	975					落差工終り												
76.4	976.4				距離板　1.5km													
100	1000	勾配		4														
5	1005					落差工		32	150									
21	1021	勾配		3				33	250									
52	1052						水管橋											
64	1064						歩道橋始め											
66	1066						歩道橋終り											
69	1069						久原橋始め											
77	1077						久原橋終り											
81	1081					ブロック補修(対岸も同様)始め												
84	1084					ブロック補修終り												
121.4	1121.4						JR始め											
	1154	勾配		2														スキップ
	1163						JR終り											
0	1163							34	250									
17	1180				堰堤始め			35	150									
18	1181				堰堤終り													
31	1194				堰堤始め													
33	1196	勾配		8	堰堤終り													
46	1209				堰堤始め													
47	1210				堰堤終り													
68	1231						水管橋											
71	1234	勾配		6			住吉橋始め(国道2号)											
86	1249	勾配		4														
99	1262						住吉橋終り											
100	1263	方向	S30E				水管橋											
10	1273					落差工始め		36	150									
16	1279					落差工終り		37	250									
22	1285					道路へ上る階段												
29	1292					階段始め												
81	1344					階段終り												
100	1363																	
36	1399					落差工始め		38	250									
42	1405					落差工終り		39	150									
47.5	1410.5				観測孔													
100	1463																	
13	1476				距離板　1.0km			40	150									
23	1486	勾配		2		落差工		41	250									
50	1513	勾配		3														
63	1526					階段始め												
78	1541					階段終り												
100	1563	方向	S14E	2														

調査名　住吉川左岸地中レーダ探査
調査日　2006/12/17　天候:晴れのち雨　調査者:宮田、苦瓜　No.16～23

距離	累加距離	変化点	方向	勾配(度)	地中構造物	河川構造物	橋梁	ファイル名	レンジ	ゲイン								備考
0	1563							42	250	-5	10	30	45	52	52	63	75	
8	1571					落差工始め		43	150	-1	7	25	38	48	58			
15	1578					落差工終り												
51	1614	勾配		2		階段始め												
74.5	1637.5					道路へ上る階段												
82	1645	勾配		0		階段終り												
88	1651						新反高橋始め											
93	1656					落差工												
100	1663	方向	S12E															
6	1669						新反高橋終り	44	150									
42	1705	勾配		2				45	250									
78	1741	勾配		0		落差工始め												
95	1758					落差工終り												
100	1763	方向	S10E															
23.65	1786.65				観測孔			46	250	-5	10	30	43	52	52	58	72	
42	1805	方向	S8E					47	150									
57	1820						反高橋始め											
66	1829	勾配		2														
73	1836						反高橋終り											
77	1840	勾配		0		落差工始め												
93	1856					落差工終り												
97	1860					道路へ上る階段												
100	1863	方向	S6E															
2	1865					道路へ上る斜路		48	150									
16	1879	勾配		2				49	250									
27	1890					階段始め												
48	1911					階段終り												
57	1920					量水標(H=3m)												
61	1924	勾配		1		落差工始め												
77	1940					落差工終り												
84	1947	勾配		2														
100	1963																	
2	1965				観測孔			50	250									
4	1967					階段始め		51	150									
13	1976				距離板　0.5km													
16	1979					橋始め												
21	1984					橋終り												
25	1988					階段終り												
29	1992					道路へ上る階段												
46	2009	勾配		1		落差工												
72	2035	勾配		2														
100	2063					階段始め												
21	2084					階段終り		52	150									
31	2094	勾配		1		落差工		53	250	-5	10	28	40	49	49	55	68	
60	2123						橋始め(阪神電車)											
98	2161						橋終り(阪神電車)											
100	2163	方向	S2W															
5	2168					道路へ上る階段		54	250									
13	2176					落差工始め		55	150									
15	2178				止水弁													
28	2191	勾配		2														
34	2197					落差工終り												
82	2245					落差工始め												
89	2252					落差工終り												
92	2255						水管橋											
95	2258						国道43号(阪神高速)始め											
100	2263																	
1	2264	勾配		4				56	150									
11	2274					階段始め		57	250									
47	2310						国道43号(阪神高速)終り											
52	2315	勾配		2		階段終り												
62	2325	勾配		4														
63	2326					落差工												
77	2340					道路へ上る階段												
87	2350					落差工												
100	2363	方向	S10W	2														

調査名　住吉川左岸地中レーダ探査
調査日　2006/12/23　天候:晴れ　調査者:宮田、苦瓜、平井　測線No.23～27

距離	累加距離	変化点	方向	勾配(度)	地中構造物	河川構造物	橋梁	ファイル名	レンジ	ゲイン								備考
0	2363							58	250	-5	10	28	40	49	49	55	68	
2.65	2365.65				観測孔			59	150	-1	7	25	38	48	58			
84	2447	方向勾配	S12W	2														
100	2463																	
13	2476				距離板　0m			60	150									土
14	2477					落差工		61	150									アスファルト
27	2490					ここから擁壁際は土		62	250									アスファルト
33	2496				観測孔													
50	2513						水管橋始め											
51	2514						水管橋終り											
80	2543	勾配		1		道は道路へ上る												
83	2546	方向勾配	S22W	-6														
0	2546					ここから矢板護岸		63	250									高さ-1m
56	2602						水管橋	64	150									
62	2608						島崎橋始め											
73	2619						島崎橋終り											
74	2620						水管橋始め											
75	2621						水管橋終り											
86	2632				観測孔													
100	2646																	
21.5	2667.5				観測孔			65	150									
80	2726				観測孔			66	250									
84	2730	方向勾配	S28W	1														道路終点

150 ns

150ns

0 101

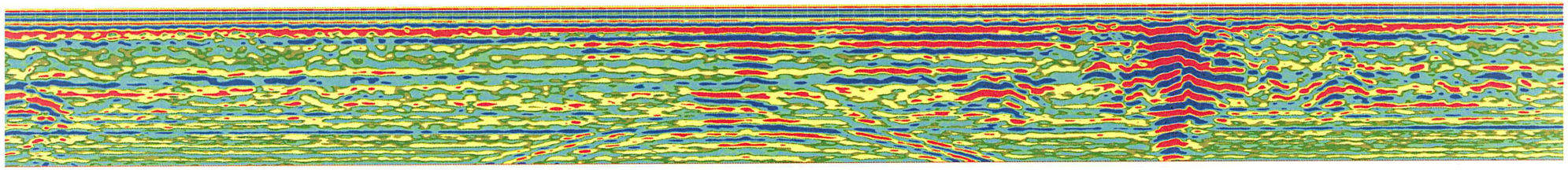

09f.bmp

100 201

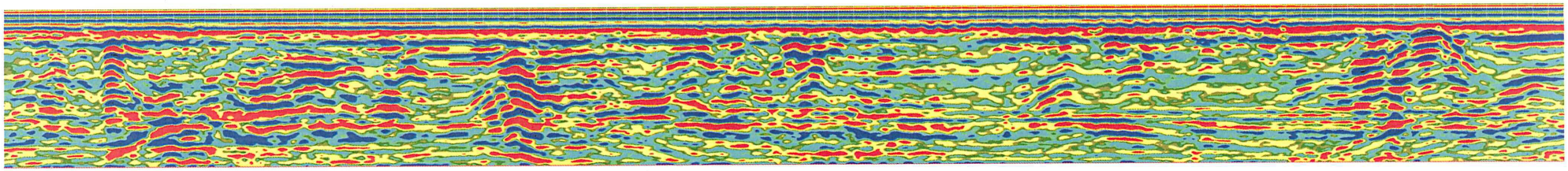

12f.bmp

200 (204-220新落合橋) 301

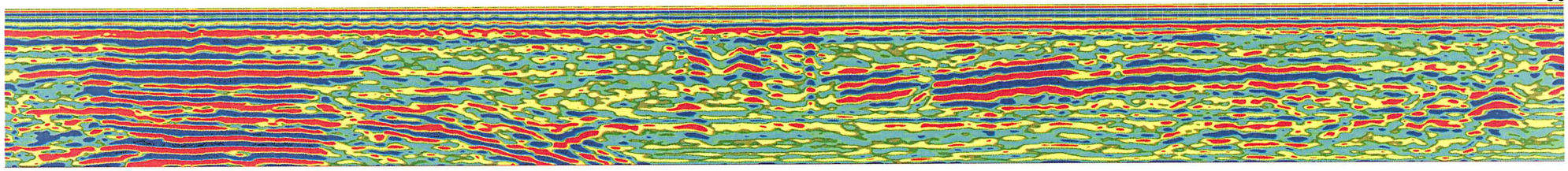

13f.bmp

300 401

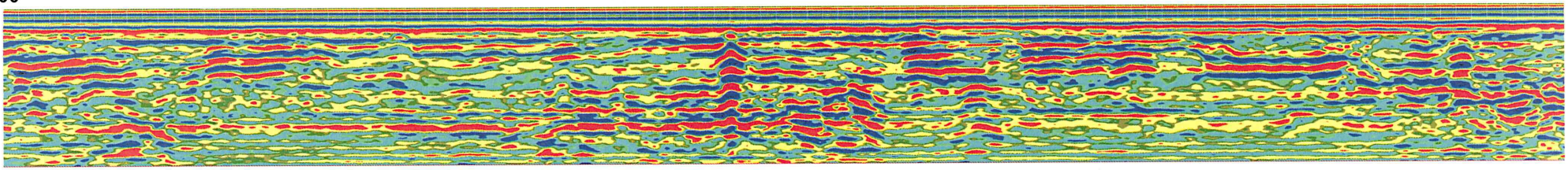

16f.bmp

150ns

400 (464-473観音橋) 501

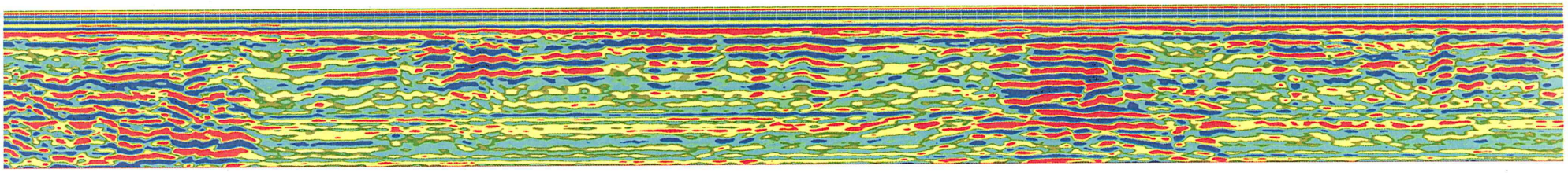

17f.bmp

500 (534-544阪急) 601

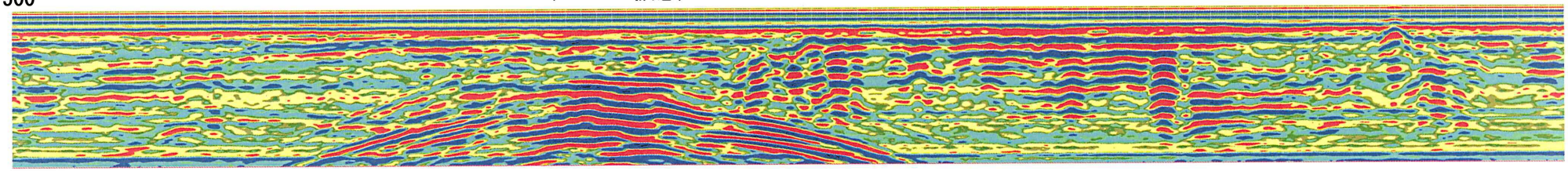

20f.bmp

600 701

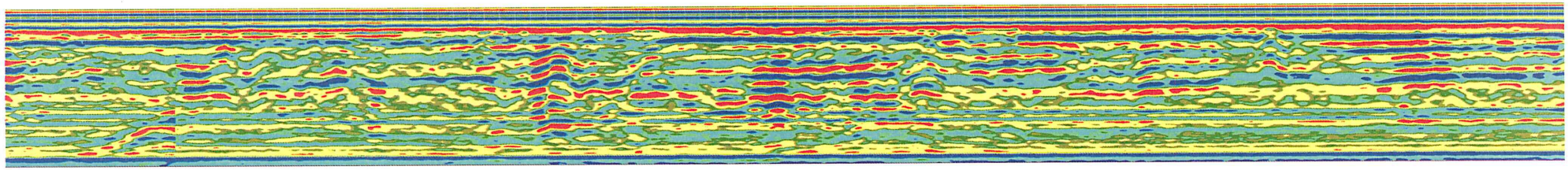

21f.bmp

711
700 水管橋 (729-765水道橋：山手幹線) 801

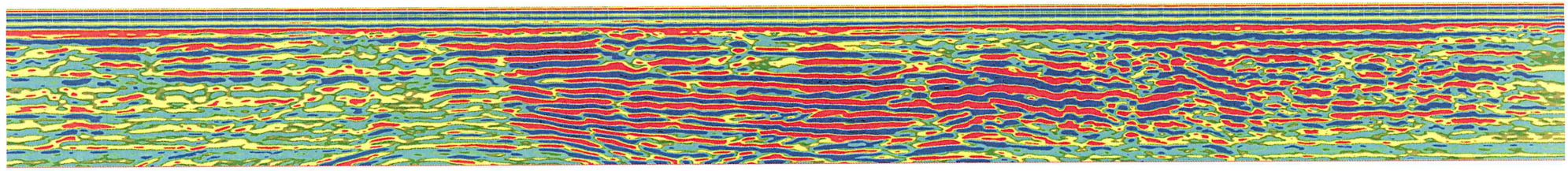

26f.bmp

150ns

800

901

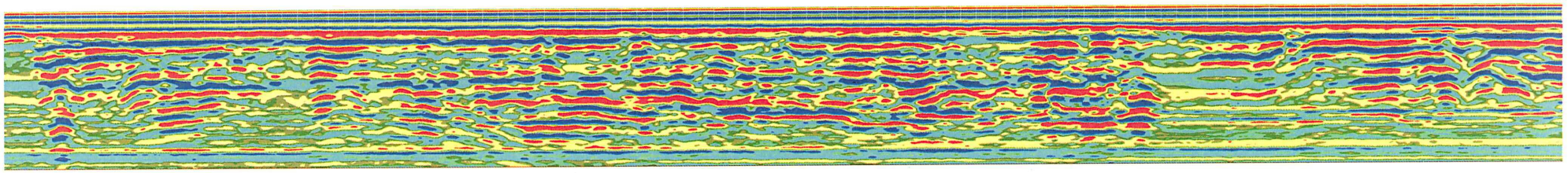

27f.bmp

900

1001

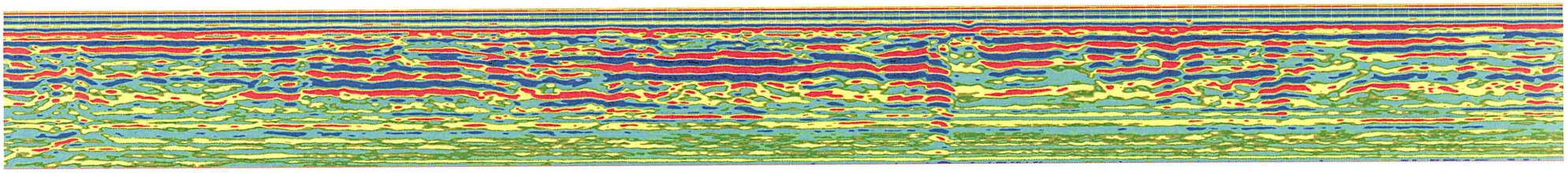

31f.bmp

1000

1052
水管橋

1064-
1066
歩道橋

1069-1077
久原橋

1123

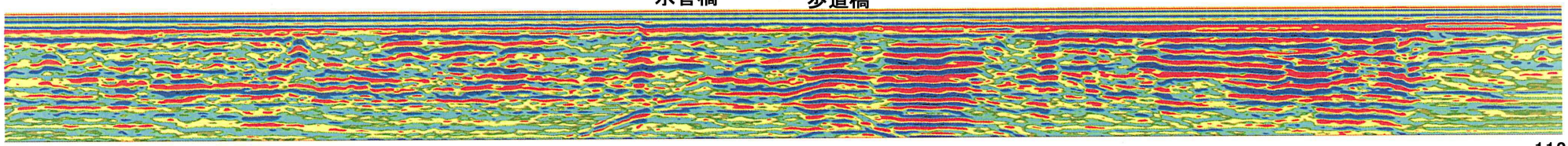

1121.4
JR

32f.bmp

1163

(1231-1263住吉橋：国道2号

)1264

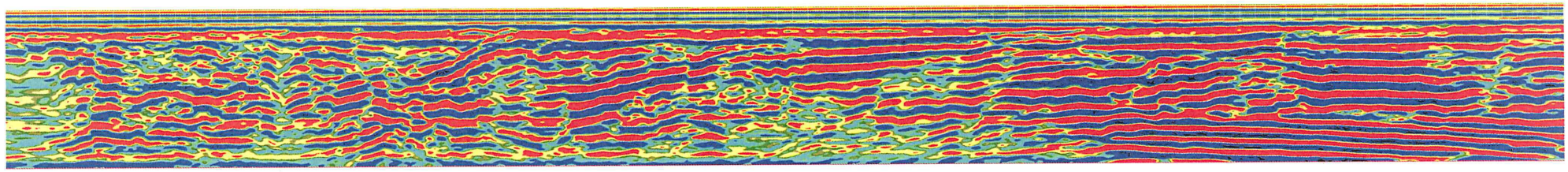

1163
JR

35f.bmp

-1263
住吉橋
国道2号

150ns

1263

1364

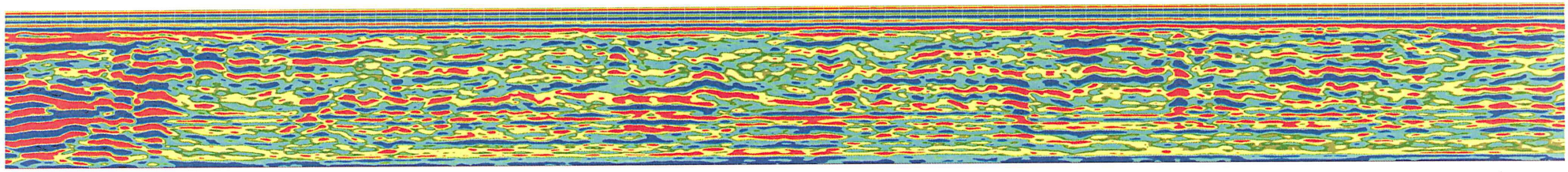

36f.bmp

1363

1464

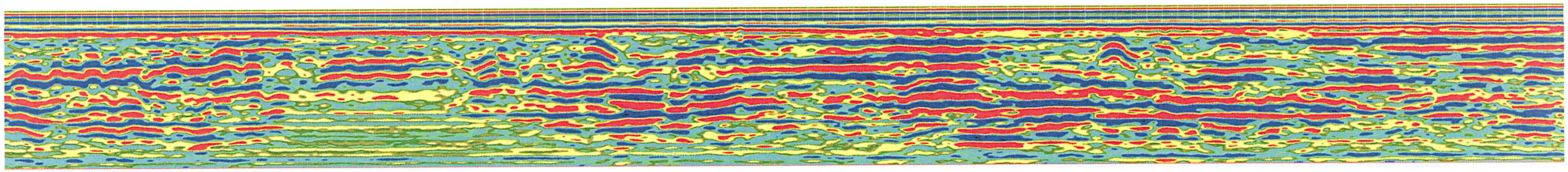

39f.bmp

1463

1564

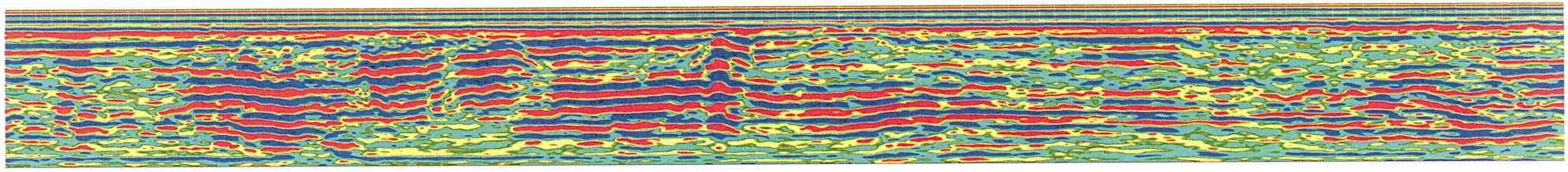

40f.bmp

(1651新反高橋　　)

1563

1664

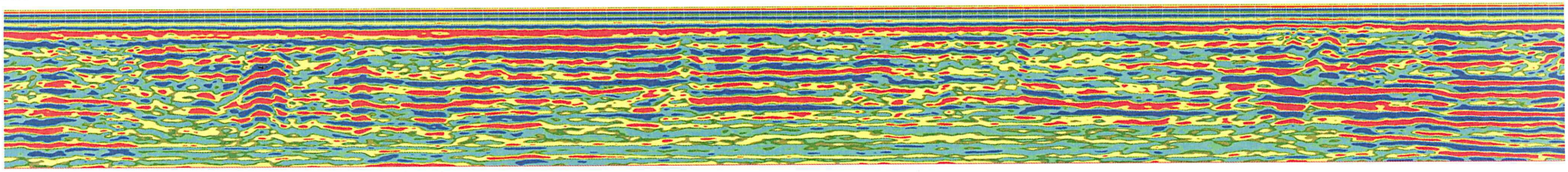

43f.bmp

150ns

-1669新反高橋）

1663

1734

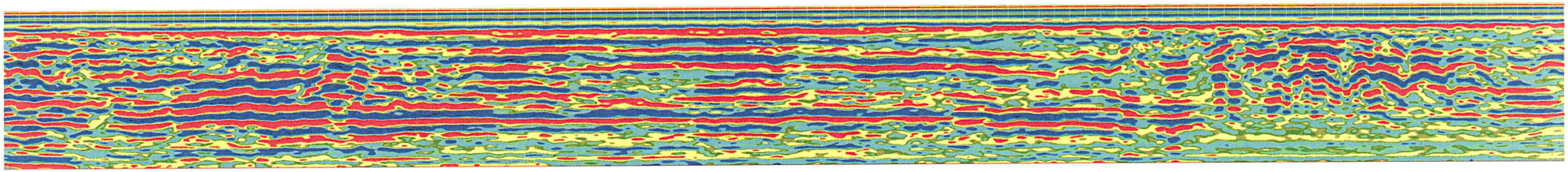

44f.bmp

（1820-1836反高橋　　）

1763

1864

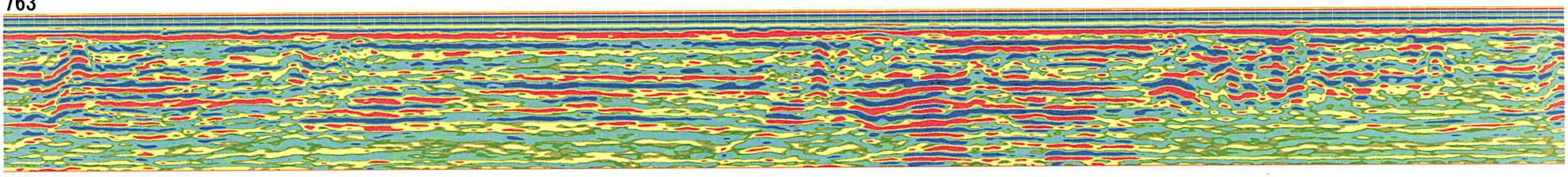

47f.bmp

1863

1964

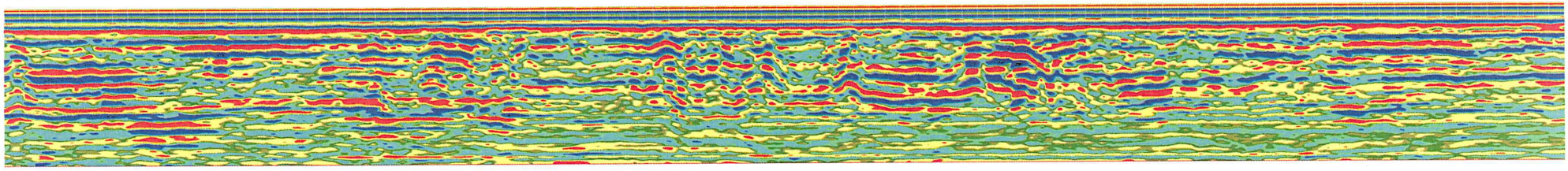

48f.bmp

1963

2064

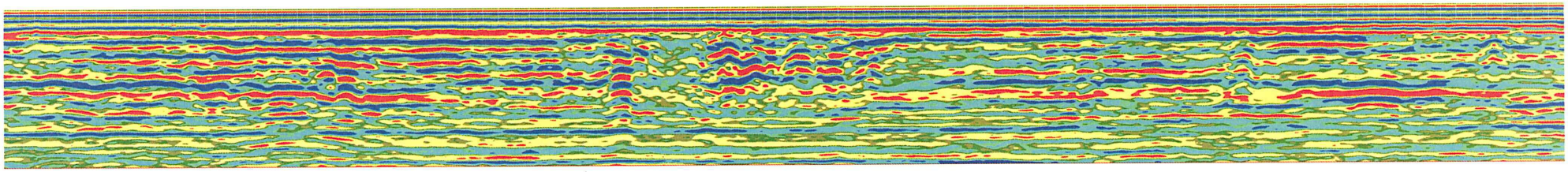

51f.bmp

150ns

2063 (2123-2161阪神電車) 2164

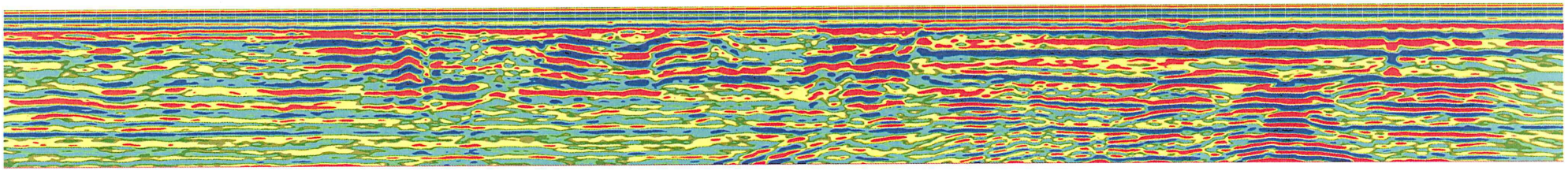

52f.bmp

(2255国道43号

2163 2264

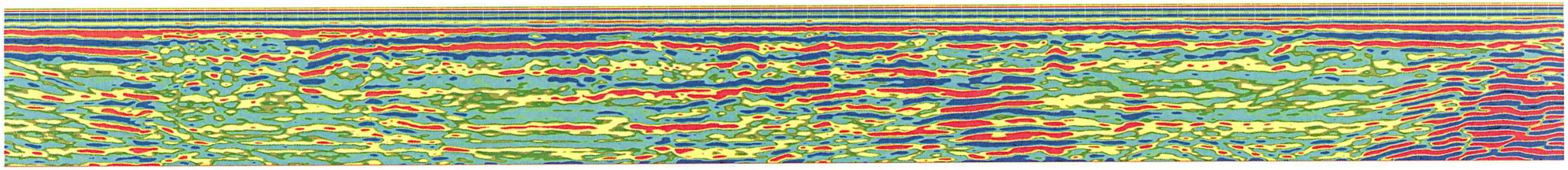

55f.bmp

-2310国道43号)

2263 2364

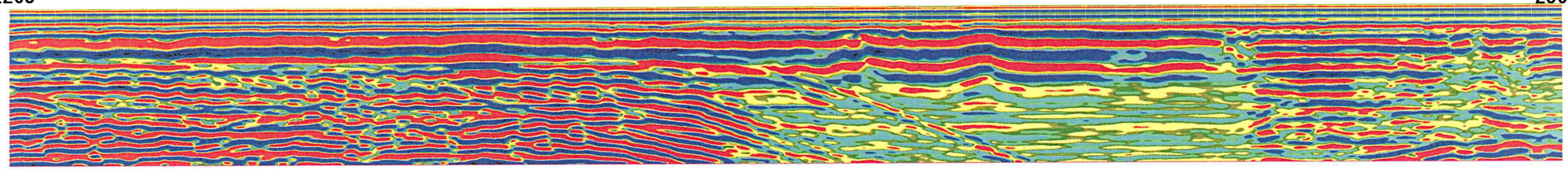

56f.bmp

2363 2464

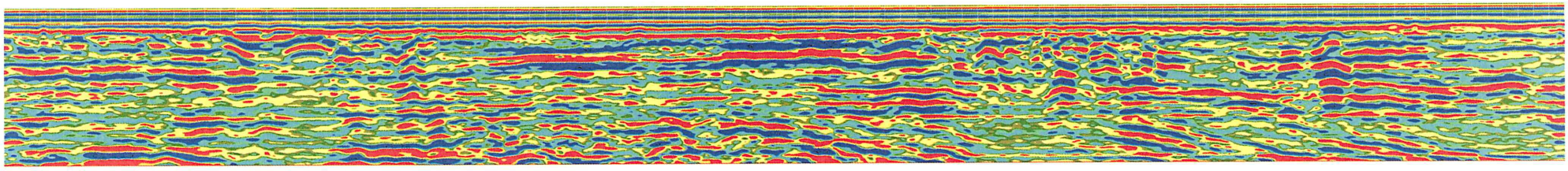

59f.bmp

150 ns

2463 2513 水管橋 2546

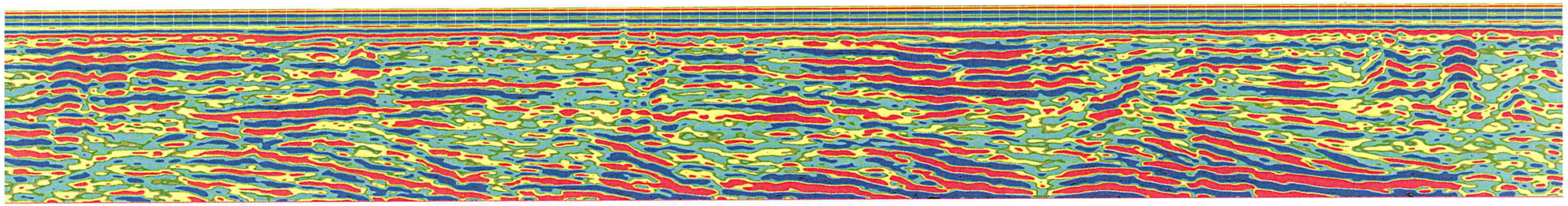

61f.bmp

2546 2602 水管橋 (2608－2621島崎橋) 2647

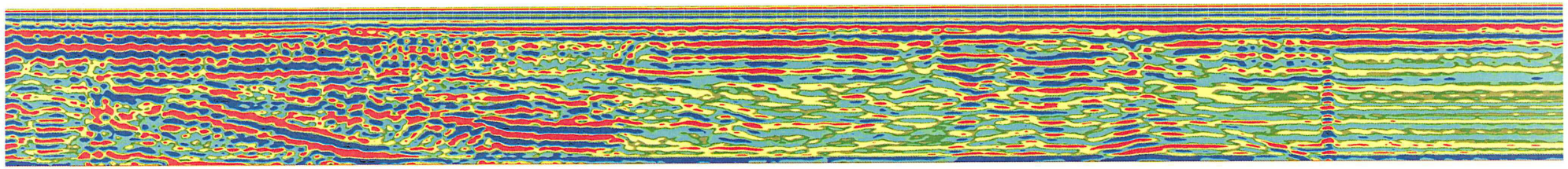

64f.bmp

2646 2730

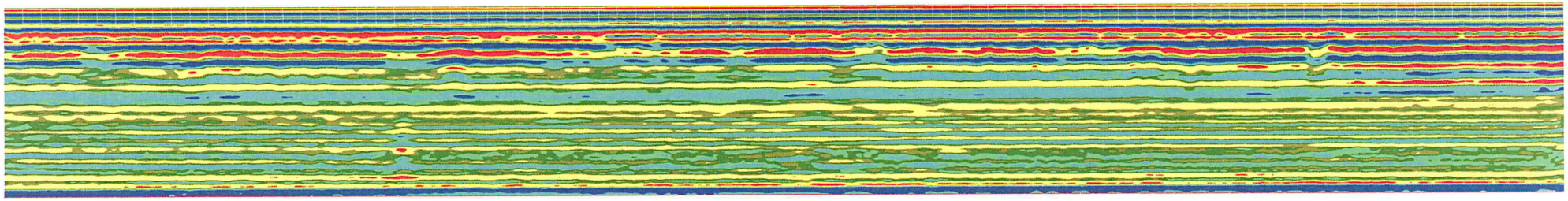

65f.bmp

250 ns

250ns

0

101

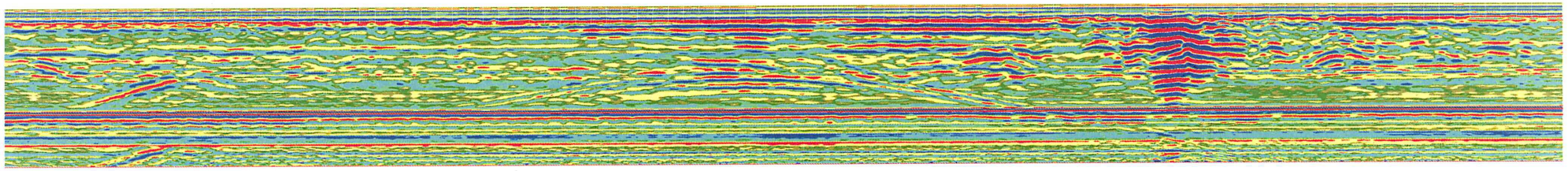

10f.bmp

100

201

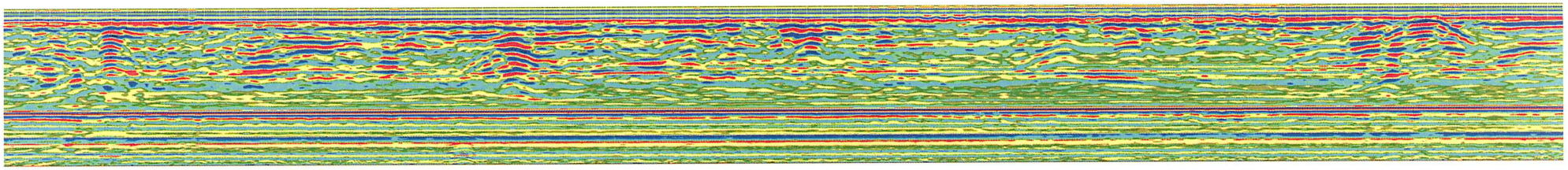

11f.bmp

200 (204-220新落合橋　　)

301

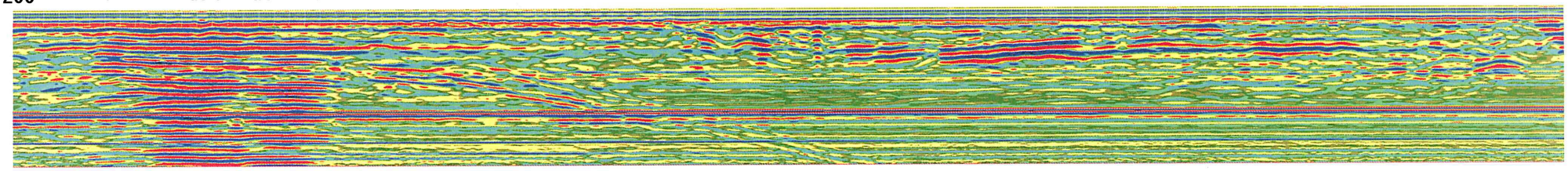

14f.bmp

300

401

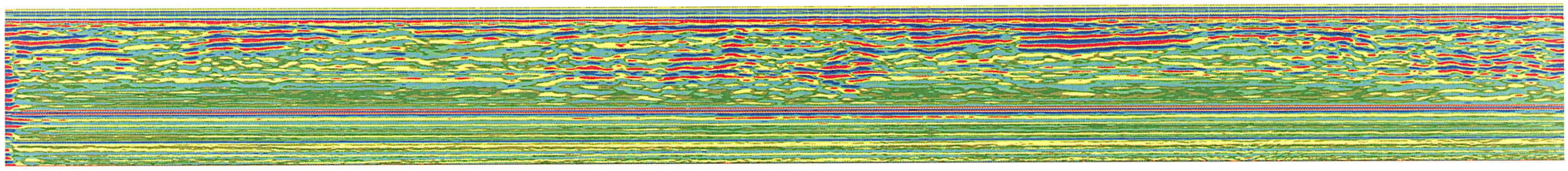

15f.bmp

250ns

400 (464-473観音橋) 501

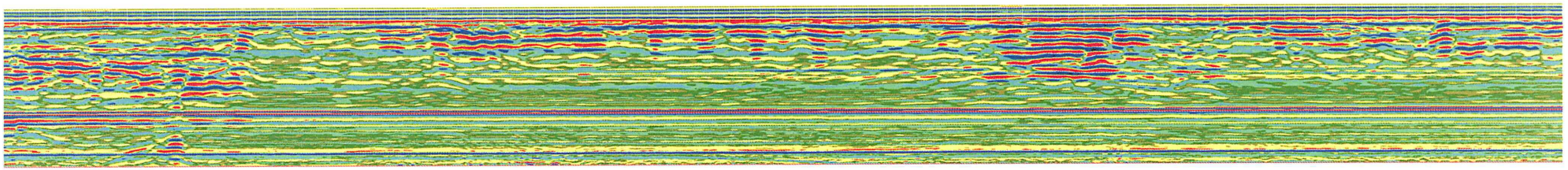

18f.bmp

500 (534-544阪急) 601

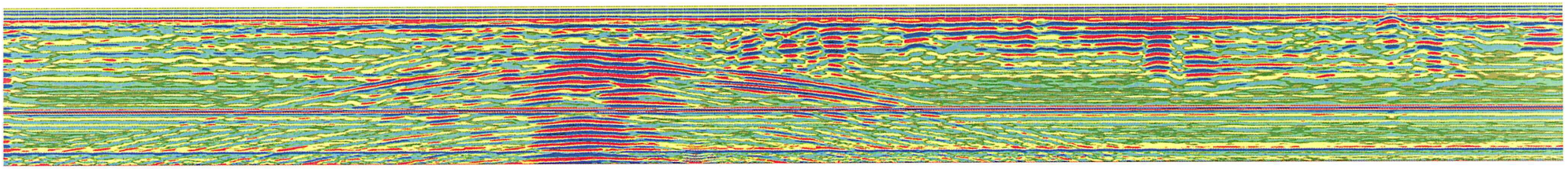

19f.bmp

600 701

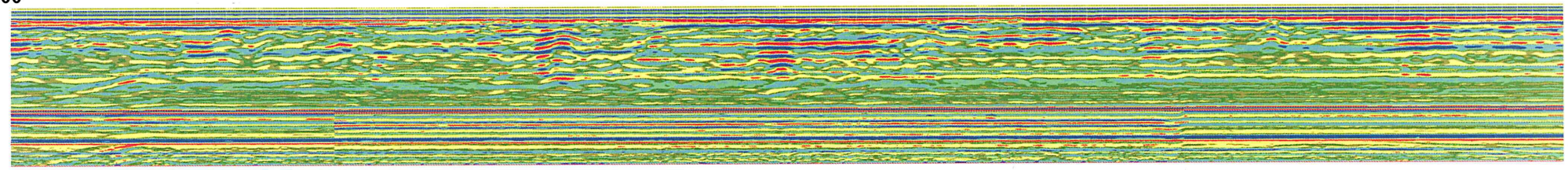

23f.bmp

700 711 水管橋 (729-765水道橋：山手幹線) 801

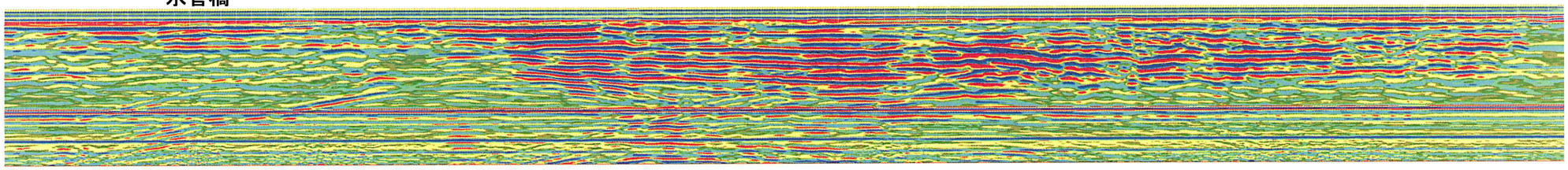

25f.bmp

250ns

800

901

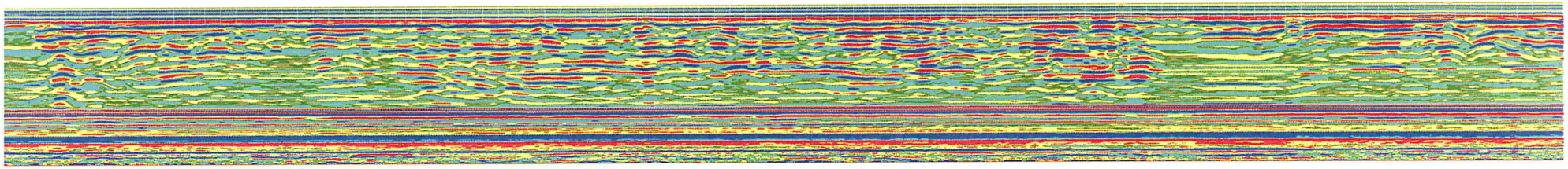

29f.bmp

900

1001

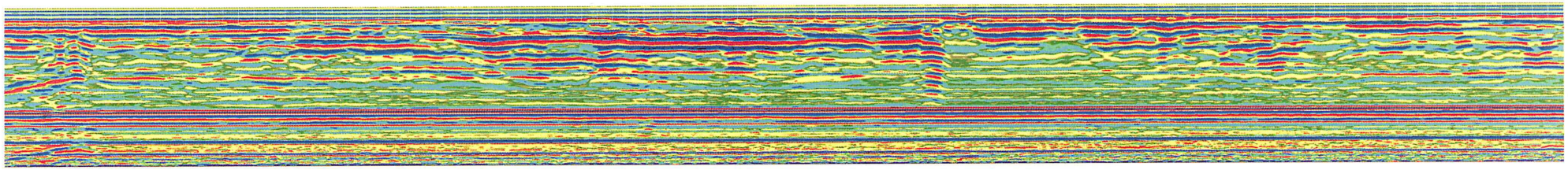

30f.bmp

1064-
1066
歩道橋

1069-1077
久原橋

1000

1052
水管橋

1123

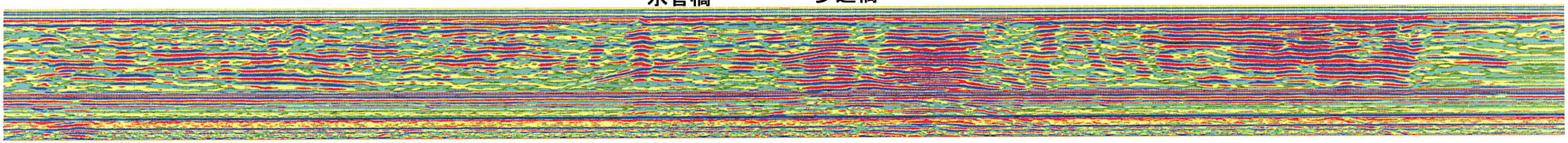

1121.4
JR

33f.bmp

1163

(1231-1263住吉橋：国道2号

)1264

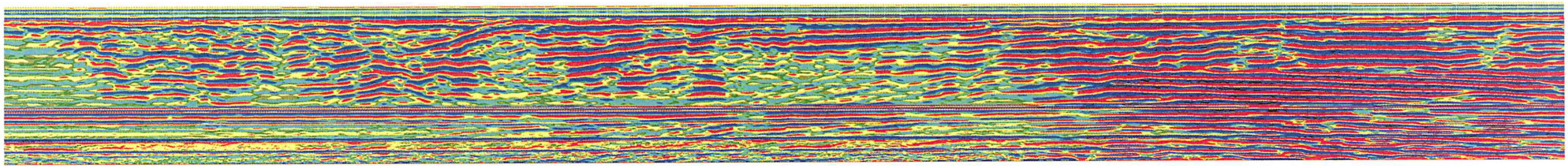

1163
JR

34f.bmp

住吉橋
国道2号

250ns

1263

1364

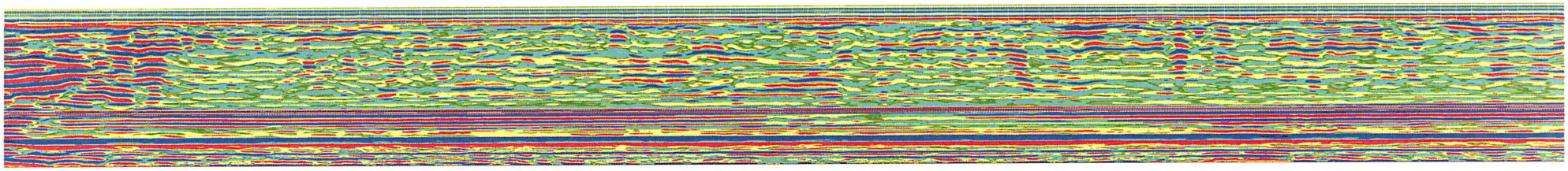

37f.bmp

1363

1464

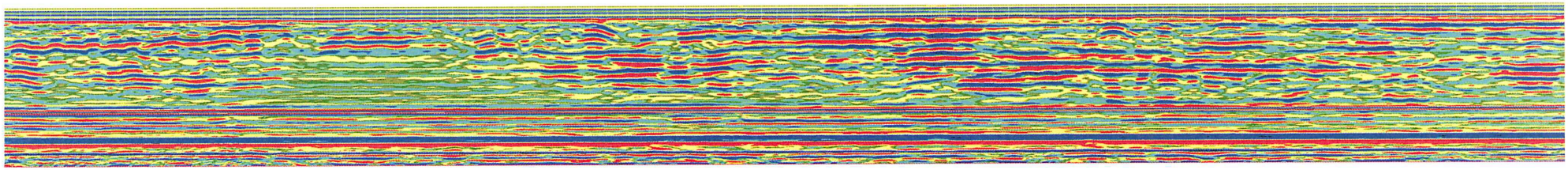

38f.bmp

1463

1564

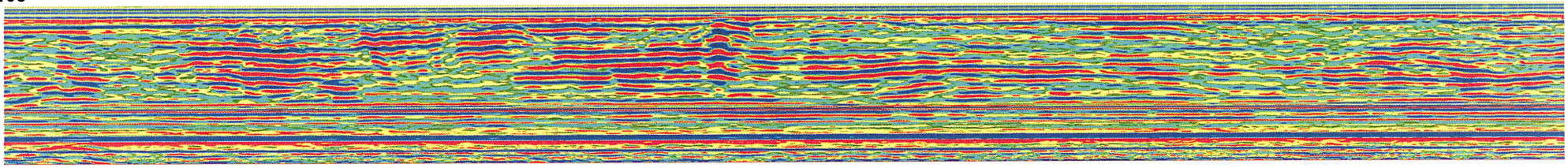

41f.bmp

(1561新反高橋　)

1563

1664

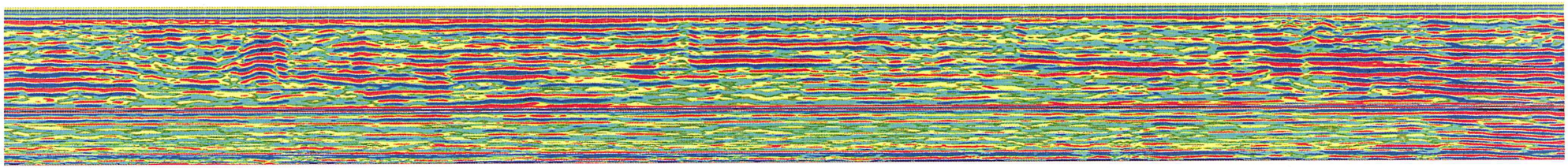

42f.bmp

-1669新反高橋）

250ns

1663

1734

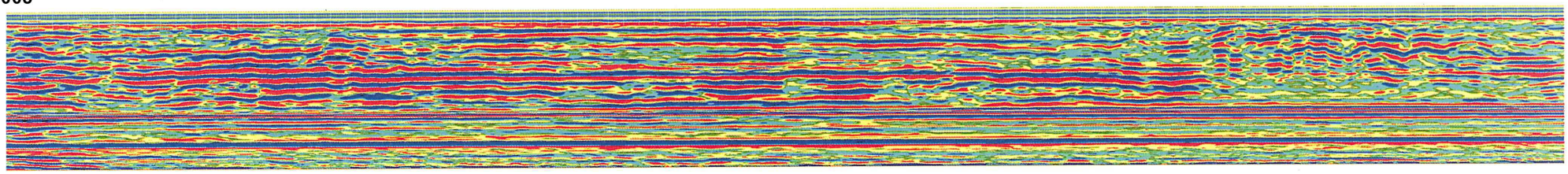

45f.bmp

1763

（1820-1836反高橋　　）

1864

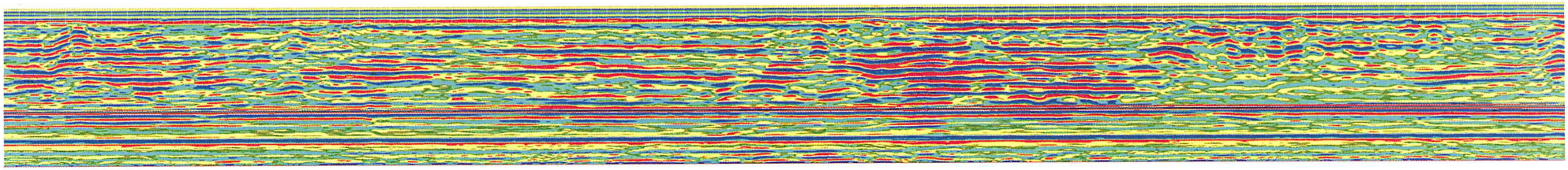

46f.bmp

1863

1964

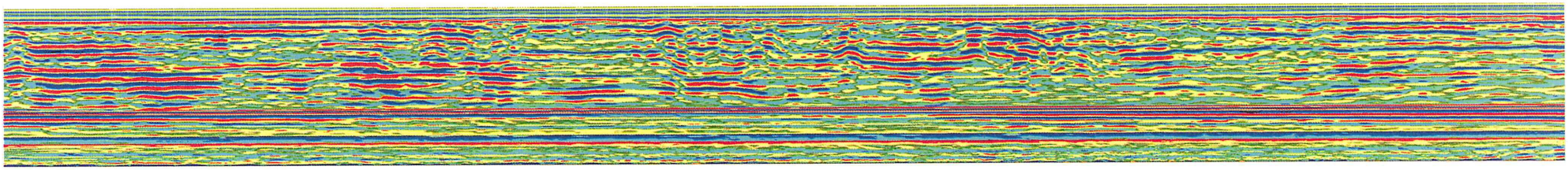

49f.bmp

1963

2064

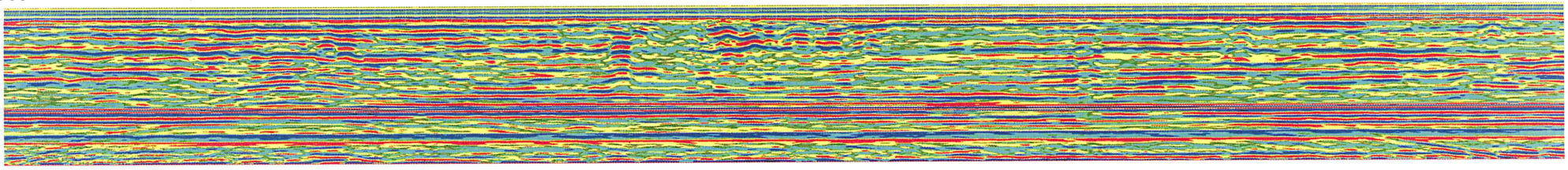

50f.bmp

250ns

2063 (2123-2161阪神電車) 2164

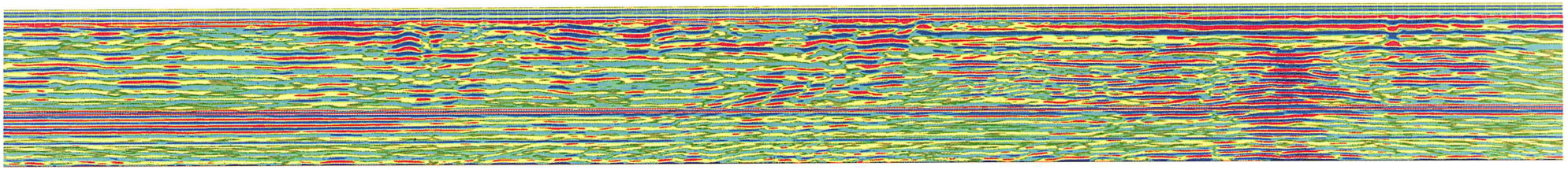

53f.bmp

(2255国道43号

2163 2264

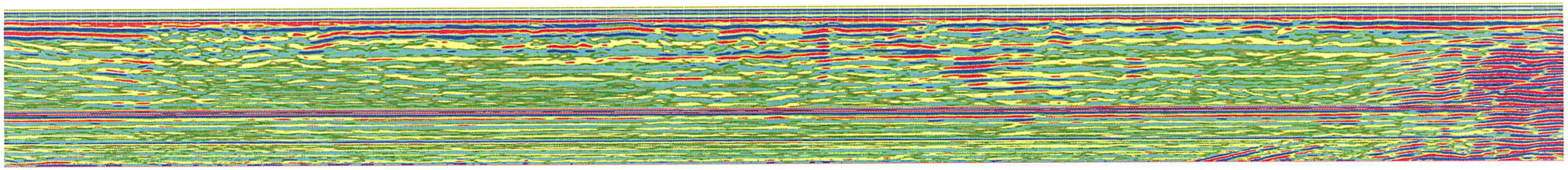

54f.bmp

2263 -2310国道43号) 2364

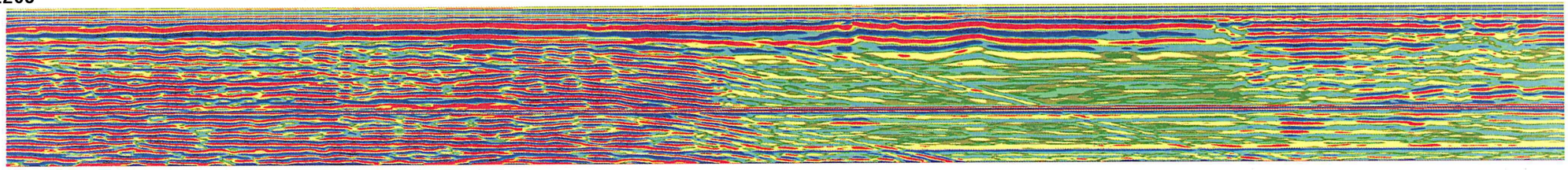

57f.bmp

2363 2464

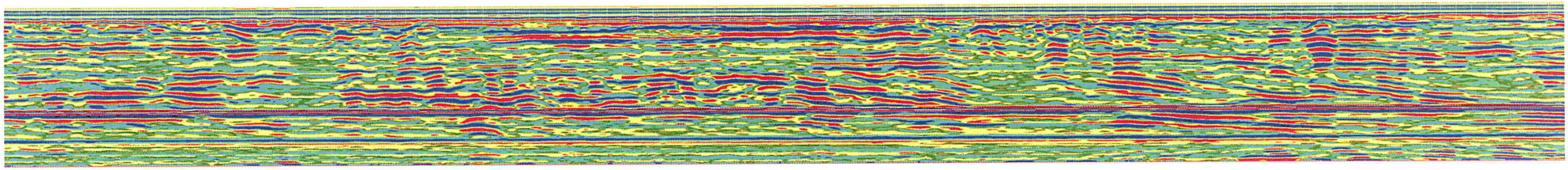

58f.bmp

250ns

2513
水管橋

2463

2546

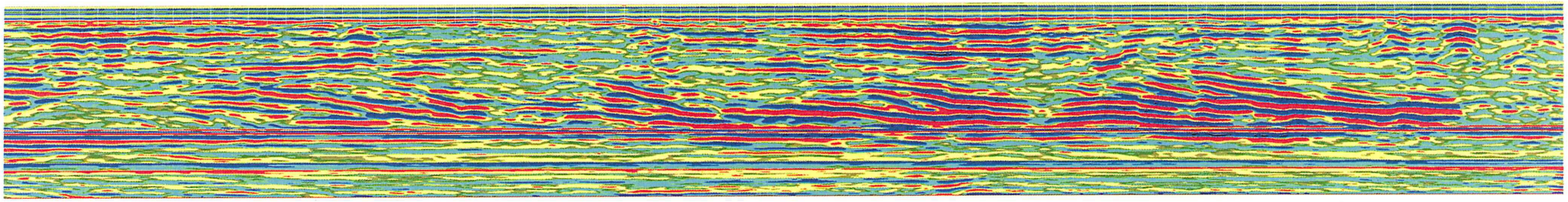

62f.bmp

2602
水管橋　　(2608-2621島崎橋)

2546

2647

高さ-1m

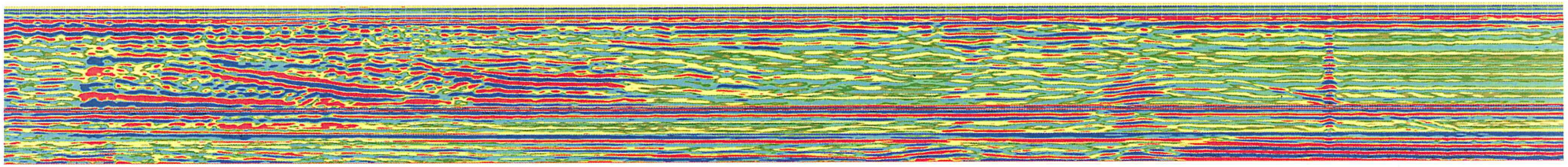

63f.bmp

2646

2730

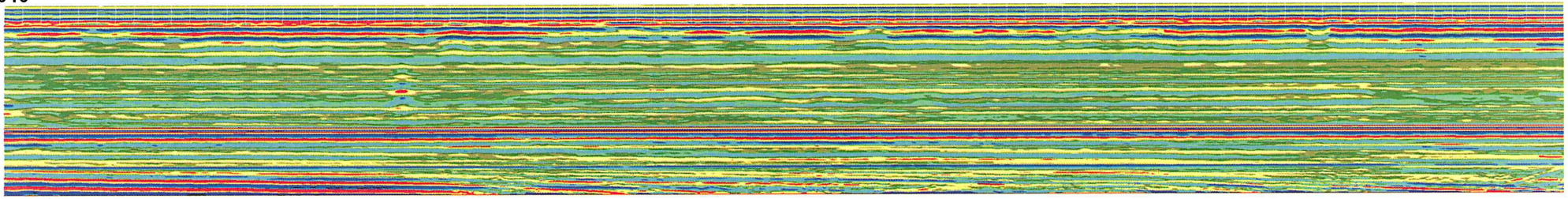

66f.bmp

Ishiya River GPR Sections

調査名　石屋川GPR

調査日　2008/11/3　天候:くもり　調査者:宮田、苦瓜、平井、上岡

距離	累加距離	変化点	方向	勾配(度)	地中構造物	目印	橋梁	ファイル名	レンジ	ゲイン							備考
0	0				マンホール位置	交差点		61	150	15	35	45	52	57	62	67	石屋川水位なし
20	20	勾配		7	0, 22, 43, 61, 64, 79, 82, 111												
42	42				130, 139	交差点											
83	83					交差点											
131	131	勾配		4													
139	139		N44W	6		交差点											
							阪急電鉄										
0	0					山麓線		62	150								
74	74	方向	N45W														
90	90	勾配		5													
110	110				右側道路側溝より湧水？	交差点											
163	163	勾配		2													
177	177	方向	N48W														
185	185					交差点											
200	200																
18	218	勾配		1				63	150								
26	226	方向	N28W														
31	231	勾配		-2		交差点右斜めに横切る											
39	239	方向勾配	N18E	1													
53	253	勾配		4													
73	273	勾配		2													
97	297	勾配		1	左側マスより大量の湧水												
120	320	勾配		0													
145	345	勾配		-3													
153	353	勾配		0		交差点											
174	374	勾配		6													
178	378	方向勾配	N10W	1		交差点											
						山手幹線											
0	0					市バス石屋川車庫		65	150	15	31	40	47	54	60	65	
7	7	勾配		0		交差点											
							JR										
46	46					交差点											
79	79	勾配		2		交差点											
133	133					交差点											
187	187					交差点											
250	250	方向	N20W														
53	303					交差点		66	150								
95	345					交差点											
131	381					交差点											
160	410	勾配		1		交差点											
180	430	方向勾配	N2W	2		交差点											
						R2											
0	0							67	150								
104	104					交差点											
123	123	方向	NS														
157	157					交差点											
200	200	方向	N30W			地蔵											
8	208						阪神	68	150								
29	229																
33	233	勾配		1		交差点											
62	262	勾配		2													
76	276	勾配		0		交差点											
119	319	勾配		-1													
124	324	勾配		0		交通量の多い車道											
128	328																
168	368	勾配		4													
200	400	方向	N20W														
215	415	勾配		2													
250	450																
42	492		N6E	0				69	150								
						R43											

FILE 61 100 MHz 150 ns

0 100

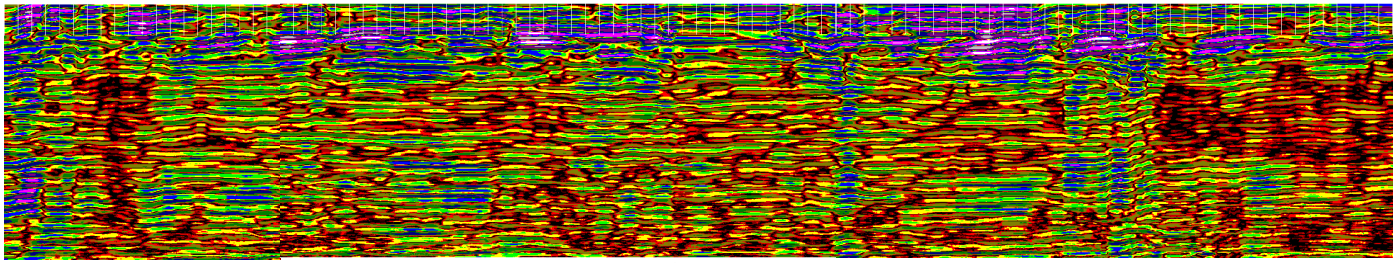

100 139 Hankyu Railway

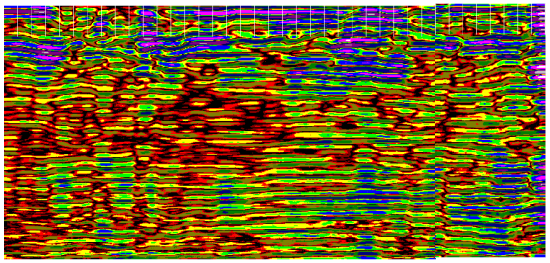

FILE 62 100 MHz 150 ns

0 90

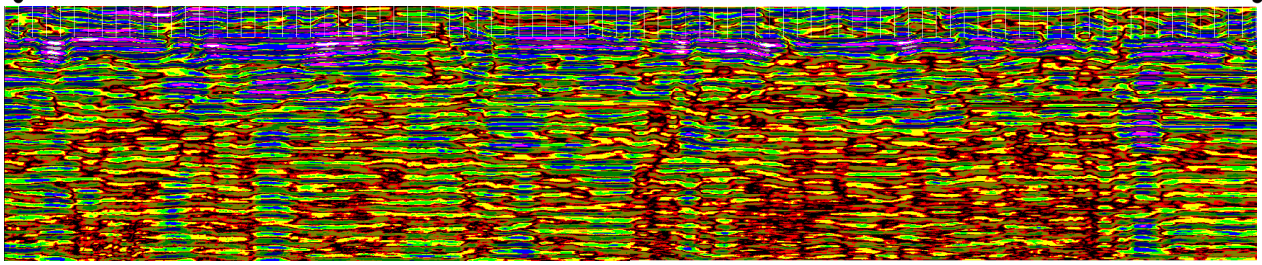

FILE 62 100 MHz 150 ns

90 200

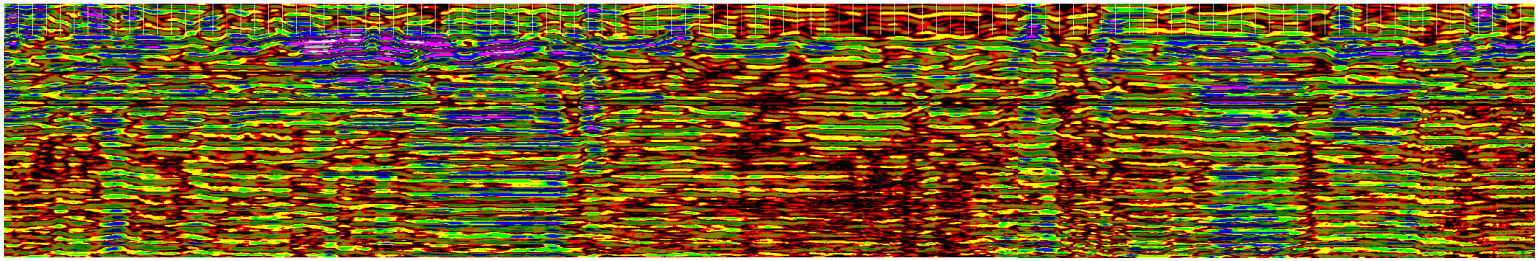

FILE 63 100 MHz 150 ns

200 297

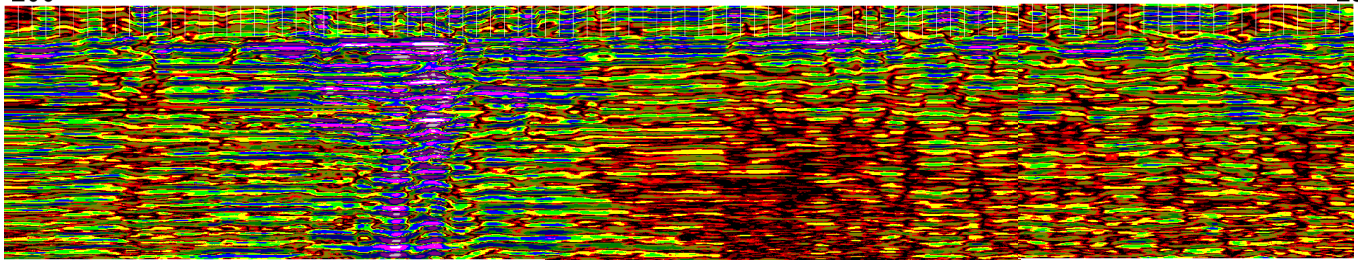

297 378 Yamate arterial road

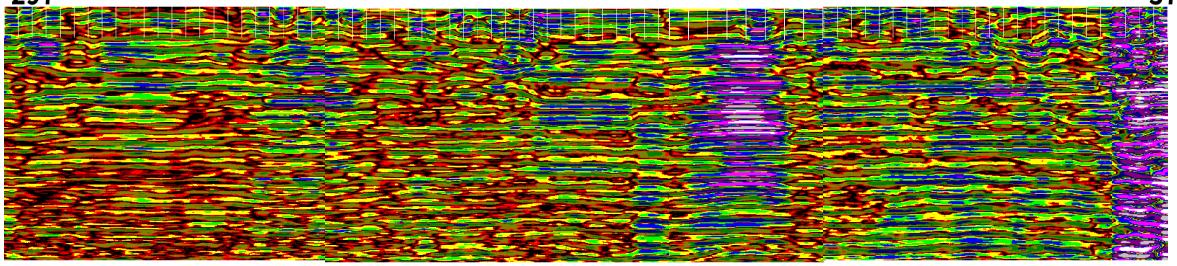

FILE 65 100 MHz 150 ns

0 120

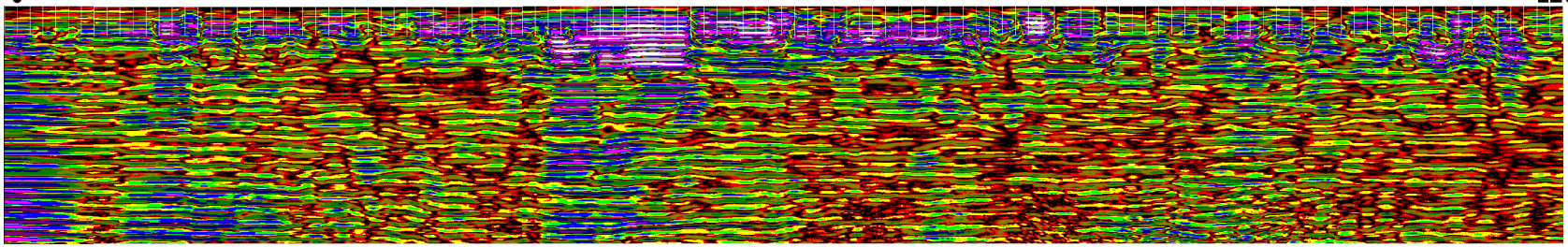

120 250

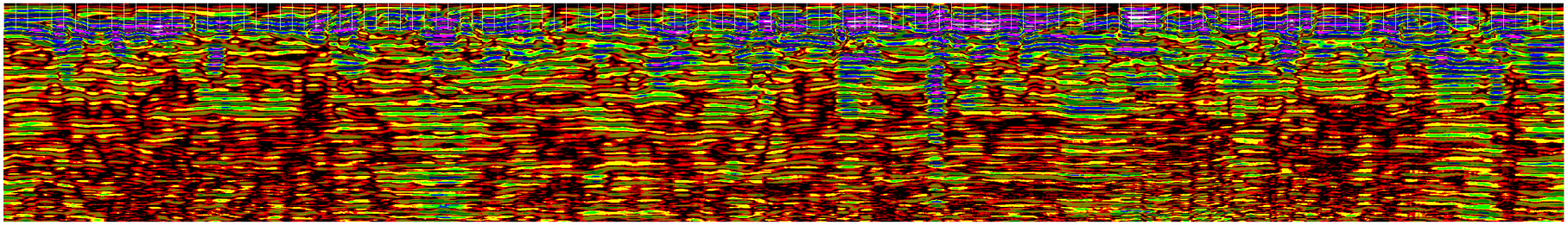

FILE 66 100 MHz 150 ns

250 330

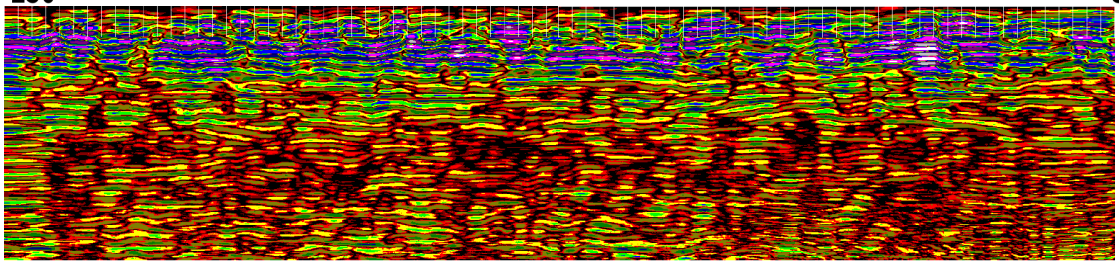

FILE 66 100 MHz 150 ns

330 430 Route 2

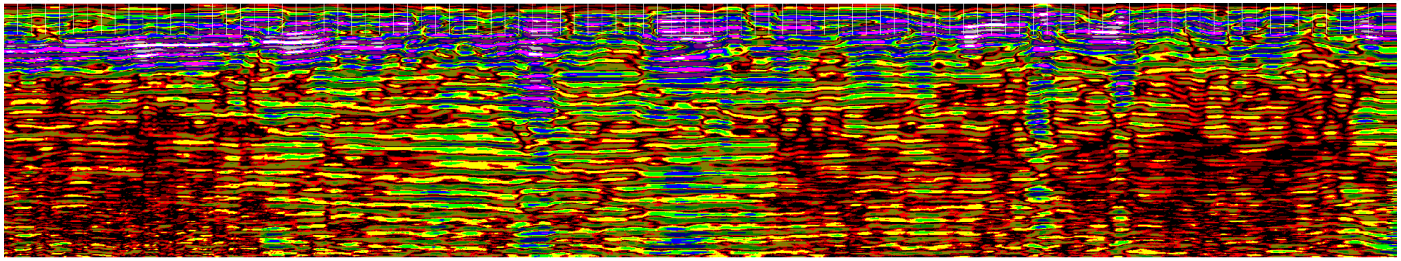

FILE 67 100 MHz 150 ns

0 123

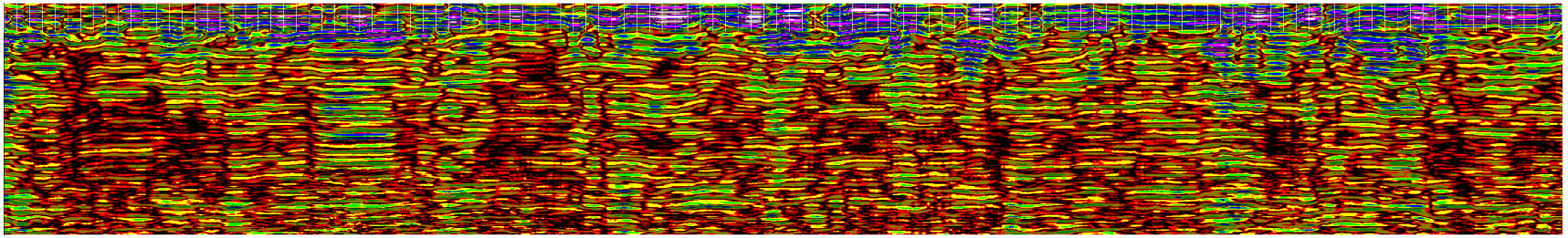

123 200

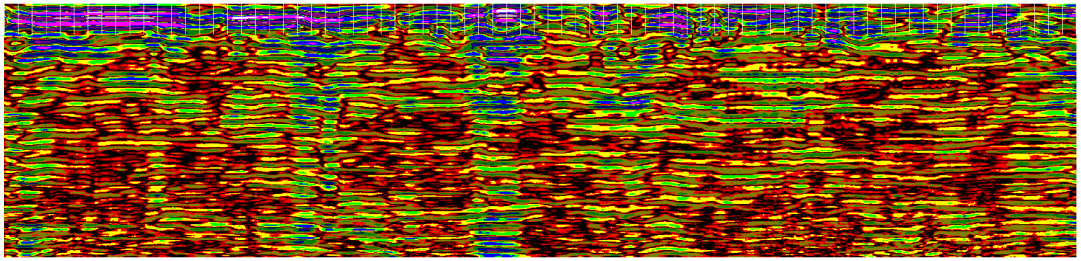

FILE 68 100 MHz 150 ns

200 328

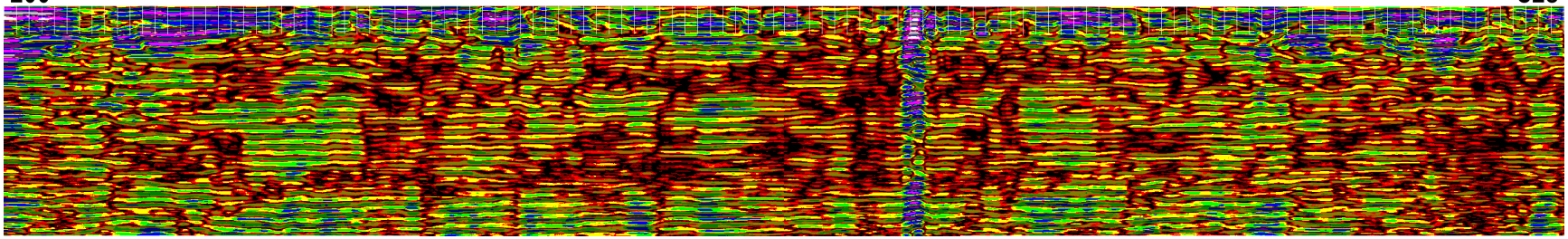

328 450

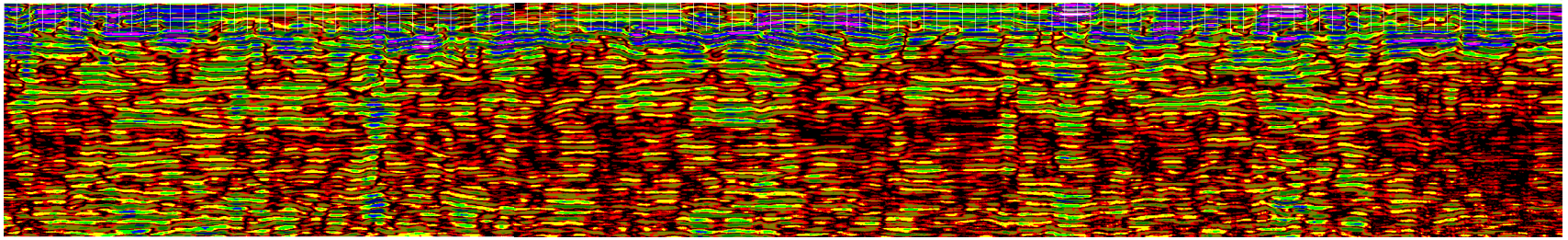

FILE 69 100 MHz 150 ns

450 492 Route 43